

DEPARTMENT OF OCEANOGRAPHY
COLLEGE OF SCIENCES
OLD DOMINION UNIVERSITY
NORFOLK, VIRGINIA 23508

Technical Report 87-2

LOAN COPY

MECHANISMS OF SAND LOSS FROM AN ESTUARINE GROIN SYSTEM
FOLLOWING AN ARTIFICIAL SAND FILL

By

John C. Ludwick, Principal Investigator

CIRCULATING COPY
Sea Grant Depository

Final Report
For the period ending March 31, 1987

Prepared for the
Virginia Sea Grant College Program
Virginia Graduate Marine Science Consortium
203 Monroe Hill House
University of Virginia
Charlottesville, Virginia 22903

Under
Research Grant R/CP-1

NATIONAL SEA GRANT DEPOSITORY
PELL LIBRARY BUILDING
URI, NARRAGANSETT BAY CAMPUS
NARRAGANSETT, RI 02882

March 1987

DEPARTMENT OF OCEANOGRAPHY
COLLEGE OF SCIENCES
OLD DOMINION UNIVERSITY
NORFOLK, VIRGINIA 23508

RECEIVED

MAR 24 1988

DEPT. OF ENVIRONMENTAL PROTECTION
PLANNING & COORD/COASTAL MGMT.

Technical Report 87-2

MECHANISMS OF SAND LOSS FROM AN ESTUARINE GROIN SYSTEM
FOLLOWING AN ARTIFICIAL SAND FILL

By

John C. Ludwick, Principal Investigator

Final Report
For the period ending March 31, 1987

Prepared for the
Virginia Sea Grant College Program
Virginia Graduate Marine Science Consortium
203 Monroe Hill House
University of Virginia
Charlottesville, Virginia 22903

Under
Project R/CP-1

Submitted by the
Old Dominion University Research Foundation
P.O. Box 6369
Norfolk, Virginia 23508



March 1987

ABSTRACT

Following the placement of 410,590 cu m of sand fill in a groin system at Willoughby Spit, Virginia, in August and September, 1984, the volume of fill retained in a test compartment was observed to decrease slowly with time as a result of sediment movement in two shorewise zones designated herein as Belt 1 (nearshore and dominated by wave and swash action) and Belt 2 (beyond the groin ends and dominated by action of strongly asymmetrical tidal currents). In the first belt, sediment is moved primarily within a compartment along the shoreline when water levels are low, i.e., below groin tops, or from compartment to compartment by groin overwashing when the water level is sufficiently elevated. In the latter case, unidirectional transports into and out of the compartment in Belt 1 were initially equal but, as shown, eventually output exceeds input leading to losses, herein termed longshore gradient losses. Sand that is shifted offshore to a position beyond the groin ends, from Belt 1 to Belt 2, by rip current action along groin walls or owing to offshore asymmetry in the wave orbital velocity field, then tends to move westward parallel to shore on a net basis under action of the tidal currents and is lost. These losses are herein termed offshore losses.

Findings of the present study show that the intensity of sediment transport decreases with elapsed time after the fill as conditions of static equilibrium are slowly approached. An equation for post-fill shoreline history was developed based on this fall-off in sediment transport intensity and was constructed so as to include the main mechanisms of sand loss described above. Two items, (1) measured growth of a new spit, formed of fill sediment, at the end of Willoughby Spit and (2) the amount of sand remaining in a test compartment at a given time, provided the means of evaluating two required rate constants in the equation. From the solution to the equation, after 10 years 11 percent of the original fill remains in the 27 compartments of the groin system, spit volume is 30 percent of the original fill volume, and offshore losses amount to 59 percent of the original fill volume. Half-life of the fill is 3.5 years; effective life of the fill, when 15 percent of the original fill volume remains in the system of groins, is estimated at 8.8 years.

If T-head groins were to be installed at the seaward end of each groin, the effective life of a new fill would be increased by reducing offshore losses of sand by inhibiting the action of rip currents along groin walls. Further, if the elevation of the top of each groin, when replaced, were to be increased by 45 cm, the longshore transfers of sediment in Belt 1 would be limited to only the times of highest storm-raised water levels, and thereby longshore gradient losses of beach sand would be postponed and fill-life lengthened. Plans for constructing the T-head groins as a field test have been incorporated in the recommended budgets prepared by appropriate local and state agencies.

TABLE OF CONTENTS

	<u>Page</u>
INTRODUCTION.....	1
TIDES AND STORM SURGE.....	4
TIDAL CURRENTS.....	15
WAVES.....	28
Wave Periodicity.....	31
Measured Wave-Generated Current Velocities.....	40
Directional Aspects of the Currents.....	41
Wave Refraction.....	47
BOTTOM SEDIMENT.....	53
SHORELINE CONFIGURATION AND EVOLUTION.....	53
BATHYMETRIC ELEMENTS AND EVOLUTION.....	60
THE PROCESS SCHEMA.....	72
THE ESTIMATION OF FILL LIFE.....	74
SUMMARY AND CONCLUSIONS.....	85
ACKNOWLEDGMENT.....	87
REFERENCES CITED.....	88

LIST OF TABLES

<u>Table</u>	<u>Page</u>
1 Highest recorded gage readings at Willoughby (Little Creek) referred to MSL.....	10
2 Wind velocities recorded at some coastal locations during the storm of November 5-8, 1953. (From Pore, et al., 1974).	13
3 Storm-elevated water levels for Willoughby Spit and their estimated recurrence times.....	15
4 Summary of tidal current observations (corrected to mean range) and sediment transport. (From Fleischer et al., 1977).....	22

TABLE OF CONTENTS - Continued

LIST OF TABLES - Concluded

<u>Table</u>	<u>Page</u>
5 Near-bed tidal currents (corrected to mean range) on a shore-normal transect off Willoughby Spit. See Figure 10 for station locations 1, 4, 5, and 6. See text for position of station number 7.....	24
6 Computed wave characteristics for the Willoughby Site. (From USACE, 1984).....	29
7 Characteristics of the spectra of wave-generated currents at the Willoughby Spit test compartment.....	32

LIST OF FIGURES

<u>Figure</u>	<u>Page</u>
1 Index map of Chesapeake Bay.....	2
2 Index map of lowermost Chesapeake Bay including Willoughby Spit.....	3
3 An example of the predicted astronomical tide at Sewells Point tide gage, 2.8 miles to the southwest of Willoughby Spit.....	5
4 Predicted hourly heights of the astronomical tide at Sewells Point, Virginia for the 19-year period 1963-1981 (from Harris, 1981). Solid curve is the frequency distribution; dotted curve is the cumulative "greater than" distribution. Note the position of the top of the outer horizontal section of the east groin of the test compartment.....	8
5 Observed storm surge and computed storm surge for the November 5-8, 1953 storm. Solid curves are observed storm surges. Dashed lines join calculated values of surge. Arrows indicate times of astronomical high tides. The date of each day is placed at the 1200 EST position. Maximum value of observed surge is placed near the peak of each curve. (From Pore, et al., 1974).....	12
6 Index map to tidal current stations off Ocean View and Willoughby Spit. (From Fleischer, et al., 1977).....	18
7 The threshold for initiation of sediment motion at the bed compared to observed tidal current velocity averaged over two levels above the bed (1.50 and 2.50 ft.) and plotted versus time. Ocean View Tidal Current Station 1; water depth 21.5 ft. (MLW). (From Fleischer, et al., 1977).	19

TABLE OF CONTENTS - Continued

LIST OF FIGURES - Continued

<u>Figure</u>		<u>Page</u>
8	The threshold of initiation of sediment motion at the bed compared to observed tidal current velocity averaged over two levels above the bed (1.50 and 2.75 ft.) and plotted versus time. Ocean View Tidal Current Station 2; water depth 24.75 ft. (MLW). (From Fleischer, et al., 1977).....	20
9	The threshold for initiation of sediment motion at the bed compared to observed tidal current velocity averaged over two levels above the bed (1.50 and 3.00 ft.) and plotted versus time. Ocean View Tidal Current Station 3; water depth 20.0 ft. (MLW). (From Fleischer, et al., 1977).	21
10	Index map of tidal current stations off the study site at Willoughby Spit. See Table 5 for data.....	23
11	Relative timing between tidal currents and elevation of the water surface at Willoughby Spit. When the groins are submerged, the tidal current is in flood. Note the asymmetry of the tidal currents and the great asymmetry in effective currents (ruled areas).....	27
12	A simple local wind wave spectrum derived from E-M current meter measurements. Peak period 3.8 sec.; propagation direction 208 deg. A subordinate peak occurs at 32.1 sec.; direction 182 deg. Water depth 95 cm.....	33
13	Wind waves from the Atlantic. Peak wave period 8 sec.; direction 210 deg. Water depth 110 cm. Local wind speed 4-7 knots from the west. Estimated wave height 8 to 18 cm..	35
14	Waves from several sources. Principal peak occurs at a period of 3.8 seconds and a direction of 181 deg. A second peak occurs at a period of 69 seconds and a direction of 211 deg. A third peak occurs at a period of 7.9 seconds and a direction of 184 deg. Water depth 90 cm. Wind from 065 degrees at 15-20 mph.....	37
15	Wave periods 3.2-4.6 seconds, 16 seconds, and 56.2 seconds. The direction of the latter motion is alongshore towards 105 degrees.....	38
16	Low frequency motion dominates at a period of 56 seconds. See Fig. 17D for the distribution of velocity vectors.....	39
17	Current measurements in the test compartment at Willoughby Spit. See text for location of stations within the compartment. A (WAV33) and B (WAV35), a current couple (see text). C Orbital asymmetry (WAV26) D Low-frequency oscillations (WAV31).....	42

TABLE OF CONTENTS - Continued

LIST OF FIGURES - Continued

<u>Figure</u>		<u>Page</u>
18	Forward-favored asymmetry of wave orbital velocity near the bed at a location 20 feet west of the east groin. Wind speed was 13-17 knots from 065 degrees. Note that some forward runs are more than 7 sec. in duration; although the mean is 1.61 sec.....	44
19	Forward-favored asymmetry of wave orbital velocity near the bed at a location 115 feet east of the west groin. Wind speed 12 knots (estimated) from 247 degrees. Reverse runs were lacking due to a superimposed current in the direction of wave propagation.....	45
20	Wave refraction diagram for pre-fill bathymetry, MHW, 3-sec. wave period, and approach from 030 deg. CTN.....	49
21	Wave refraction diagram for pre-fill bathymetry, MHW, 3-sec. wave period, and approach from 300 deg. CTN.....	50
22	Wave refraction diagram for post-fill bathymetry, MHW, 3-sec. wave period, and approach from 030 deg. CTN.....	51
23	Wave refraction diagram for post-fill bathymetry, MHW, 3-sec. wave period, and approach from 300 deg. CTN.....	52
24	Sediment distribution in the test compartment at Willoughby Spit. The sampling period is prior to the placement of fill.....	54
25	A re-sampling of bottom sediment in the test compartment. Sampling period is pre-fill.....	55
26	Shoreline changes in the test compartment. A. Recession towards the pre-fill shoreline. Each band or envelope contains many shoreline surveys taken in the noted period; the average for the band is the central line. B. Details of a prolonged overwash episode at the east groin followed by redistribution of the overwashed sediment.....	56
27	Growth of a new spit at the western end of Willoughby Spit following the placement of fill in the updrift groin system. Where the terminal groin is represented by broken lines, it has been covered by sand in transit to the west along the shore in the shore zone. (Provided to the author by R. Neville Reynolds).....	59
28	Beach topography and shoreface bathymetry in the test compartment. Contour labels are in centimeters. MLW (1983) corresponds to the +30 cm contour. A. May 13, 1984; pre-fill. B. October 4, 1984; post-fill.....	61

TABLE OF CONTENTS - Concluded

LIST OF FIGURES - Concluded

<u>Figure</u>	<u>Page</u>
29 Beach topography and shoreface bathymetry in the test compartment. Contour labels are in centimeters. MLW (1983) corresponds to the +30 cm contour. A. January 9, 1986; pre-fill. B. August 5, 1986; post-fill.....	63
30 Difference map; post-fill. September 27 to November 8, 1985.....	65
31 Difference map; post-fill. November 8, 1985 to January 9, 1986.....	67
32 Difference map; post-fill. January 9 to March 26, 1986.....	68
33 Difference map; post-fill. March 26 to May 5, 1986.....	69
34 Time-history of sediment volume in the test compartment. The shaded area gives the cumulation of values derived from the sequence of elevation difference maps. The dashed line is a corrected time-history curve allowing for whether erosion at a point is in fill or pre-fill sediment.....	71
35 Groin effectiveness related to sand level and water level. A. East groin, pre-fill profiles taken along the east and west sides of the groin. B. East groin, post-fill profiles taken along the east and west sides of the groin. C. West groin, pre-fill profiles taken along the east and west sides of the groin. D. West groin, post-fill profiles taken along the east and west sides of the groin.....	73
36 Definition sketch. Three compartments of a rectilinear system of groins. Symbols are defined in the text.....	77
37 Sediment remaining in the various compartments as a function of time post-fill. The results were obtained from Eq. 2 of the present report.....	80
38 Time history of the partitioning of the placed fill at Willoughby Spit among the groin compartments, terminal spit, and offshore losses.....	84

INTRODUCTION

Groins have been widely utilized by man for a long time in his attempts to control beach erosion (e.g., Balsillie and Bruno, 1972; Tomlinson, 1980). Today, a system of constructed groins, particularly in estuarine settings, is often filled artificially with sand in the hope that the structures will hold the protecting sediment in place. In this report, transfers of filled sediment in and near a groin compartment are explored with the ultimate aims of 1) developing a technique for predicting fill life in estuarine settings, where tidal currents are significant, through a mathematical analysis of the acting processes and 2) prolonging the life of a fill by modifying the structural design of estuarine groins from the style presently in common use.

Willoughby Spit lies at the western end of the beach system that forms the southern boundary of Chesapeake Bay, Virginia (Figs. 1, 2). The spit is 3.2 km long, 135 to 535 m wide, 2 m (MLW) in average elevation, and is developed residentially. The feature became recognizable ca. 1800 (Melchor, 1970) and, from the start, lengthening to the west (Fleischer, et al., 1977) was accompanied by a shoreward shifting of depth contours on the northern shoreface. Along the actual shoreline, from 1852 to 1937, net recession to the south ranged from 55 to 180 cm per year (Brown, 1938). More recently the shoreline retreat rate was estimated at 7.6 cm per year (Byrne and Anderson, 1977).

From 1920 to 1937, property owners built 62 groins along the north shore of the spit. Most of these were replaced in 1939 with a system of 37 designed structures along a 5.5-km shore reach. These groins are straight, shore normal, of timber construction, 79 to 100 m in length, and spaced 152 m apart on average. Each has an inner level section at +183 cm (MLW), an

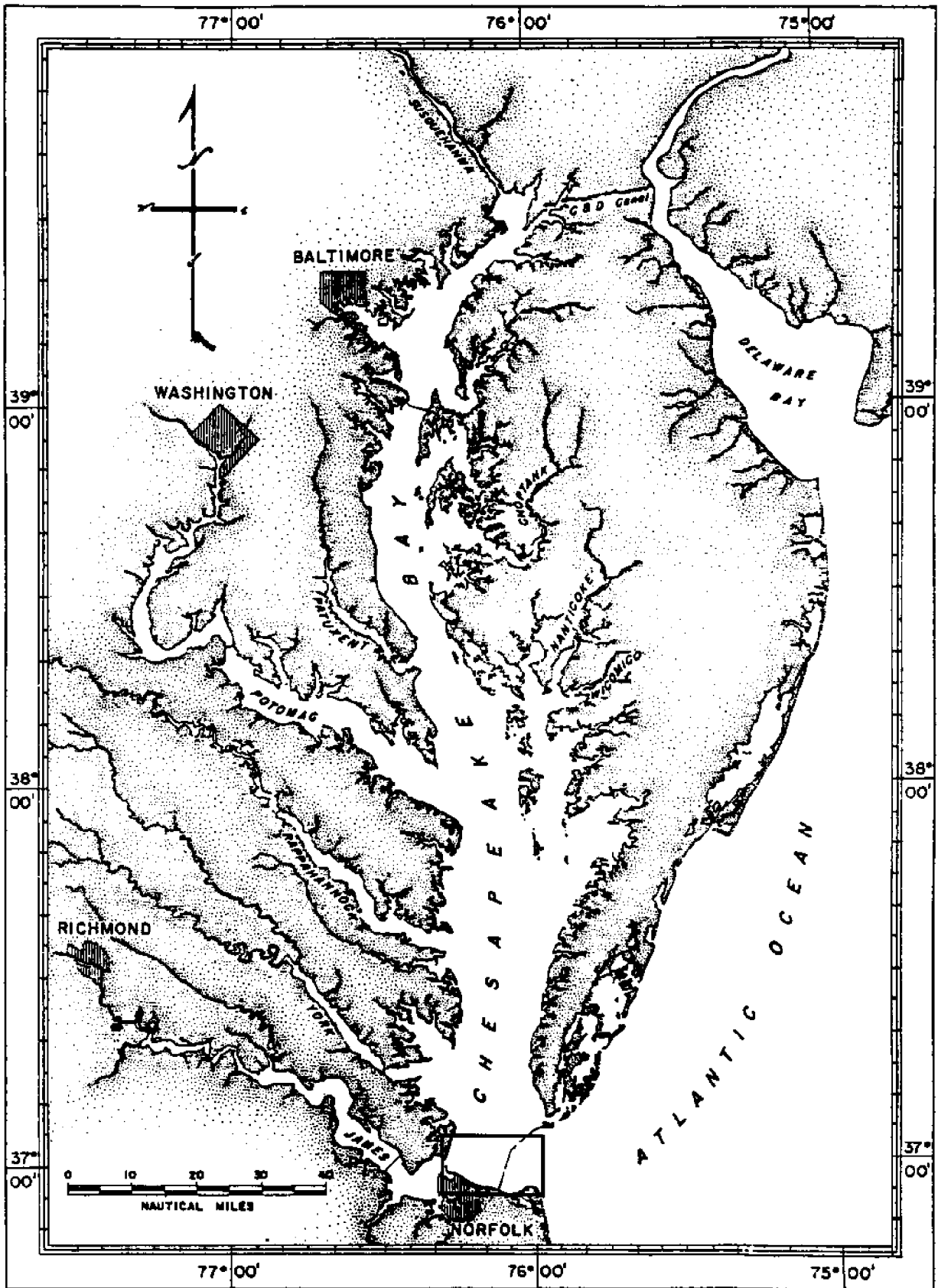


Fig 1. Index map of Chesapeake Bay.

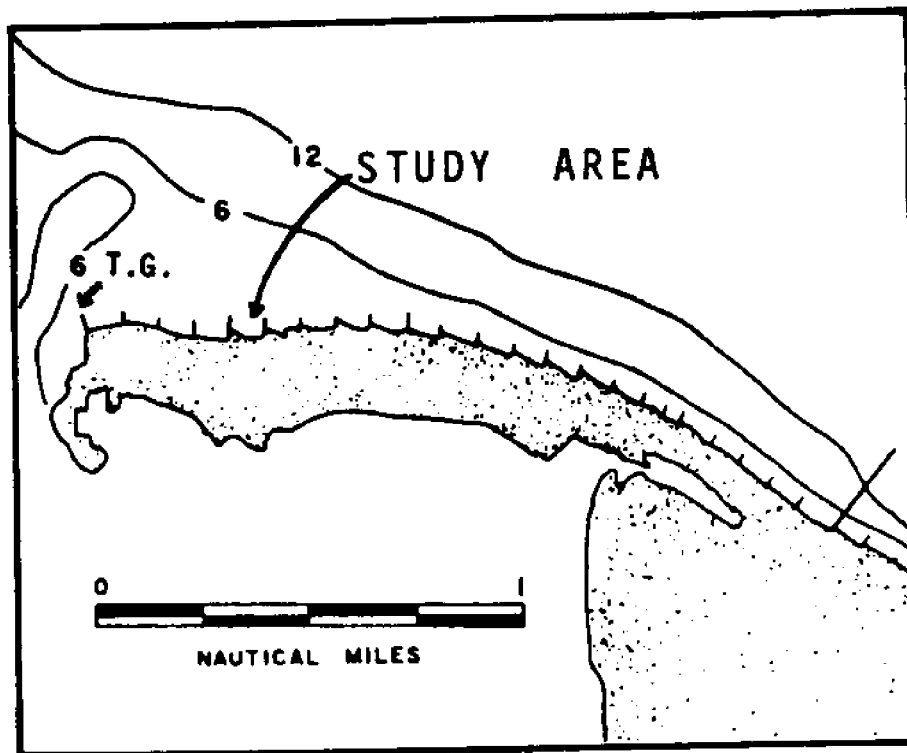
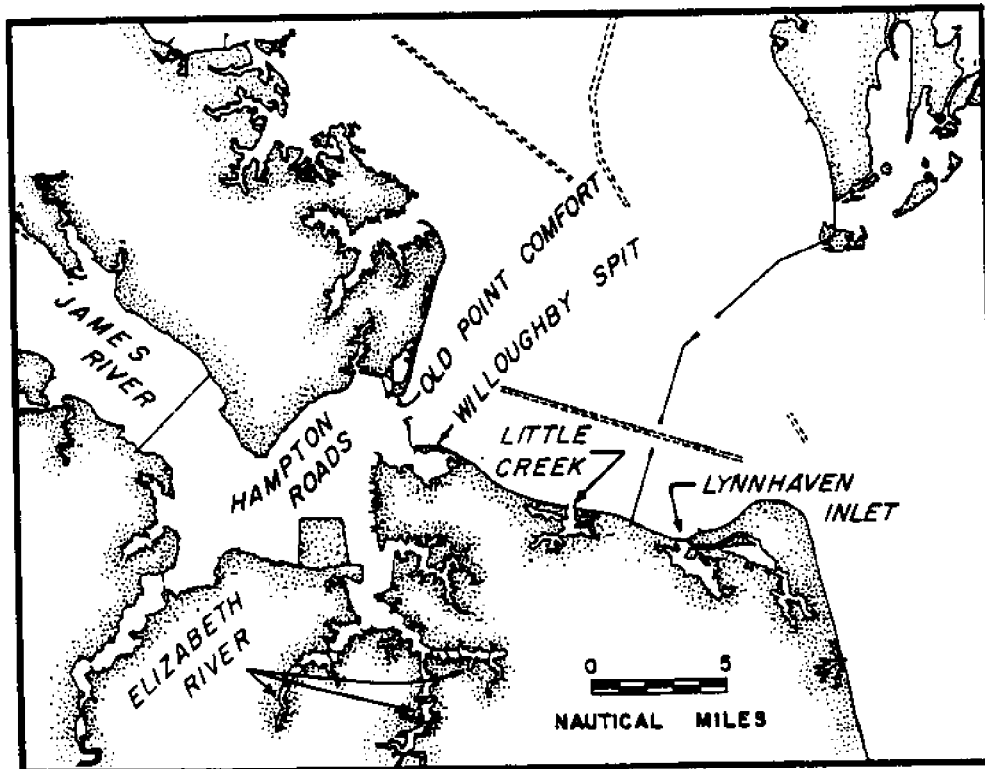


Fig. 2. Index map of lowermost Chesapeake Bay including Willoughby Spit.

outer level section at +61 cm (MLW), and an intermediate inclined section approximately 23 m in length. In a recent report (USACE, 1984) it is observed that relative to common practice of the present-day (Tomlinson, 1980), the described groins are longer, more widely spaced, and lower.

In September, 1984, a sand fill of 410,590 cu m was placed in the 27 westernmost groin compartments of the groin system at Willoughby Spit along a 3.9-km reach. The sediment was obtained by cutter-head dredging in the Elizabeth River from the upper part of the Yorktown formation which is a shelly carbonate-cemented iron-stained poorly-sorted coarse-grained pebble-, cobble-, and concretion-bearing quartz sandstone of Miocene age. The fill surface was bulldozed to a plane dipping seawards to the groin ends at a slope of 1:20. On the backshore, fill was formed into a dune-like ridge with a top elevation of approximately +3.7 m (MLW).

In the sections of this report that follow, the main environmental processes that affect the movement and transport of sediment in the near-shore zone in the Willoughby Spit area are examined in some detail as background for the construction of a process schema and an equation for fill life prediction. Suggestions for design modifications to estuarine groins are derived from the results.

TIDES AND STORM SURGE

The astronomical tide at the Willoughby Spit study site is semidiurnal, and produces typically two high and two low waters each tidal day which is 24 hours and 50 minutes in duration (Fig. 3). Elevations of the tidal datums that are conventionally used to characterize the magnitudes of the vertical motions are taken as being the same as those at the nearby reference tide station of the National Ocean Survey for Hampton Roads (Sewells

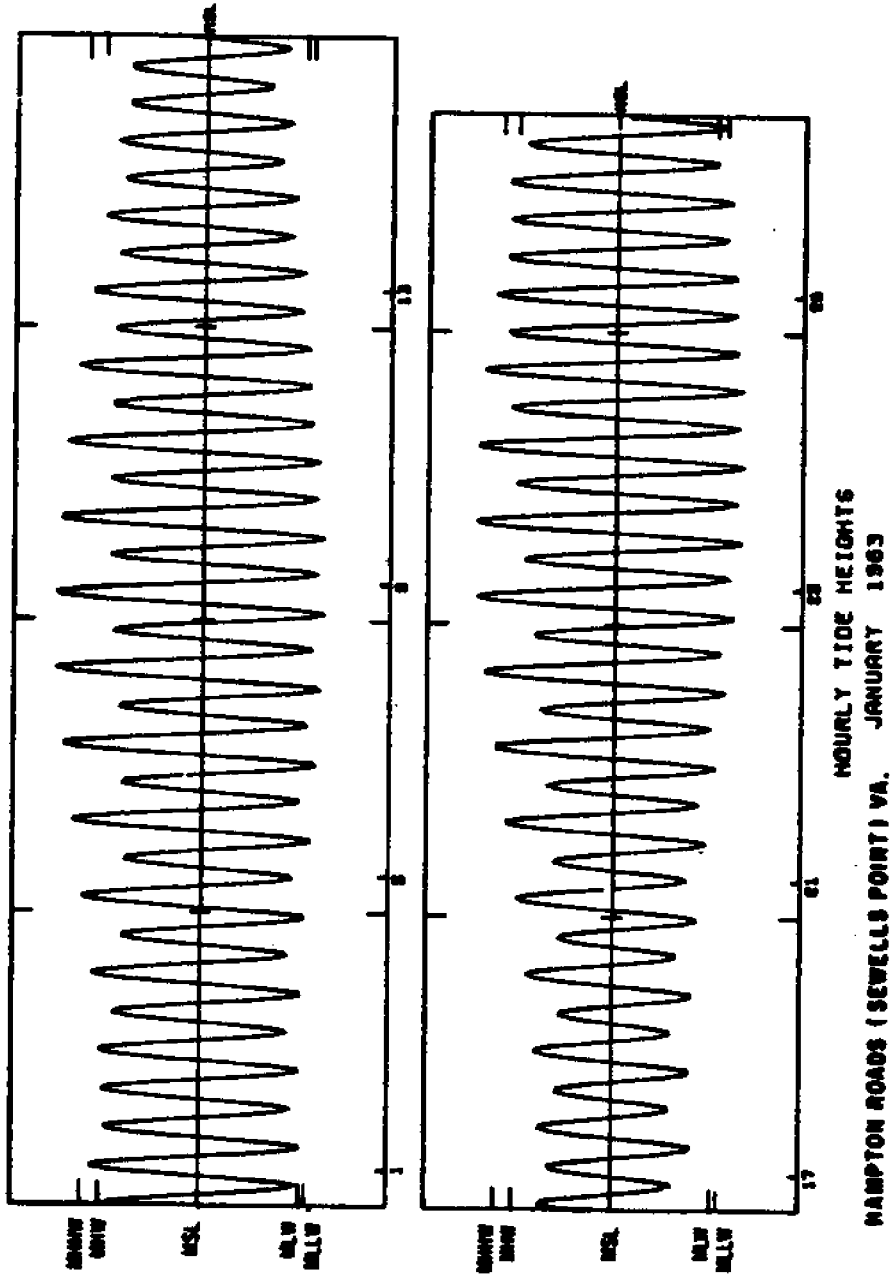


Fig. 3. An example of the predicted astronomical tide at Sewells Point tide gage, 2.8 miles to the southwest of Willoughby Spit.

Point) which is 2.8 statute miles distant to the southwest. Relative to mean sea level (MSL), the principal datums are (Harris, 1981):

Mean Higher High Water (MHHW)	1.41 feet (43.0 cm)
Mean High Water (MHW)	1.22 feet (37.2 cm)
Mean Sea Level (MSL)	0.00
Mean Low Water (MLW)	-1.22 feet (-37.2 cm)
Mean Lower Low Water (MLLW)	-1.26 feet (-38.4 cm)

These values were calculated by Harris from hourly predictions of water level for the 19-year period 1963-1981 and are based on harmonic constants for 17 tidal constituents derived from the Sewells Point gage record for the 365-day period January 1 to December 31, 1974. Constants for two of the constituents came from the analysis of longer records of monthly mean sea level.

An idea of the reliability of these recent predictions can be formed by comparing them with the elevations of datums established observationally from the Sewells Point gage record for the 19-year period 1941-1959 (Harris, 1981, p. 417):

Mean High Water	1.2 feet (36.6 cm)
Mean Sea Level	0.0
Mean Low Water	-1.3 feet (-39.6 cm)

The differences arise from residual effects in the observational records of storm-related changes in water level despite the use of both mechanical and

procedural steps taken to suppress these effects. Overall agreement between predicted and observed values is better than 0.1 ft. (3 cm).

During the 19-year period 1963-1981 for which predictions were made there are 166,440 hourly values of predicted water level elevation relative to mean sea level. The distribution of this population of elevations is presented in Figure 4 in both frequency and cumulative forms. Over the 19-year period, the extreme elevations due to the astronomical tide alone are +2.4 ft. (73.1 cm) and -2.0 ft. (-61.0 cm) relative to MSL. The double peaked shape of the distribution is characteristic of similar plots for other stations on the eastern seaboard of the United States (Harris, 1981) and is a consequence of the fact that the speed of the tidal rise and fall of the surface of the water is greatest at the level of MSL and hence the residence time is relatively shorter there than at the elevations of high water and low water where the surface dwells before moving downward or upward.

The elevation of the outer horizontal section of the east groin at the Willoughby Spit site is +0.8 ft. (24.4 cm) relative to MSL; for the west groin, +1.0 ft. (30.5 cm). Utilizing these groin crown elevations and the cumulative distribution of tidal water levels (Fig. 4), it is found that the east and west groins are tidally submerged by the astronomical tide 23 and 20 percent of the time, respectively. Alternatively stated, the inner near-shore area of the Willoughby Spit site is divided by a system of groins into a series of compartments approximately 78 percent of the time and is a series of submerged weirs approximately 22 percent of the time.

In addition to the tidal rise and fall of the water surface, meteorological processes also lead to short term changes in the level of the Bay. Storms affecting the region are associated chiefly either with the passage

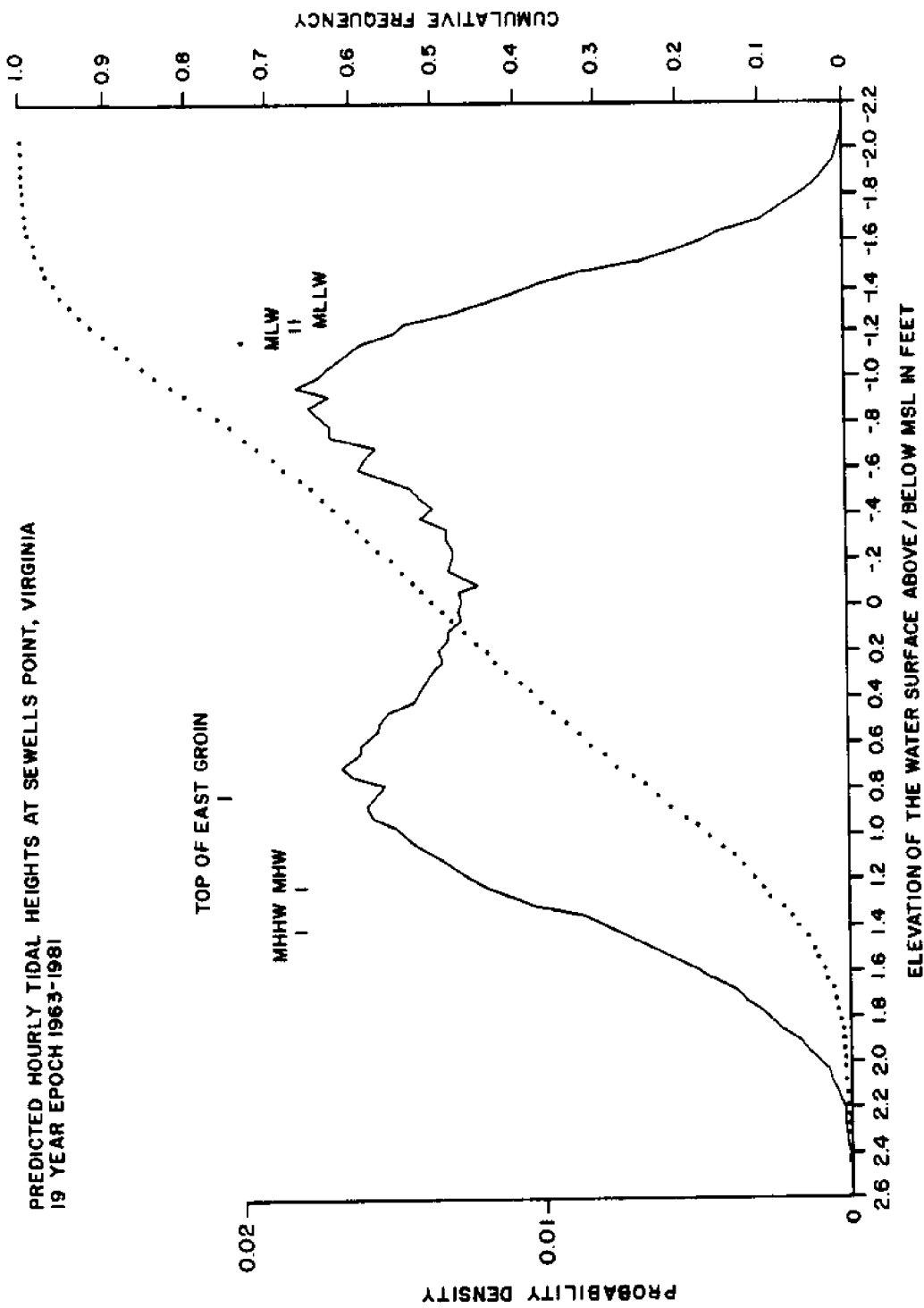


Fig. 4. Predicted hourly heights of the astronomical tide at Sewells Point, Virginia for the 19-year period 1963-1981 (from Harris, 1981). Solid curve is the frequency distribution; dotted curve is the cumulative "greater than" distribution. Note the position of the top of the outer horizontal section of the east groin of the test compartment.

of extra-tropical low pressure cells during the fall, winter, and spring, i.e., "northeasters," or with tropical storms or hurricanes. The average duration of a northeaster is approximately 2 to 3 days; however, they may persist for as long as a week or 10 days (USACE, 1983, p. 9). In the intense northeaster of April 26-27, 1978 that severely affected the southern shoreline of Chesapeake Bay, water level rose to more than 4.8 ft. (1.46 m) above MSL (USACE, 1983, p. 26).

At Little Creek, 6.9 statute miles to the east of the study site, the highest water level readings each month on a tidal gage for the period 1954 to 1959 (Table 1) indicate that of 68 monthly maximum readings 49, or 72 percent, are greater than 2.4 ft. (above MSL) which is the maximum predicted water level for the astronomical tide in the 19-year, or metonic, tidal cycle. During the period of 68 months one reading (in April) indicates a rise in water level of 5.7 ft. (1.74 m) above MSL. Superelevations of this magnitude are often associated with the unwanted loss of sand from the beaches of the area.

The term storm surge denotes the algebraic difference between the observed tide and the normal astronomical tide (Pore, Richardson, and Perrotti, 1974, p. 2). Factors that determine the height of the storm surge are: 1) wind stress on the surface of the water; 2) atmospheric pressure effect, i.e., the "inverse barometer" effect; 3) mass transport onshore of water by waves and swell; 4) effects of coastline configuration, bathymetry, and frictional resistance of the bed. Of these, the wind stress factor is of prime importance. The evaluation of this factor must include consideration of the wind intensity, duration, and direction. The magnitude of storm surge at the Willoughby Spit study site is not as much a function of the local wind speed, duration, and direction as it is of the meso-scale

Table 1. Highest recorded gage readings at Willoughby (Little Creek) Referred to MSL.

Year	Gage Reading in Feet above Mean Sea Level											
	Jan	Feb	Mar	Apr	May	Jun	Jul	Aug	Sep	Oct	Nov	Dec
1954	3.4	2.4	1.8	2.6	3.0	2.7	2.4	3.3	3.0	2.9	2.3	3.8
1955	2.9	1.8	2.0	3.0	1.9	3.1	1.9	3.5	3.3	3.0	2.6	2.1
1956	3.7	2.3	2.4	5.7	2.3	2.7	2.1	2.9	4.6	3.5	3.2	2.2
1957	2.4	2.9	2.8	2.1	2.0	2.8	2.2	3.2	2.7	5.2	3.1	2.6
1958	2.9	2.9	3.1	3.1	2.7	2.6	2.1	2.7	3.3	4.3	2.6	2.9
1959	2.2	1.9	3.3	3.2	1.9	2.4	1.9	2.4	-	-	-	-

From USACE (1983, p. 36). Gage reading corrected to NGVD by subtracting 6.5 ft.; and then corrected to MSL by subtracting 0.1 ft.

wind field in relation to the entire body of the Chesapeake Bay (Fig. 5 and Table 2).

The historical incidence of storm-related high water levels at Willoughby Spit has been determined by the Corps of Engineers by listing the annual maximum elevation of the water surface for each year since 1928 for a gage at Fort Norfolk, 8 statute miles to the south of the study site (USACE, 1983). The values, which reflect both tide and storm surge, were corrected by an elevation correlation procedure to reflect more closely water levels at Willoughby Spit relative to mean sea level. The maximum value at Fort Norfolk was 8.0 ft. (MSL) as recorded on August 23, 1933; the corresponding value for Willoughby Spit is 7.8 ft. (MSL). Exceedence (cumulative) frequencies expressed as percentages were calculated at intervals of 0.5 ft. down to a level of +4.0 ft. (MSL) and extrapolated for high levels above 8 ft.

If, for example, in a period of 50 years for each of which the annual maximum level has been tabulated, there are 41 values >4.0 ft. (MSL), and if these 41 values were assumed to occur at equal intervals of time, then an elevation >4.0 ft. (MSL) would be expected to occur every 1.22 years. Results of this kind for the different levels appear in Table 3.

To illustrate the use and relative reliability of Table 3, consider the observed data of Table 1 which spans a period of 5.75 years at Willoughby Spit (Little Creek). From Table 3, it would be predicted that:

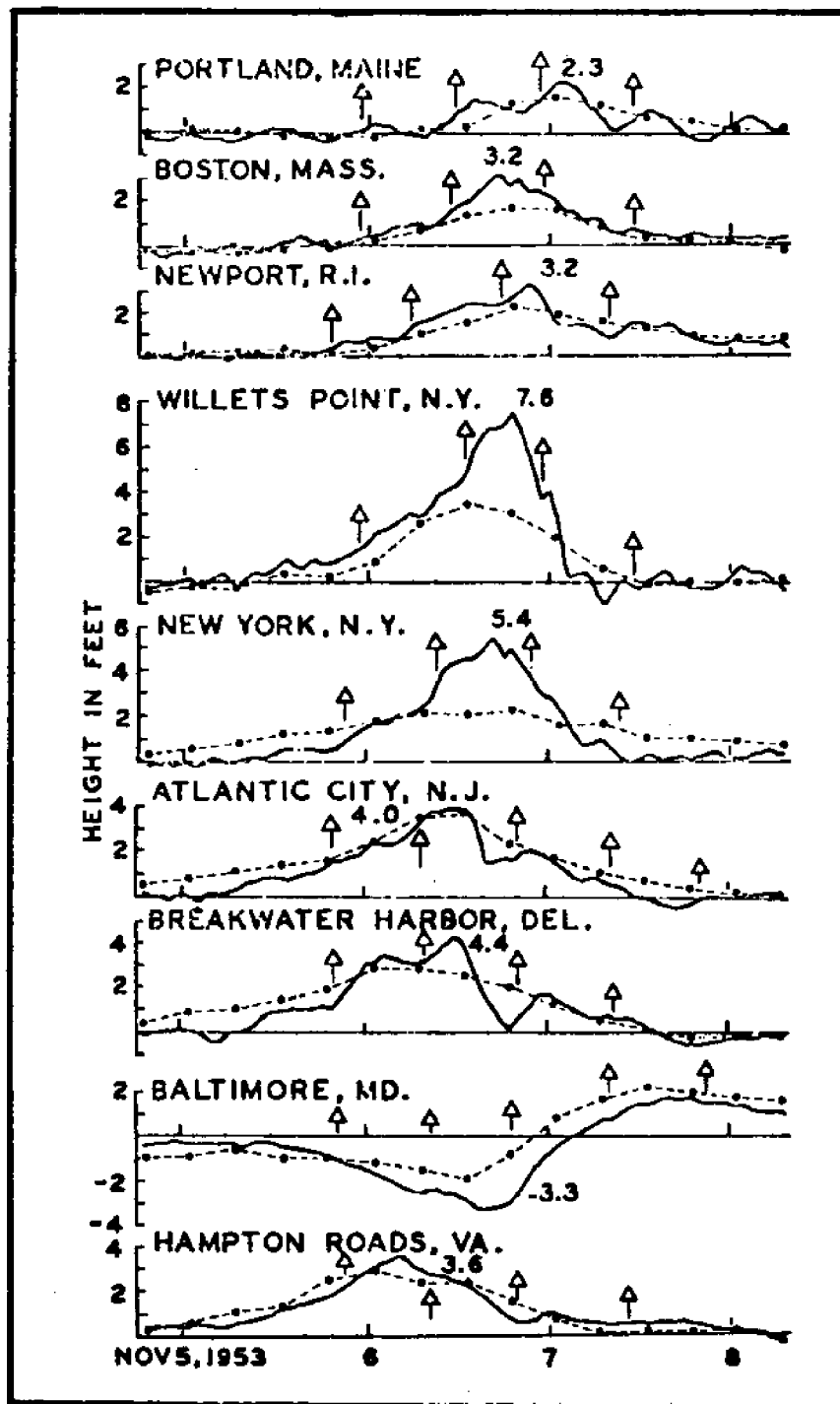


Fig. 5. Observed storm surge and computed storm surge for the November 5-8, 1953 storm. Solid curves are observed storm surges. Dashed lines join calculated values of surge. Arrows indicate times of astronomical high tides. The date of each day is placed at the 1200 EST position. Maximum value of observed surge is placed near the peak of each curve. (From Pore, et al., 1974).

Table 2. Wind velocities recorded at some coastal locations during the storm of November 5-8, 1953. (From Pore, et al., 1974).

Nov. 1953	Portland Me.	Boston Ma.	Willets Point N.Y.	New York N. Y.	Atlantic City N.J.	Baltimore Md.	Hampton Roads Va.
06/01	N/10 mph	N/24 mph	NNE/22 mph	N/12 mph		NE/22 mph	NE/18 mph
07	N/11	N/18	NE/28	NE/18		NE/23	NNE/24
13	NNE/13	NE/29	NE/36	NE/35		NNE/22	NNE/26
19	NNE/18	NE/39	NE/42	NE/30		NNE/23	N/24
07/01	NNE/21	NE/53	NE/46	NE/27		NNW/30	NNW/20
07	NNE/30	ENE/49	E/23	SW/26		WNW/20	NW/18
13	ENE/32	SE/11	SSW/18	SW/17		W/25	WNW/14
19	SSE/10	SSW/12	SSW/16	S/16		SW/16	W/6
Nov. 06	NE/25 mph	NE/49 mph		Fastest mile NE/35 mph	NE/69 mph	NW/32 mph	NE/30 mph
Nov. 07	E/41	NE/67		SW/36	NE/68	NW/36	NW/24

levels >6.0 ft. (MSL) would occur 0.42 times; whereas, the actual number of occurrences was (0);

levels >5.5 ft. (MSL) would occur 0.69 times; whereas, the actual number of occurrences was (1);

levels >5.0 ft. (MSL) would occur 1.26 times; whereas, the actual number of occurrences was (2);

levels >4.5 ft. (MSL) would occur 2.40 times; whereas, the actual number of occurrences was (3);

levels >4.0 ft. (MSL) would occur 4.70 times; whereas, the actual number of occurrences was (4).

On an interval basis using results derived from Table 3, it would be predicted for the 5.75-year record at Willoughby (Little Creek) that:

levels 6.0 - 5.5 ft. would occur 0.27 times; whereas, the actual number was (1);

levels 5.5 - 5.0 ft. would occur 0.57 times; whereas, the actual number was (1);

levels 5.0 - 4.5 ft. would occur 1.14 times; whereas, the actual number was (1);

levels 4.5 - 4.0 ft. would occur 2.30 times; whereas, the actual number was (1).

The extreme elevation (5.75 ft., MLW) during the 5.75 year period covered by Table 1 is, according to Table 3, a 10-year event.

Table 3. Storm-Elevated Water Levels for Willoughby Spit and their Estimated Recurrence Times

Feet Above Mean Sea Level	Estimated Recurrence Time In Years	Feet Above Mean Sea Level	Estimated Recurrence Time In Years
>9.5	345	>6.5	20.0
>9.0	200	>6.0	13.7
>8.5	117.6	>5.5	8.3
>8.0	71.4	>5.0	4.55
>7.5	47.6	>4.5	2.38
>7.0	29.4	>4.0	1.22

TIDAL CURRENTS

Present knowledge of the speed, duration, and direction of tidal currents near the study site at Willoughby Spit is based chiefly on four different but related sets of measurement data: 1) three 30-hour current meter stations off Willoughby Spit occupied during the fall of 1974, taken by the present author and reported in Fleischer, et al. (1977, pp. 28-49); 2) two current meter stations off the study site occupied in the winter of 1984, taken by the author in connection with the present study; 3) a single deployment made by Dr. Donald R. Johnson of a near-surface current meter of his own design for 9.5 hours at a location immediately off the study site--the processed but uninterpreted data from which deployment were made available to the author by Johnson; and 4) repeated deployments of an electromagnetic current meter at various sites in the groin compartment at Willoughby Spit--deployments from which the speed and direction of the tidal

currents and other were extracted by filtering the raw data so as to remove those parts associated with local wind waves.

Tidal currents in the 10.6-mile wide entrance to Chesapeake Bay are of the reversing type as regards the shape of the M2 constituent tidal ellipse and of the progressive wave type with respect to timing, i.e., maximum currents on ebb and flood occur at the times approximately of low water and high water, respectively (Ludwick, 1974). In contrast, the tidal currents in Lower Chesapeake Bay further inland at the narrows between Fort Wool and Old Point Comfort are of the standing wave type, i.e., maximum currents, both ebb and flood, occur when the water is approximately at mid-tide level. At the times approximately of low water and high water, the tidal current is slack or nil or of near-minimum speed.

In most estuarine areas, at a fixed location near the bed, if attention is directed to the speeds of ebb and flood currents at strength and to the durations of ebb and flood pulses, it is found that both measures are unequal in the ebb and flood pulses. In the southernmost part of Lower Chesapeake Bay there is a geomorphic feature, here named Beach Channel, the axis of which trends approximately parallel to the southern shoreline of Chesapeake Bay from Cape Henry westward past Lynnhaven Inlet, Little Creek Entrance, and on to Willoughby Spit, at a distance of 0.5 to 1.5 statute miles north of the shoreline. The water depth in this channel is approximately 28 ft. (MLW) along much of its length, compared to lesser depths both closer to shore and farther offshore. The channel is the southernmost of four master channels that lead inwards at the sea floor into Lower Chesapeake Bay from its entrance. In bed channels of this kind there is nearly always a marked asymmetry in the strength and duration of ebb and flood tidal currents. The study area at Willoughby Spit is situated onshore

of the westward terminus of Beach Channel where it grows shallower and hooks northward into the curved side of Willoughby Bank, a ramp-margin shoal associated with the narrows that connect Hampton Roads and Chesapeake Bay.

Measurements cited in Fleischer et al. (1977) show that at three stations between Willoughby Spit and Willoughby Bank and off East Ocean View (Fig. 6), flood currents near the bed are stronger at strength and longer in duration than ebb currents (Figs. 7-9). In Table 4, it is seen that among the three stations the degree of dominance of flood-directed currents over ebb-directed currents increases with distance to the west from Location 3 which is off East Ocean View (Fig. 6). Maximum near-bed velocity and also the duration of sediment transport increase from Location 3 to Location 1.

In the second set of data referred to in a previous paragraph, two additional tidal current stations were occupied: Locations 4 and 5 (Fig. 10). When these are combined with Location 1 above, a crude shore-normal transect is defined off the study site at Willoughby Spit. With reference to Locations 1, 4, and 5 only it is seen in Table 5 that:

- 1) the speed of the average maximum flood current near the bed, corrected to mean range, is approximately $1.14 \text{ ft. sec}^{-1}$ (34.7 cm sec^{-1}) compared to $0.80 \text{ ft. sec}^{-1}$ (24.5 cm sec^{-1}) on ebb;

- 2) duration of flood greatly exceeds the duration of ebb and this exceedance increases with nearness to the beach and ranges from 7.1 hours to 8.1 hours compared to ebb duration which ranges from 5.2 to 4.4 hours;

- 3) for the three stations, the direction of the flood current at strength near the bed ranges from 278 to 295 degrees, i.e., essentially parallel to the local contours of water depth; whereas, the ebb direction is not at all the reverse of the flood direction but rather is turned counter-clockwise (from the flood back-azimuth) by 9 to 45 degrees so as to flow on

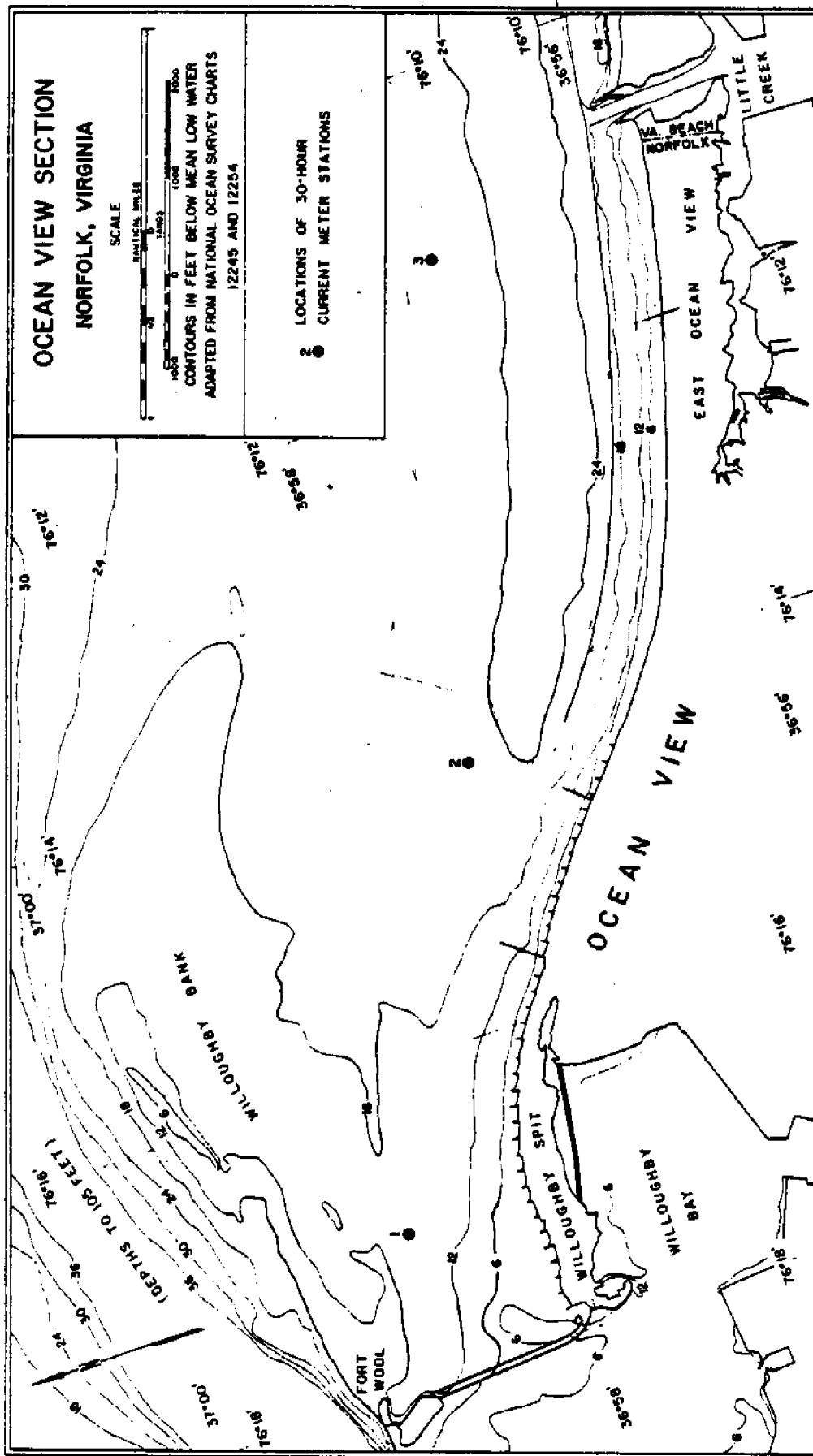


Fig. 6. Index map to tidal current stations off Ocean View and Willoughby Spit. (From Fleischer, et al., 1977).

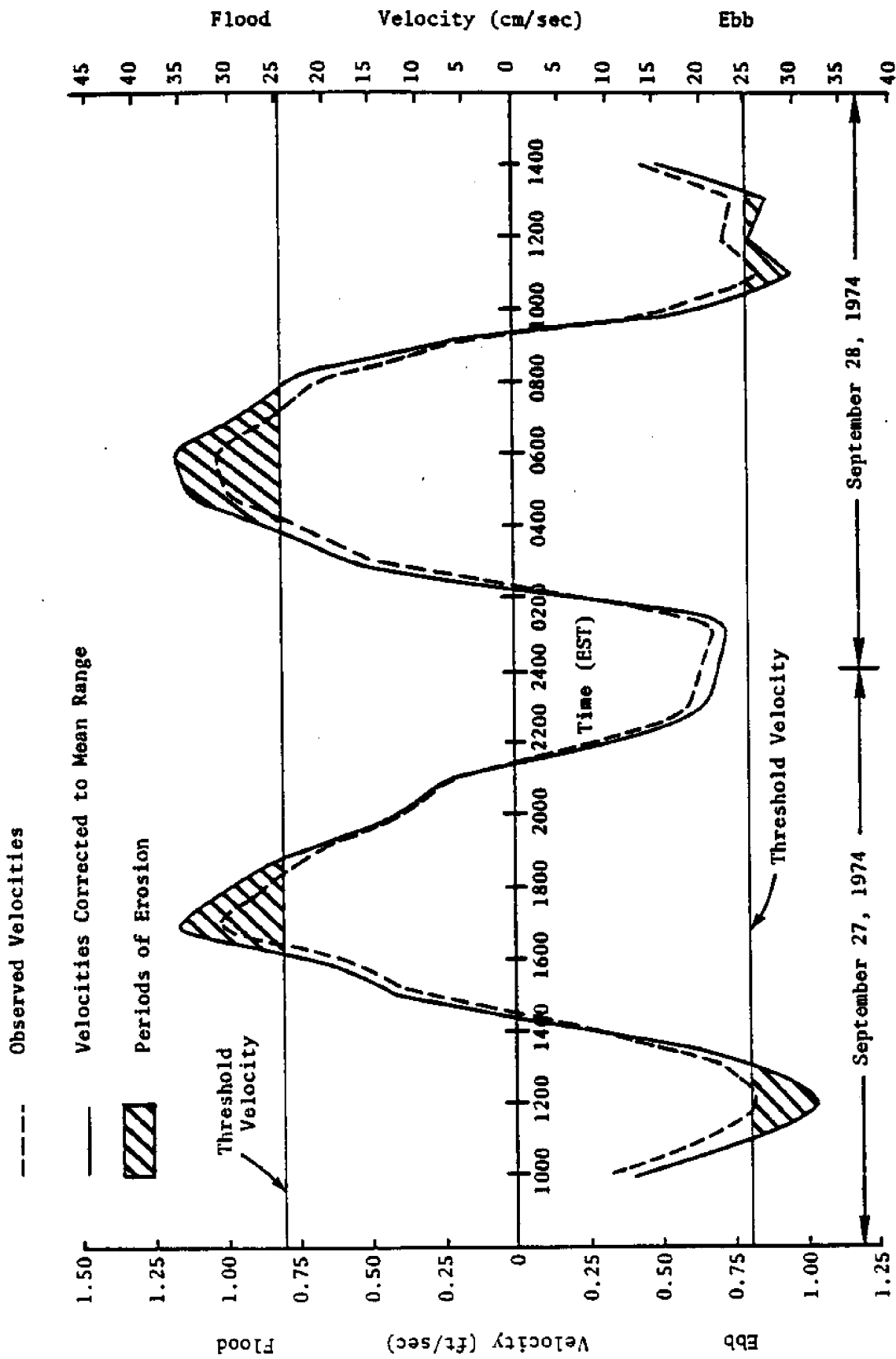


Fig. 7. The threshold for initiation of sediment motion at the bed compared to observed tidal current velocity averaged over two levels above the bed (1.50 and 2.50 ft) and plotted versus time. Ocean View Tidal Current Station 1; water depth 21.5 ft. (MLW). (From Fleischer, et al., 1977).

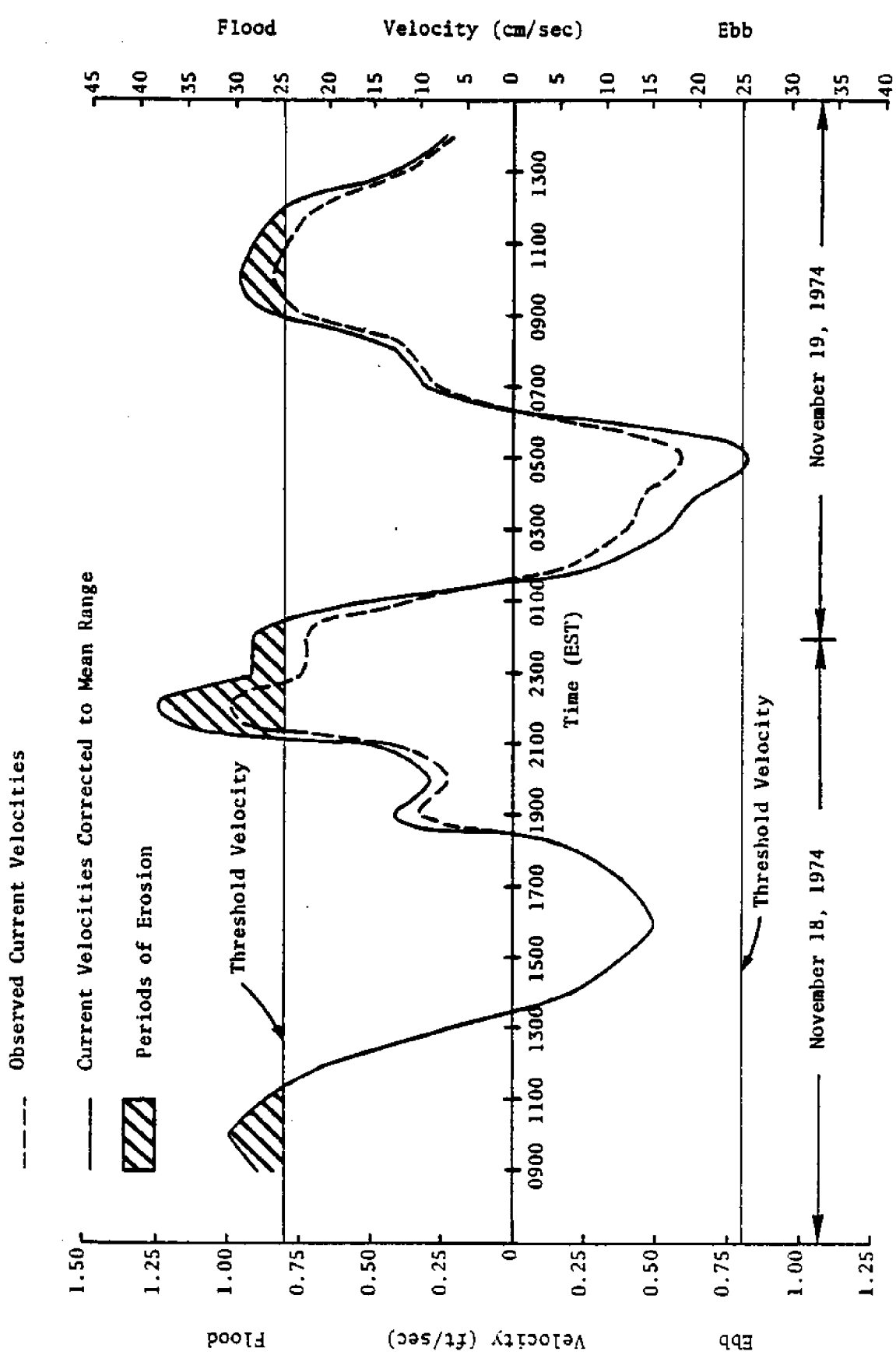


Fig. 8. The threshold for initiation of sediment motion at the bed compared to observed tidal current velocity averaged over two levels above the bed (1.50 and 2.75 ft.) and plotted versus time. Ocean View Tidal Current Station 2; water depth 24.75 ft. (MLW). (From Fleischer, et al., 1977).

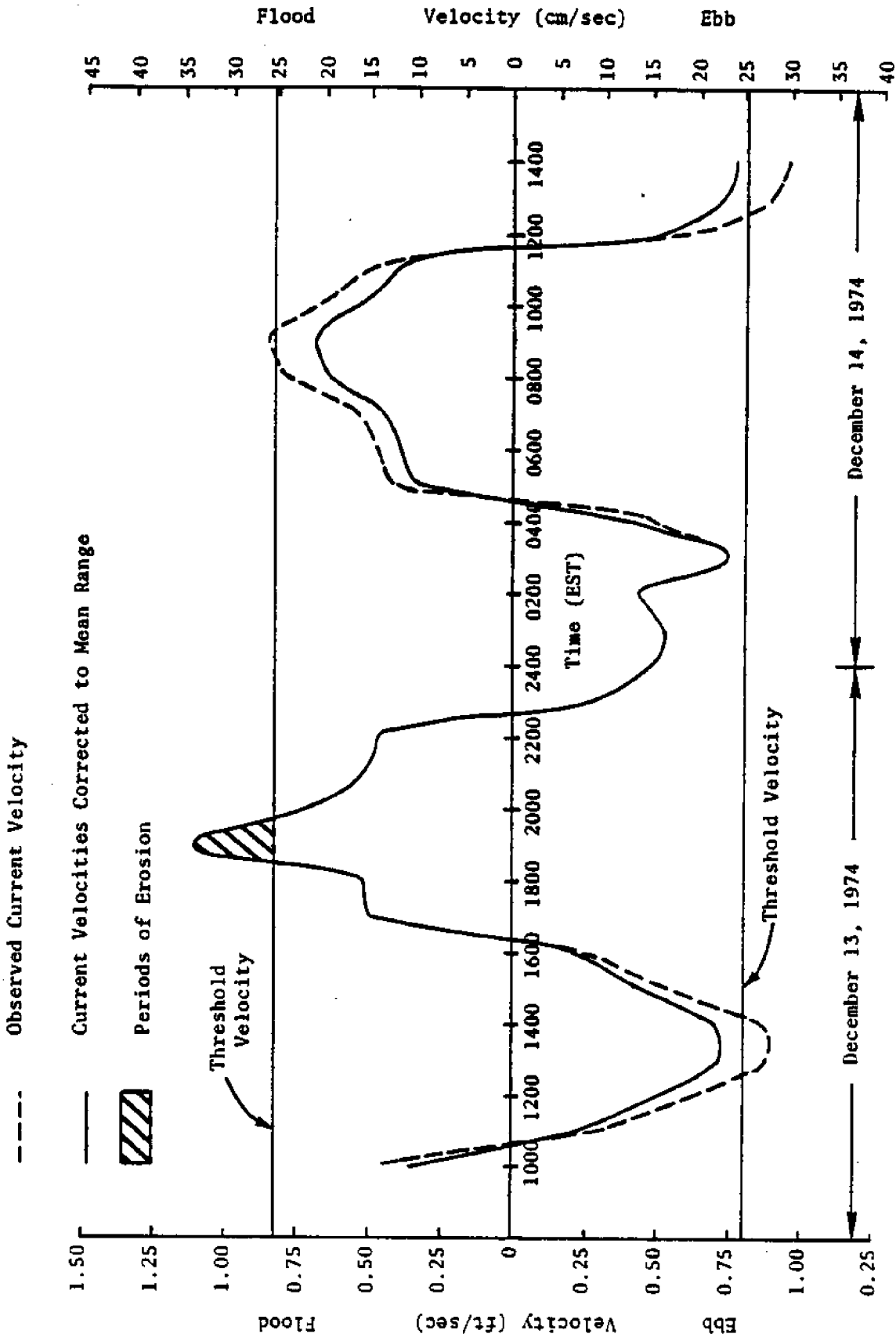


Fig. 9. The threshold for initiation of sediment motion at the bed compared to observed tidal current velocity averaged over two levels above the bed (1.50 and 3.00 ft) and plotted versus time. Ocean View Tidal Current Station 3; water depth 20.0 ft. (MLW). (From Fleischer et al., 1977).

Table 4. Summary of Tidal Current Observations (Corrected to Mean Range) and Sediment Transport.
From Fleischer et al. (1977).

	Station	Average Duration of Cycle (hrs)	Average Maximum Near-Bottom Velocity per Cycle (ft/sec)	Average Duration of Sediment Transport per Cycle (hrs)	Average Direction of Sediment Transport (Degrees True)
Flood Cycle	1	7.1	1.16	3.3	295
	2	7.3	1.06	3.1	320
	3	6.6	0.90	0.6	282
Ebb Cycle	1	5.2	0.91	1.6	106
	2	4.9	0.66	0.2	128
	3	5.9	0.74	0	---

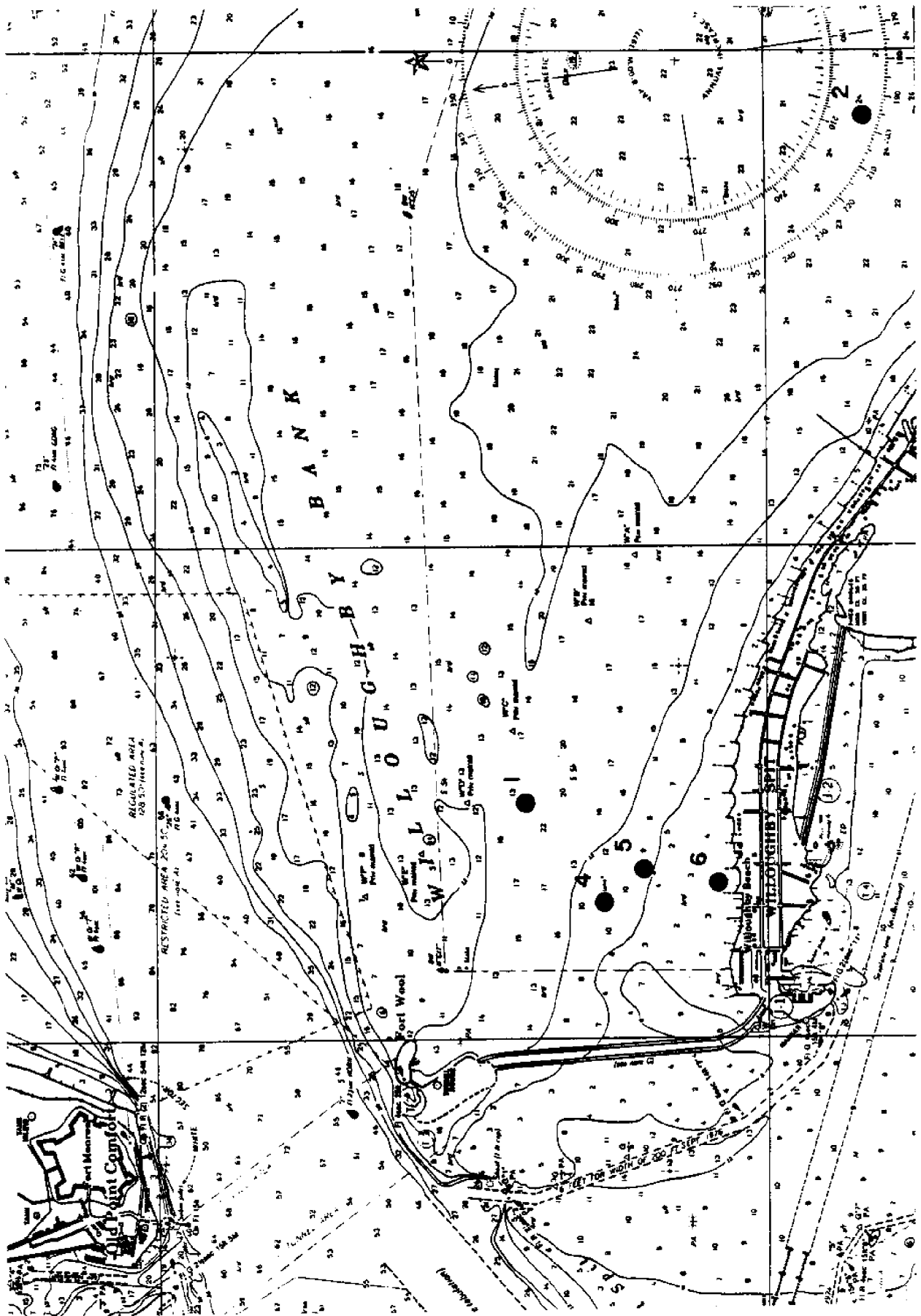


Fig. 10. Index map of tidal current stations off the study site at Willoughby Spit. See Table 5 for data.

Table 5. Near-bed Tidal Currents (Corrected to Mean Range) on a Shore-normal Transect off Willoughby Spit. See Figure 10 in station locations 1, 4, 5, and 6. See text for position of station number 7.

	Station Number	Distance From Shore, ft.	Water Depth (MLW), ft.	Avg. Max. Velocity, ft. sec ⁻¹	Avg. Duration hours	Avg. Direction degrees, True
FLOOD CYCLE	1	4050	21.5	1.16	7.1	295
	4	2550	14.0	1.12	7.5	278
	5	1800	8.5	1.15	8.1	287
	6	320	3.5	—	—	264
	7	160	2.8	0.87	7.0	266
	1	4050	21.5	0.91	5.2	106
	4	2550	14.0	0.82	4.8	085
EBB CYCLE	5	1800	8.5	0.68	4.2	075
	6	320	3.5	—	—	087
	7	160	2.8	0.60	5.4	082

ebb in a direction sub-parallel to the direction of Thimble Shoal Channel, the master ebb channel of the area, at its closest point off Fort Wool.

A description of the timing of the tidal currents in relation to the rise and fall of the surface of the water can be extracted from the measurements taken at the three stations. In seven instances available for analysis, it is found that, at the bottom, the cessation of ebb-directed flow occurs near the time of low water.

For a more exact evaluation of the actual correspondence in time between the time of low water and the cessation of ebb, the observed time of low water is used when it is well-defined by data or if this event cannot be assessed with sufficient preciseness because of its flatness, the predicted time of low water is used. The time of cessation of ebb flow is taken as the zero-crossing of the curve of observed current-speed-versus-time when linearly interpolated between segments of established flood and ebb flows. On average, the time of zero current at the end of ebb occurs 13 minutes before the time of low water.

A half lunar day is 12.4 hours. This must necessarily on average be equal to the elapsed time from the end of an initial ebb flow to the end of the next ebb pulse. It is this 12.4 hours which is now partitioned into the duration of flood and the duration of ebb. From Table 5, the average duration of flood, based on the three outermost stations, is taken to be 7.7 hours; the average duration of ebb is 4.7 hours. A significant consequence of the foregoing is that the end of a flood episode does not occur at the time of high water but instead is reached, on average, 1.5 hours later than the time of high water.

The shapes of the pulses of flood and ebb currents, as seen on a plot of current-speed-versus time, are neither notably symmetrical nor smooth nor

regular; although, an average taken over several such pulses exhibits more regularity. Nevertheless when averaged, the times of maximum flood and ebb currents do not occur at mid-tide, as would be the case in a standing wave, but instead are delayed by 45-60 minutes from the time of mid-tide but with considerable variation. The foregoing relations are shown in Fig. 11 along with the times of covering and uncovering of the groins. Also shown is a threshold for sediment movement at 0.6 ft. sec^{-1} (18 cm sec^{-1}) which is applicable to medium to fine grained sand when waves and currents act together.

It is evident from Fig. 11 that, considering only the astronomical tide, sediment input to and output from the groin compartment by flows which overtop the groins can occur only on flood. This process, when it occurs at all, takes place in shallow water near the shore where waves are nearly at breaking, thereby releasing enough kinetic energy to mobilize and suspend bed sediment to elevations high enough in the water column to allow the washing of the sediment over the shallowly submerged groin and into the adjacent compartment.

The third set of data, Location 6 (Fig. 6) in Table 5, is that taken using a near-surface current meter at a point approximately 40 meters seaward (north) of the line connecting the seaward (north) end of the groins, and approximately one-half the way between the two groin ends. The tidal currents here are found to be reversing to within 3 degrees, are nearly shore-parallel (slightly onshore in flood; slightly offshore on ebb), and are flood dominant.

The fourth set of data (Location 7 in Table 5) was taken using a tripod-mounted electromagnetic current meter at a point approximately 3 m seaward (north) of the line connecting the ends of the two groins and one-

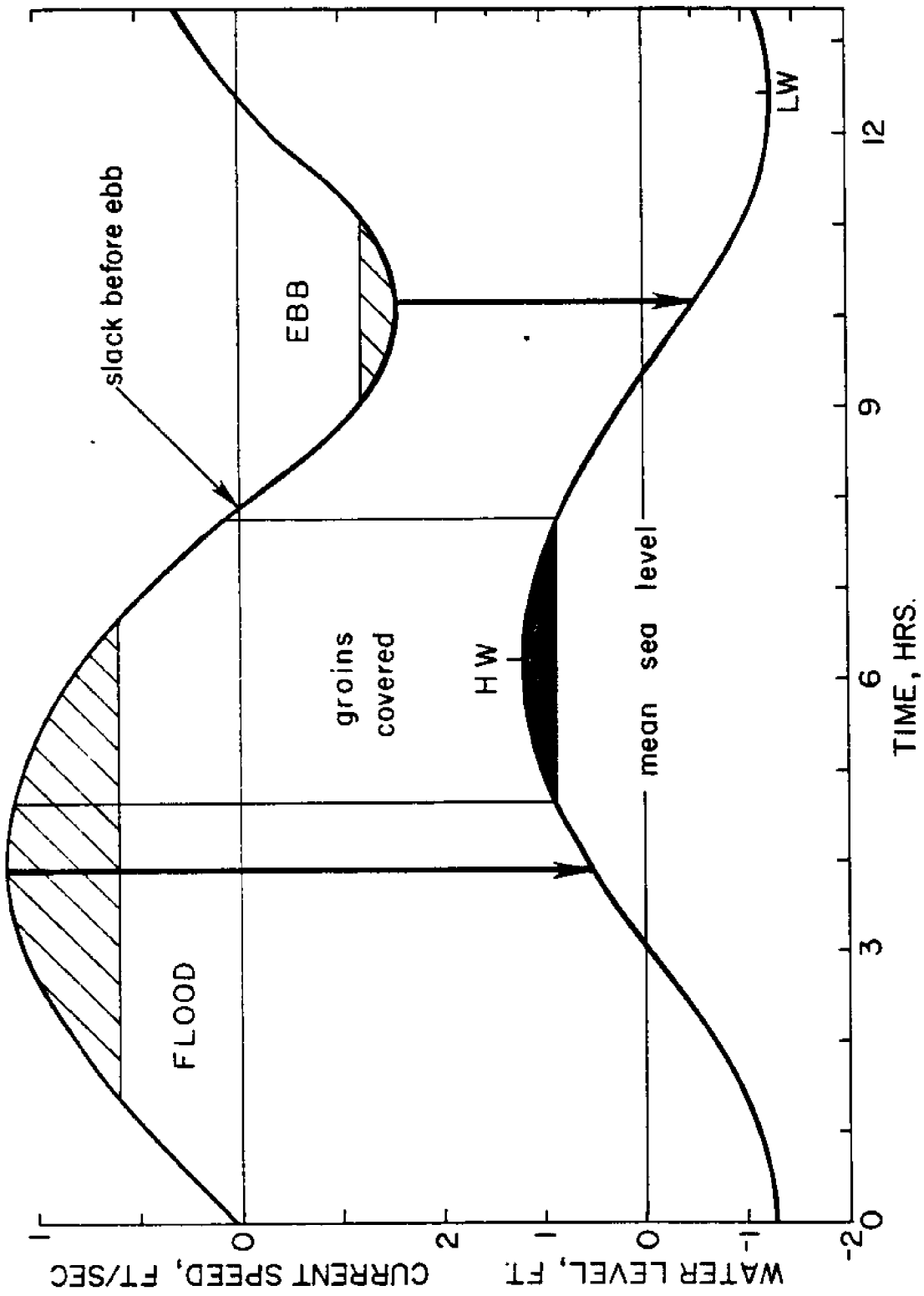


Fig. 11. Relative timing between tidal currents and elevation of the water surface at Willoughby Spit. When the groins are submerged, the tidal current is in flood. Note the symmetry of the tidal currents and the great asymmetry in effective currents (ruled areas).

half the way between them. As shown in Table 5, current speeds, near the bottom, of the 17-sec low-pass currents at strength, corrected to mean range, are 0.87 ft. sec⁻¹ on flood and 0.60 ft. sec⁻¹ on ebb. Duration of flood is 7 hours; duration of ebb is 5.4 hours. Direction of flood is 266 degrees (True); direction of ebb is 082 degrees (True). These directions are within 4 degrees of being reversed.

In summary, tidal currents near the bed at the seaward limit of the groin compartment are approximately shore-parallel, nearly reversing, flood dominant, and at flood strength reach 0.9 ft. sec⁻¹ (27.4 cm sec⁻¹) and at ebb strength reach 0.6 ft. sec⁻¹ (18.3 cm sec⁻¹) both of which values equal or exceed a reasonable threshold for the movement of the bed sediment when waves and currents act together. The near-bottom flood-directed tidal currents are far more effective in power and duration in moving bed sediment than are the ebb currents of the area.

WAVES

For Chesapeake Bay as a whole there is no published long term climatology of waves based on actual wave gage records. For the southern part of the Bay, as far as known to the author, there is only a single, very short-term record taken with a wave gage on South Thimble Island, the southernmost island of the Chesapeake Bay-Bridge Tunnel system which spans the Bay entrance. The site of this gage was eight nautical miles to the east of the Willoughby Spit study site and as a result of being located in the entrance area of the Bay is somewhat differently exposed than the Willoughby Spit site. Thus, except for the few measurements of the present study, the characteristics of the waves that impinge on the Bay beaches of Willoughby Spit must be assessed visually or must be deduced using theoretical and empirical

relationships from available information on wind speed, directional fetch, and water depth.

Some computed estimates of wave height and period obtained by applying the above methods to the site of the present study are contained in a report of the U.S. Army Corps of Engineers (1984). The results, reproduced below, are for north winds, and effective fetch of 22.5 nautical miles, a central fetch radial oriented at 020 degrees clockwise from true north originating at the study site at Willoughby Spit, and for a representative water depth along the radial of 34 feet MLW.

Table 6. Computed Wave Characteristics for the Willoughby Site.
(From USACE, 1984).

Wind Speed (knots)	Significant Wave Height (feet)	Wave Period (seconds)
11	1.7 (1.1)*	2.8
25	4.2 (2.8)	4.3
35	5.7 (3.8)	5.0

*The figures in parentheses are wave height estimates after correction for frictional effects along the fetch.

The question arises as to the presence of waves of other origins at the site and particularly whether wind waves generated in the Atlantic Ocean reach the test site on the Chesapeake Bay shore of Willoughby Spit with significant energy. Such waves would move along propagation paths passing through the 10-mile wide entrance to Chesapeake Bay, would experience refraction over shoals and channels within the Bay, and would suffer an amplitude loss owing to frictional affects along the propagation path. In the aforementioned report (p. 37) it is estimated that the amplitude of the

ocean waves will be reduced by one-half in traversing the 15 nautical miles from the Bay entrance to the Willoughby site.

Waves generated entirely within the Bay along the principal fetch would approach the curving shoreline of Willoughby Spit and the adjacent shoreline to the east at angles that differ with shoreline location. In the report (1984) it is noted that beginning at a point 0.6 statute miles to the east of the present study site, for at least a shoreline distance of 2 miles farther to the east, the breaker angle α would open to the east. However, there was at least the appearance that waves from the Atlantic would impinge on the same shore with a westward opening α and produce an overbalancing or net westward longshore current as required by the sense of the shoreline offsets at the groins in that reach.

Currents, primarily generated by waves, were measured at 15 sites in the test compartment with an oriented electro-magnetic meter positioned 30 cm above the bed ($y = 30$). Two orthogonal components of the instantaneous velocity vector are obtained in a coordinate system whose compass orientation is known to within plus or minus 3 degrees. An experiment typically consisted of moving the meter among a group of locations cyclically for 12 hr. Single sites were occupied for 12 min. with readings of the components taken at intervals of 0.5 sec. Plots were made in which successive vectors were drawn from the center of a coordinate system and marked with a cross at the head (e.g., Fig. 17). When only waves occurred, and these were directionally restricted, the crosses formed an ellipse whose long axis was in the direction of propagation.

In the present study, 48 separate records of wave-generated currents were measured in the selected groin compartment. Observations were taken in the months of March, April, May, July, September, and November on 6

different days. Four patterns of sampling with the E-M meter were used: 1) single station, single record; 2) three to seven stations in a random pattern in the compartment with one-time sequential occupancy or with some repeat occupancy on the same day; 3) three stations on a shore normal profile with seven cycles of re-occupancy over an 11-hour period; 4) single station with 13 records taken over a 12-hour period. The mean of the measured water depths over all stations and occupancies is 105 cm; maximum observed water depth when a record was taken was 200 cm.

The data obtained are presented below under three headings: 1) wave periodicity as revealed by spectral analysis; 2) current velocities of the motions and the associated potential for sediment movement; and 3) directional aspects of the motions as derived from directional spectra and wave refraction studies.

Wave Periodicity

For a given data set, an angular transformation was made initially such that N-S and E-W components of the instantaneous velocity were obtained. By coincidence, the N-S component is within two degrees of parallelism with the alignment of the groins of the study compartment. Thus the two derived component directions are referred to below as shore-normal (or cross-shore) and shore-parallel (or alongshore) components. A spectral analysis was made following a FFT method (Bloomfield, 1976) applied to record segments each of which is 128 data points in length. A final spectrum was obtained from 11-36 such segments (typically 12), by averaging the spectral estimates at each Fourier frequency.

The observed spectral peaks, primary and other, in the shore-normal spectra are classified into 6 bands:

Table 7. Characteristics of the spectra of wave-generated currents at the Willoughby Spit test compartment.

Period Band (sec)	Occurrences*	Occurrences as Primary Peak*	Modal Period(s) (sec)
< 2	3	0	—
2 to 5	41	25	3.5-4.0
5 to 12	25	12	8.0-8.5
12 to 16	19	5	12.5-13; 15-15.5
32.1 to 32.7	4	1	32.1-32.7
52.9 to 56.2	8	2	52.9-56.2

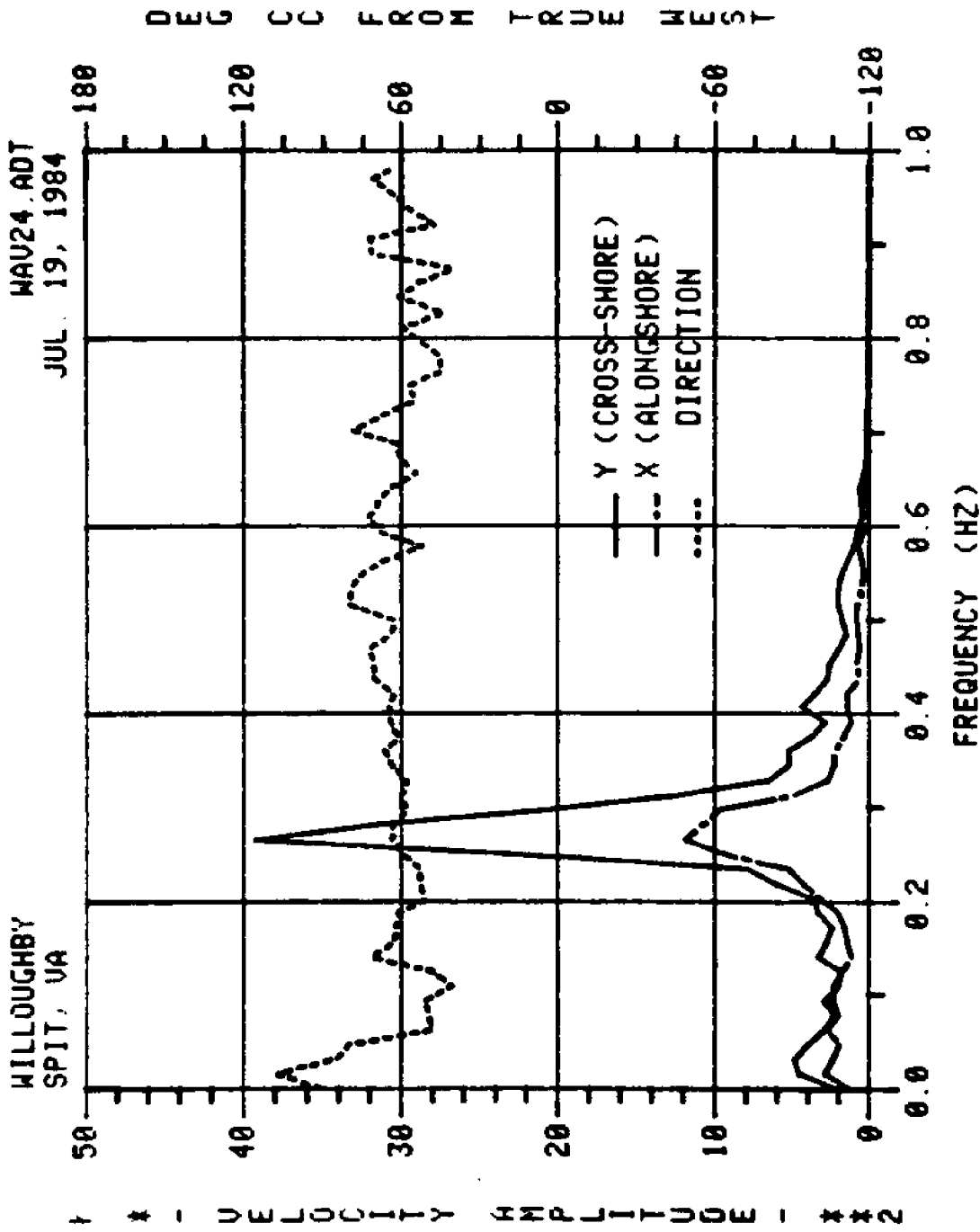
*Out of 48 records

At the Willoughby Spit test site, waves in the < 2 sec range correspond to local wind chop typically developed for a period of several hours following a temporary increase in wind speed as in an afternoon seabreeze.

Waves in the 2 to 5 sec. band are local wind waves, developed over a Bay fetch, at persistent wind speeds in the range from 10 to 35 knots. (See Table 6). A simple wind wave spectrum typical of this class is shown in Fig. 12. The observation site for this record is 9 m seaward the mid-point of a line connecting the ends of the groins in the test compartment. Shore-normal and shore-parallel spectra are presented in the figure. An estimate of the direction of propagation of each spectral component was obtained using the method of Nagata (1964a) with some analytical steps coming from the work of Longuet-Higgins (1957), Cartwright (1962), and Nagata (1964b).

Waves in the 5 to 12 sec. band are interpreted according to information presented in the paragraph below as wind waves propagating in from the Atlantic Ocean through the entrance to Chesapeake Bay.

It is well established in published data that the period of wind-generated waves in coastal Atlantic waters off the central United States is in the range from 4 to 17 sec. For example, in a summary of wave climate at 10



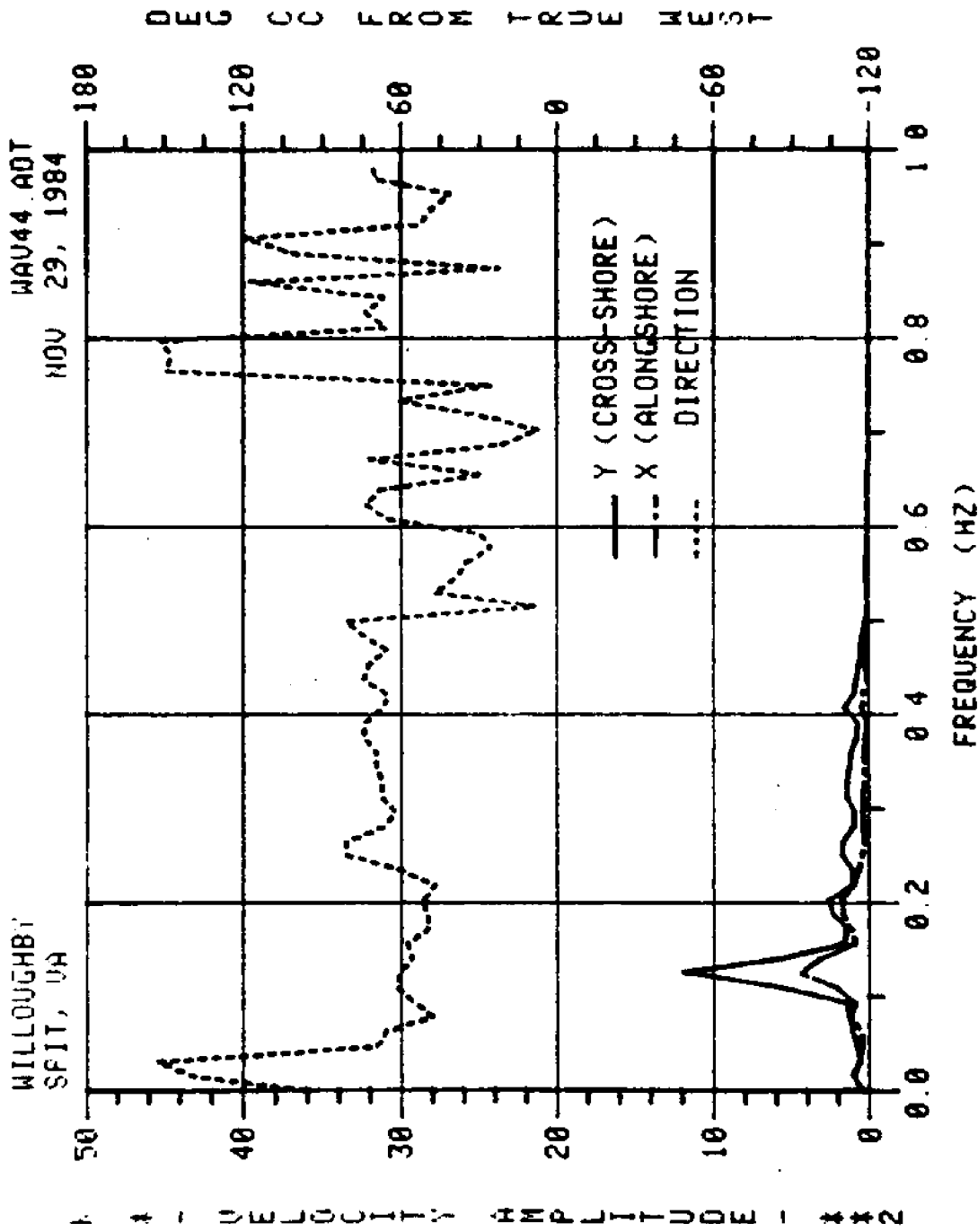
K = CONSTANT **CC=COUNTERCLOCKWISE**

Fig. 12. A simple local wind wave spectrum derived from E-M current meter measurements. Peak period 3.8 sec.; propagation direction 208 deg. A subordinate peak occurs at 32.1 sec.; direction 182 deg. Water depth 95 cm.

selected locations along the Atlantic seaboard from Buzzards Bay, Massachusetts to Lake Worth, Florida, Thompson (1977, p. 54) shows that annual mean significant period of the waves from actual records ranges from 6 to 9 sec. Buoy data off Ocean City, Maryland, in 20 m of water, for 2717 records taken in a 12-month period in 1982-1983 show that 85 percent of the peak wave periods are greater than 5 sec. and 92.5 percent are greater than 4.06 sec. At Duck, North Carolina, for the five-year period, 1980 to 1984, at 3 stations ranging in water depth from 8 to 18 m, peak wave period averaged 8.8 sec. with a standard deviation of 2.8 sec.

An example is shown in Fig. 13 of low waves of 8-second period observed in the compartment when the local wind had been too weak for too long a time to generate significant local wind waves in the Bay. The observed waves are believed to have propagated to the Willoughby Spit test site from the Atlantic Ocean through the entrance to the Bay, 15 nautical miles to the east.

Those occasionally occurring spectral peaks in the 12 to 16 sec. band are interpreted as surf beat originating possibly from the interaction of Bay-generated wind waves and Atlantic wind waves. For example, two sine waves of equal amplitude, propagating in the same direction, whose periods are 4 and 6 sec., respectively, when summed form a beat wave characterized by a rising and falling amplitude. The period of the envelope function of the interaction is 24 sec., but the time difference between the arrival of packets of high waves is 12 sec. and the piling-up and relaxation from the beach face of the associated water would generate an oscillatory current motion with a periodicity of 12 sec. Alternatively, two wave trains of 3.75 and 5 sec. period on interacting would produce packets of higher waves at time intervals of 15 sec.



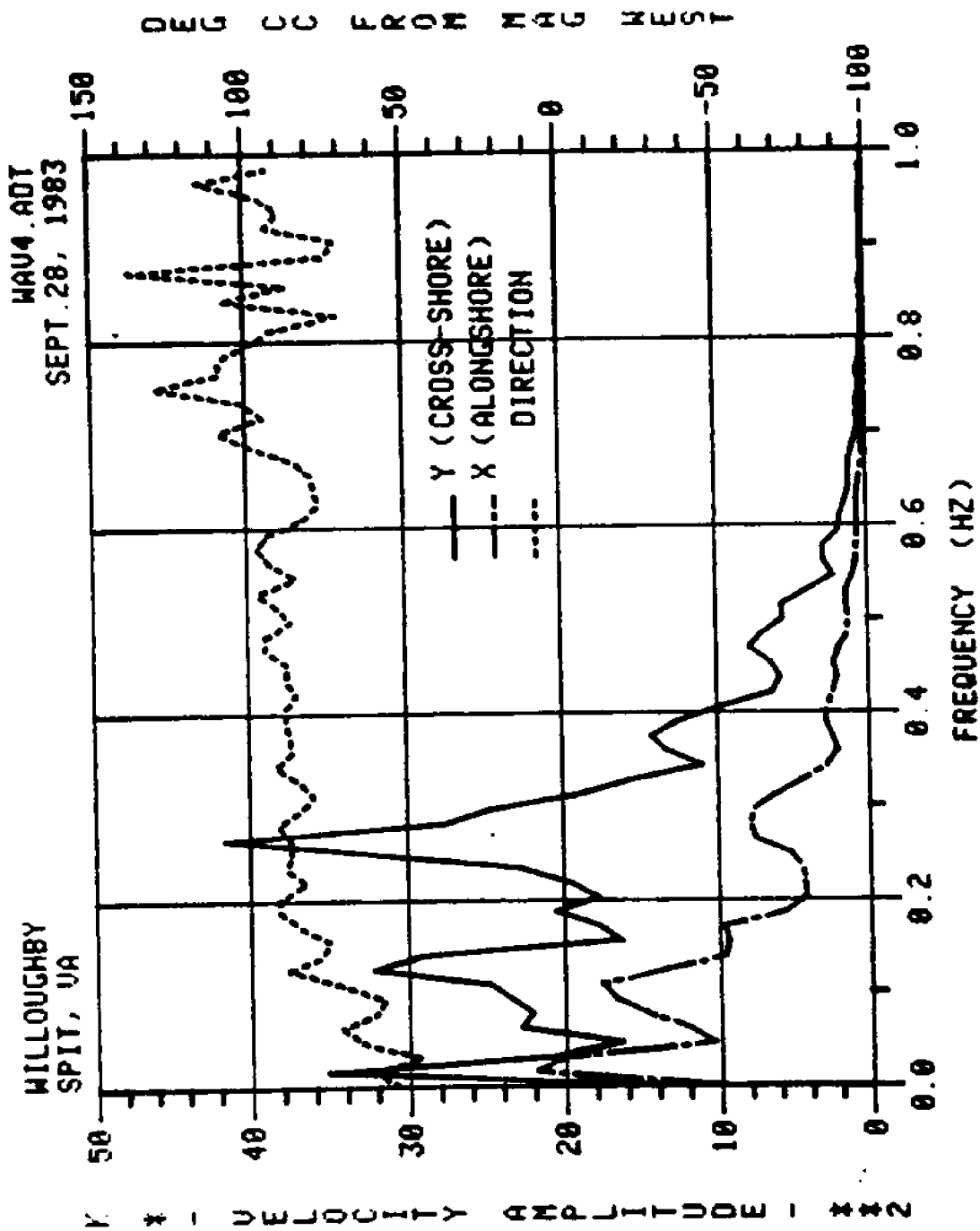
K = CONSTANT **CC=COUNTERCLOCKWISE**

Fig. 13. Wind waves from the Atlantic. Peak wave period 8 sec.; direction 210 deg. Water depth 110 cm. Local wind speed 4-7 knots from the west. Estimated wave height 8 to 18 cm.

Spectral peaks in the band from 32.1 to 32.7 sec. may be standing waves in mono-nodal oscillation between groins (i.e., wavelength of the wave is twice the spacing between groins). Using the Ursell (1952) formulation with the offshore modal number $\underline{n} = 1$, a beach slope of 3.6 degrees, and a wavelength of 2×497 or 994 feet, an edge wave period of 32.2 sec. is obtained. Some supportive observational evidence is presented below regarding the direction of the motions at this period. A more easily excited edge wave of offshore modal number $\underline{n} = 0$, and other parameters as before, has a computed period of 55.6 sec.

The relative heights of the spectral peaks discussed above when averaged over occurrences among the 48 measured spectra are of interest in that the results permit at least a generalized comparison of the relative velocity amplitudes of the motions at the different frequencies. In the spectra, distance along the y-axis is proportional to the square of the velocity amplitude. In the discussion that follows, square roots of measured peak heights have been taken so that the comparisons made are between velocity amplitudes. If the mean spectral peak height of Bay-generated wind waves in the period band from 2 to 5 sec. is assigned the arbitrary magnitude of 100 (based on 55 values), then mean peak height in the band from 5.29 to 56.2 sec. is 95 (based on 9 values); mean peak height in the band from 12 to 16 sec. is 84 (based on 15 values); mean peak height in the band from 5 to 12 sec. is 82 (based on 25 values); and mean peak height in the band from 32.1 to 32.7 sec. is 72 (based on 5 values).

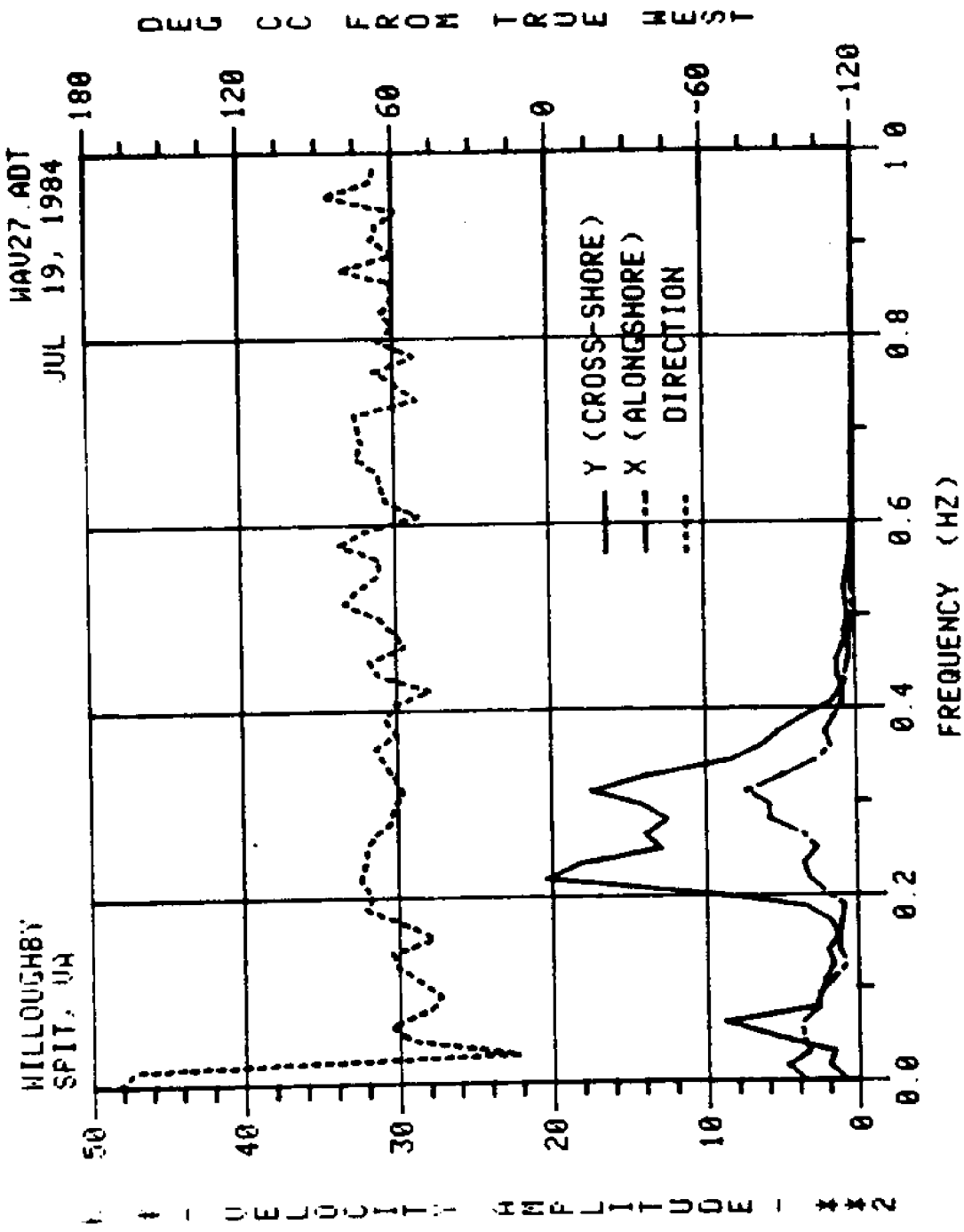
Examples of spectra in which low frequency motions are evident are shown in Figs. 14-16. The direct manifestation of the low frequency motion of Fig. 16 is seen in Fig. 17D and is discussed below.



K = CONSTANT

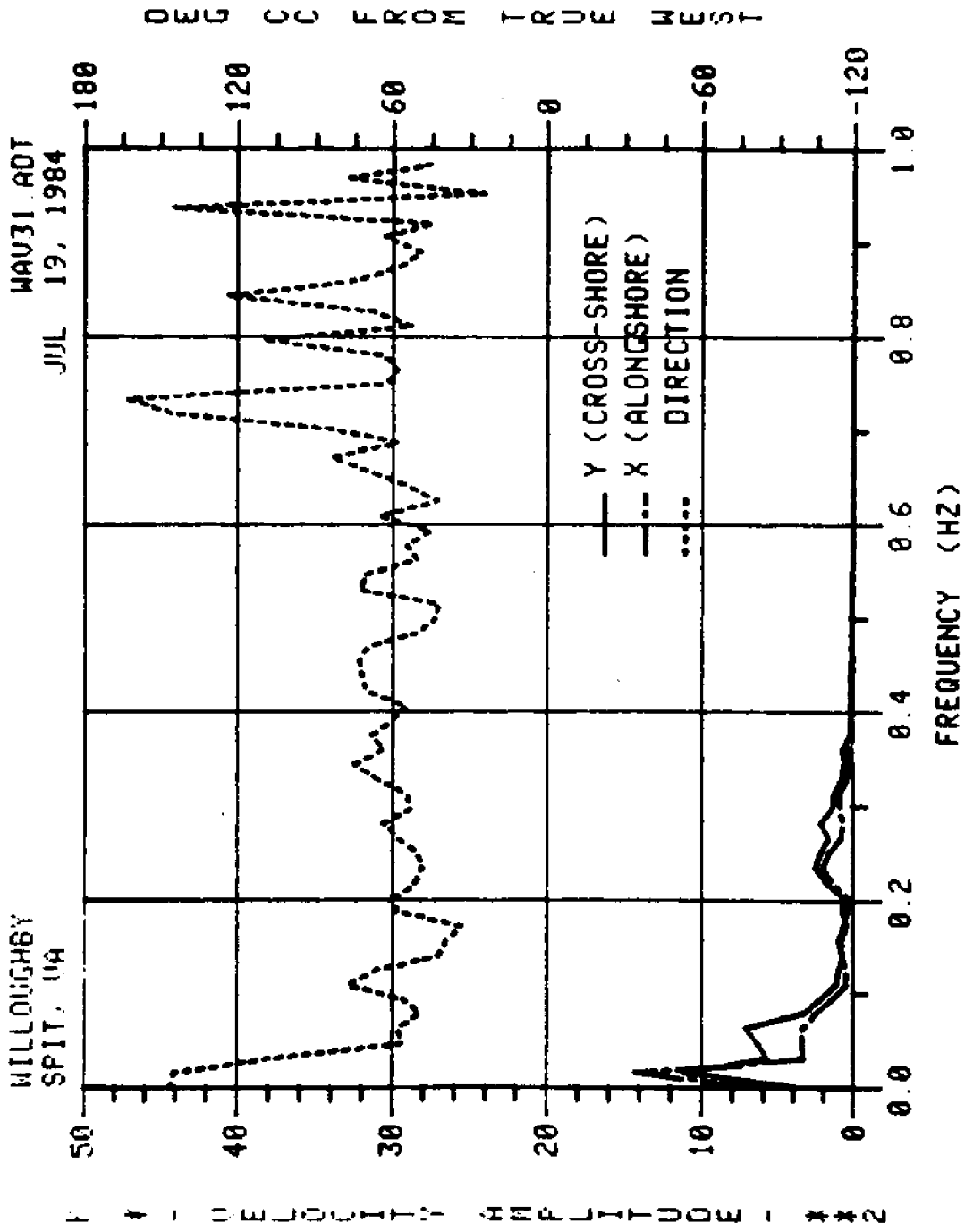
CC=COUNTERCLOCKWISE

Fig. 14. Waves from several sources. Principal peak occurs at a period of 3.8 seconds and a direction of 181 deg. A second peak occurs at a period of 69 seconds and a direction of 211 deg. A third peak occurs at a period of 7.9 seconds and a direction of 184 deg. Water depth 90 cm. Wind from 065 degrees at 15-20 mph.



K = CONSTANT **CC=COUNTERCLOCKWISE**

Fig. 15. Wave periods 3.2-4.6 seconds, 16 seconds, and 56.2 seconds. The direction of the latter motion is alongshore towards 105 degrees.



K = CONSTANT CC=COUNTERCLOCKWISE

Fig. 16. Low frequency motion dominates at a period of 56 seconds. See Fig. 17D for the distribution of velocity vectors.

From the comparisons of relative current amplitudes as evaluated on a scale of 100, it is seen that Bay-generated wind waves produce the largest velocity amplitudes in the test compartment at Willoughby Spit but edge waves with $\underline{n} = 0$ are close behind with those of $\underline{n} = 1$ being smaller. Surf beat motions and Atlantic-generated wind waves are approximately equal, a finding whose cause is not presently understood.

Measured Wave-Generated Current Velocities

Throughout nearly all the days when the E-M current meter was deployed, wave heights in the groin compartment were observed to be less than 9 inches; only on one day, when a single record was obtained (WAV4), did the estimated height reach as much as 12 inches. At other times under severe conditions, wave heights estimated at 3 feet were observed. In these infrequent but significant circumstances, the entire area between the groins and out beyond the groin ends was a part of the surf zone. Ordinarily the sites at which the meter tripod was set were seawards of any wave breaking which was confined to a zone 3 to 5 feet in width along the shore. Only occasionally were whitecaps or incipient whitecaps present when records were being

taken. Oscillatory currents varied in strength with the size of the waves. The measured root mean square orbital velocity amplitude of the modal wave in the compartment over the observation set was 20 cm per sec. On average, waves that produced this speed were asymmetrical, unbroken, 15 cm in height, of 4 sec. period, and occurred in a water depth of 111 cm ($=d$).

Velocity at the bed for the modal wave is 0.75 times that at $y/d = 0.27$ (Wood, 1970, Figs. 14, 15) or 15 cm per sec. Accepting the Shields function as a relatively reliable criterion for the threshold of sediment movement under water waves (Madsen and Grant, 1975), the critical value of wave-

generated shear stress for modal particles of the area is between 1.6 and 4.8 dyn per sq. cm. The calculated moveable bed friction factor is 0.23 (Vitale, 1979, Eq. 27; Grant and Madsen, 1982, Eq. 7) and peak shear stress is 25 dyn per sq. cm. If grain resistance is 70 percent of total resistance, bed grains would experience 17 dyn per sq. cm, a value in excess of threshold. Bed grains which are thus temporarily resuspended come briefly under the additional influence of other currents with their potential for translation.

Directional Aspects of the Currents

A steady current, inclined to the waves, shifts the center of the ellipse of current vector heads away from the origin (e.g., Fig. 17A). Offsetting currents of this kind in and immediately outside the groin compartment were found to reverse direction at intervals of approximately 6 hours and were therefore ascribed to the action of the semi-diurnal tidal currents. However, it was also found that when the current beyond the groin ends (Fig. 17A) was ebbing, the offsetting current within the compartment (Fig. 17B) was often counter oriented. The two records cited above are from sites 50 m apart on a north-south line in mid-compartment, and 48 min. apart in time. The first was taken at maximum ebb and is located just beyond the line connecting the groin ends.

Current couples such as these are consistent with the existence of a current gyre within the compartment driven by the shorewise tidal current beyond the groin ends. Two conditions were conducive to the formation of the gyre: 1) water level below groin tops so that compartmentalization is achieved; 2) sufficient elapsed time and external current strength to spin-up the gyre. The first condition was best met during ebb; the second during

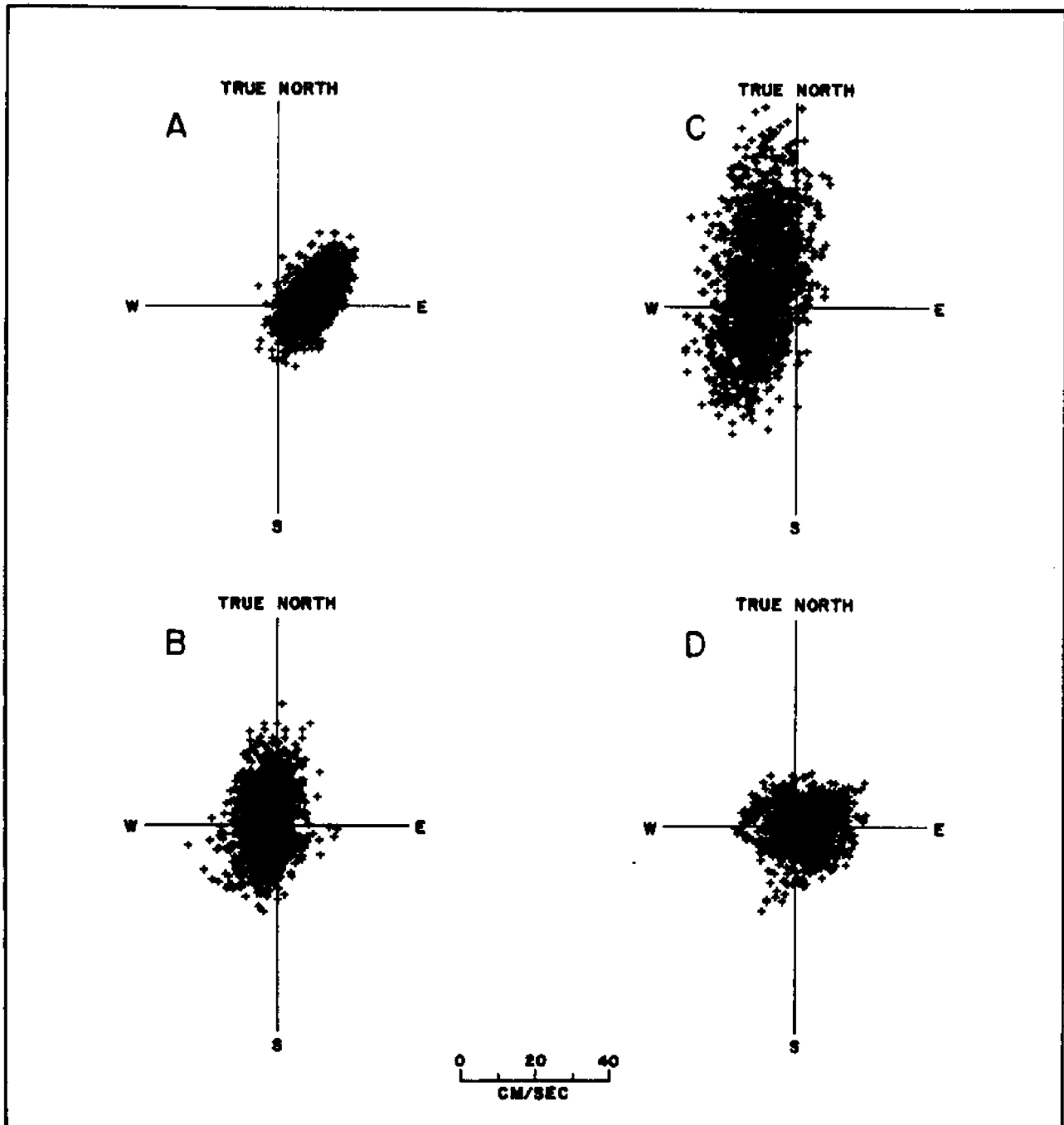


Fig. 17. Current measurements in the test compartment at Willoughby Spit. See text for location of stations within the compartment. A (WAV33) and B (WAV35), a current couple (see text). C Orbital asymmetry (WAV26) D Low-frequency oscillations (WAV31).

flood. The gyre occurred under ebb and flood, but was more frequent and stronger under ebb. Thus west-directed currents dominate in the shoreside limb of the gyre.

If the steady current has an offshore component along the line of wave propagation, offshore wave orbital motions are augmented and onshore wave orbital motions are decreased. Asymmetry is evident in Fig. 17C where the strongest offshore-directed vectors exceed the strongest onshore-directed vectors. The resultant vector for the entire distribution is 12 cm per sec. at 301 deg. CTN, i.e., offshore. The resultants from 37 of 48 available records were directed in the offshore semicircle. Although some of these vectors are within 20 deg of parallelism to shore, it is still the case that offshore movement of sand is by no means rare in the compartment and is not at all confined exclusively to the vicinity of groin walls.

The asymmetry of near-bed orbital velocity is in 11 of 48 records such that the resultant motion is directed in the onshore semicircle. In Figs. 18 and 19, the asymmetry analysis of two such records, WAV4 and WAV5, is presented. The method of analysis is described here briefly: 1) an azimuth window is defined by specifying a central azimuth in degrees CTN to the nearest degree and the angular spread of the window is defined as, say, plus or minus 10 degrees, for a total width of 20 degrees; 2) each successive vector in a vector time series under analysis is marked distinctively if its azimuth falls within the defined window; unmarked vectors are erased; 3) the run length of runs of consecutively marked vectors is determined and stored and those runs of length 2 (i.e., 1 sec.) or less are rejected and erased; 4) in each remaining run, the maximum velocity is retained and the other lesser velocities in the run are erased; 5) the frequency distribution of the retained peak velocities is formed, counted, and the mean and other

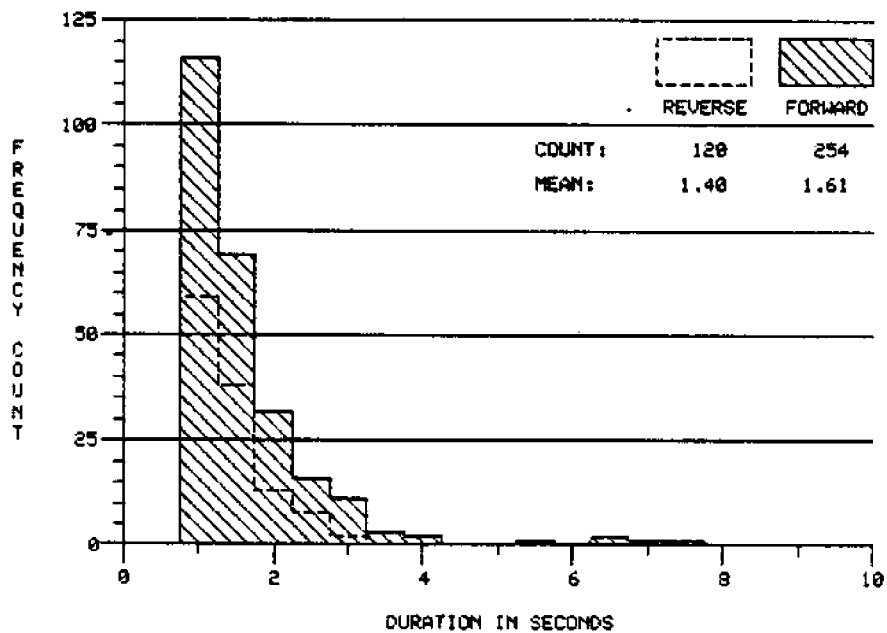
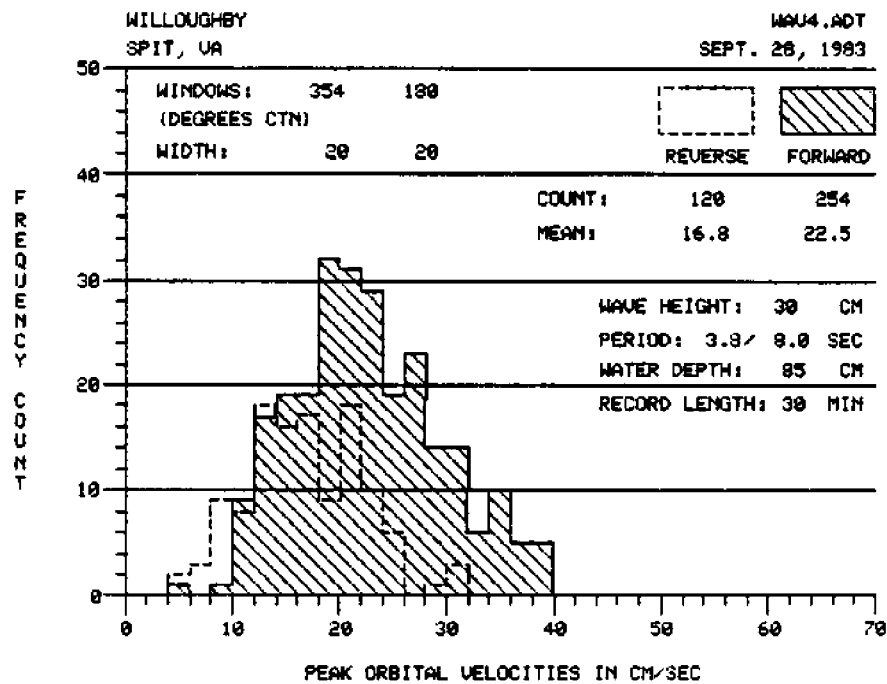


Fig. 18. Forward-favored asymmetry of wave orbital velocity near the bed at a location 20 feet west of the east groin. Wind speed was 13-17 knots from 065 degrees. Note that some forward runs are more than 7 sec. in duration; although the mean is 1.61 sec.

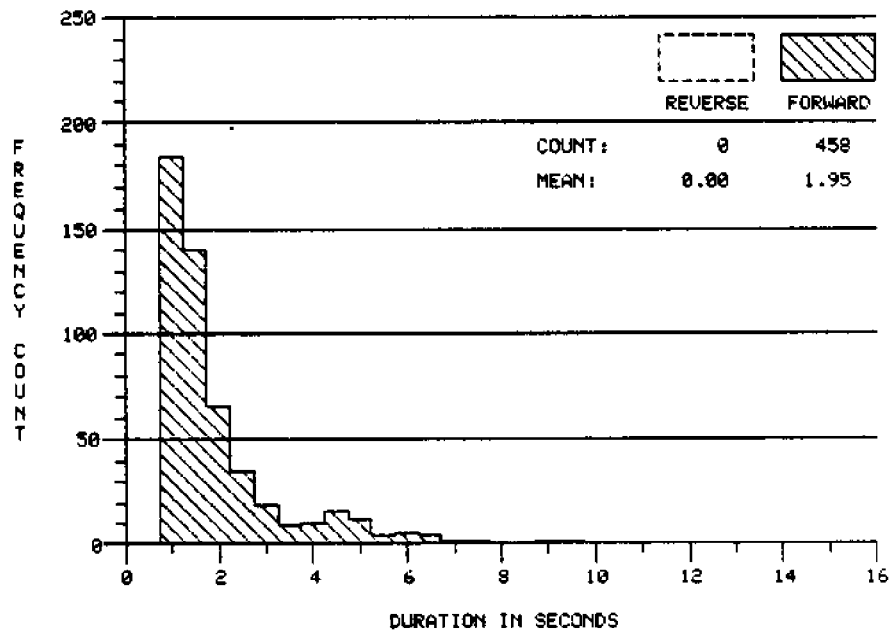
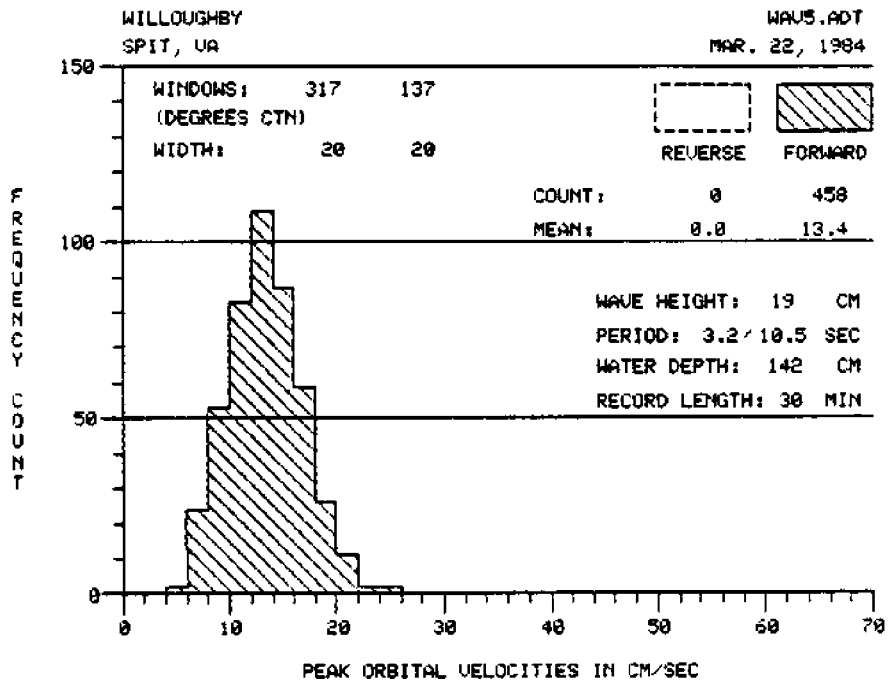


Fig. 19. Forward-favored asymmetry of wave orbital velocity near the bed at a location 115 feet east of the west groin. Wind speed 12 knots (estimated) from 247 degrees. Reverse runs were lacking due to a superimposed current in the direction of wave propagation.

percentiles calculated and stored; 6) the azimuth window is shifted one degree and steps 2 through 5 are repeated until the 360-degree circle has been traversed; 7) for each window, the product of retained run count and mean velocity is calculated; 8) the window of largest product is found, the azimuth is noted and the distribution for that window is plotted; 9) in the vicinity of the back-azimuth to the window of step 8, a window whose product is a local maximum is sought, found, and plotted on the same diagram.

Fig. 18 shows the results of the analysis for WAV4. The lower panel of Fig. 18, shows the distribution of run length (in seconds) for the forward and reverse windows. It is to be noted that for the onshore events, the mean of the peak velocities is 22.5 cm per sec.; whereas, for the reverse events, the mean of the peak velocities is 16.8 cm per sec. The mean of the largest one-third of the forward peak velocities, i.e., the significant velocity, is 30.6 cm per sec.; the corresponding value for reverse direction is 23.0 cm per sec. The asymmetry is evident and is in favor of the onshore direction both in mean magnitude and duration. The dispersion pattern of sediment on the bottom, at the site, if particles were mobilized at, say, 18 cm per sec., would display a ray of maximum length in the onshore direction.

In Fig. 19, an extreme case of onshore-favored asymmetry is shown wherein no offshore directed events occurred in the analysis. This situation arises from the existence of a bias current which flows in the same direction as the direction of wave propagation. In this particular instance, however, the significant forward velocity is only 16.8 cm per sec.

Low frequency oscillations are occasionally strong enough to be revealed directly in the plots (Fig. 17D). In this diagram, weak wind waves generated the central ellipse whose major axis is along 220 deg CTN. Also evident are two streaks oriented at 220 deg CTN offset to the sides of the

ellipse. This motion is manifested in cross-shore and alongshore spectra of the record as principal peaks at a period of 56 sec. (Fig. 16). The direction of that frequency component is along the line 300-120 deg CTN which is within 30 degrees of being shore-parallel; its velocity amplitude is 13 cm per sec. In a hypothetical pattern of dispersion of a bed sediment from a single point on the bed, azimuths of the maximum rays would doubtless be affected by low frequency motions such as these.

Wave Refraction

Wave refraction diagrams were prepared for: 1) one pre-fill and two post-fill bathymetric surveys of the compartment; 2) wave periods of 3 sec. and 6 sec.; 3) evaluation of the water surface at mean high water (MHW) and at mean low water (MLW); and 4) wave approach directions of 030 and 300 deg CTN (clockwise from true north). The method of calculation used is based on that described by Willis and Price (1975). This is a single ray method that propagates wave orthogonals through a succession of adjacent triangles the vertices of which correspond to places where water depth, i.e., wave celerity, is known. In the present case, each vertex is a point on a 10 m by 10 m surveying grid in and offshore of the compartment where water depth was determined. Unfortunately, in this and most other estuaries, a far field region is not available where the waves are unrefracted because of a sufficiently great water depth. The results obtained suffer because of this shortcoming in that the starting wave orthogonals beyond the groin ends are taken as a set of straight parallel equispaced lines; whereas, in fact some refraction would actually already have occurred by the time the wave had reached that position. Nevertheless, gross features of the refraction pattern are valid despite this limitation.

Relatively little difference was found between the refraction diagrams for 3-second and 6-second waves, or in the results taken at MHW and MLW. Thus, only four diagrams (Figs. 20-23), two for the pre-fill bathymetry and two for the post-fill bathymetry, serve to demonstrate the main features of the patterns obtained. In the first of these (Fig. 20), the wave orthogonals from 030 deg, by far the most common direction of approach, bend slightly but sufficiently so as to reach the pre-fill MHW shoreline with a normal or near-normal orientation. In the latter case, whatever non-zero small breaker angles exist tend to open to the west, thereby denoting very weak, or nearly zero, west-directed longshore currents in the narrow breaker zone.

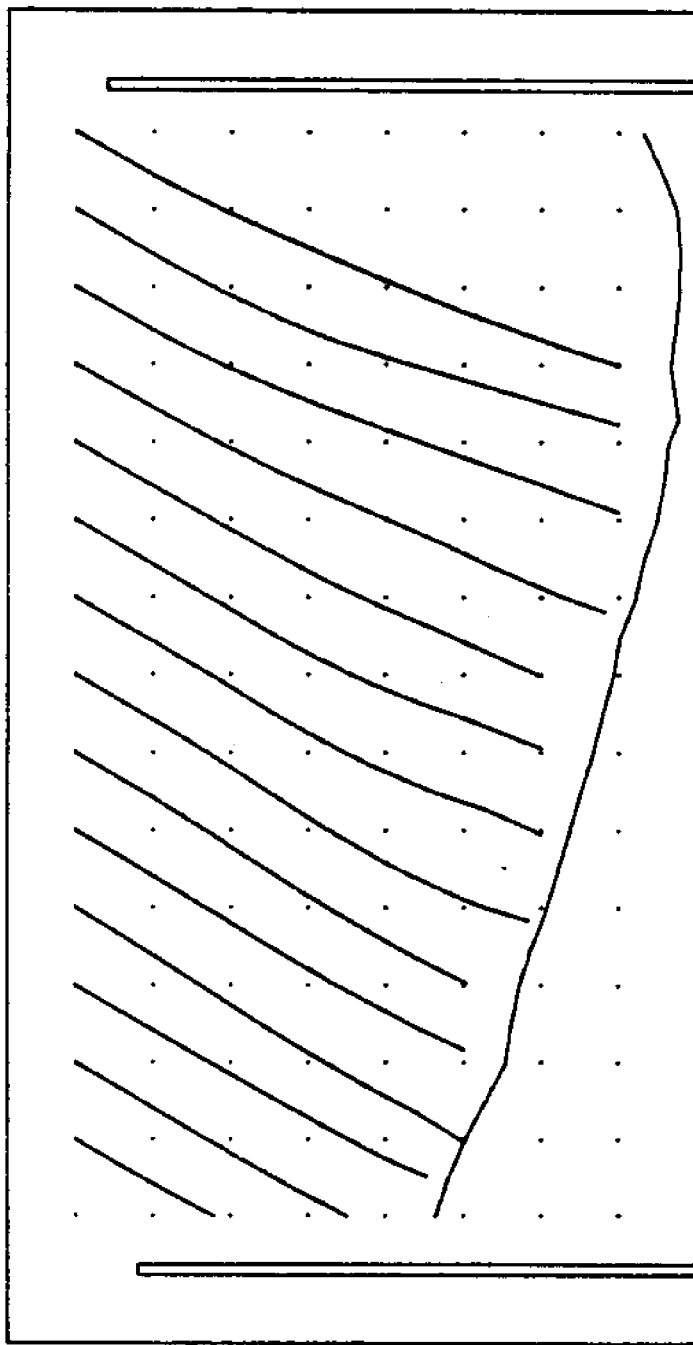
In the second of the four diagrams (Fig. 21), waves approach from 300 deg, an infrequent condition but the only other azimuth of sufficient fetch length to produce waves of note. There is much crossing and converging of orthogonals; however, the places of greatest concentration of orthogonals are along the wall of the east groin and not on the shoreline. Wave energy from 300 deg does not reach the shoreline in any significant amount.

In the third diagram (Fig. 22), which shows refraction over the 6-months post-fill bathymetry at MHW, orthogonals do not bend enough to approach the shoreline at normal angles. Instead, breaker angles of 5 to 10 degrees, open to the west, are characteristic of the pattern and denote westward flowing longshore currents in the narrow surf zone.

In the fourth diagram (Fig. 23), it is seen that the shoreline is again for the most part effectively shielded from wave energy approaching from 300 deg. A difference from Fig. 21 is that an orthogonal convergence zone now occurs at the east end of the shoreline within the compartment. The higher waves thus produced in that local convergence area may be the cause of the

WILLOUGHBY SPIT AT 13-TH VIEW

GROINS 500 FT APART



BATHYMETRY: 8-22-84

STILL WATER LEVEL: MHW + 00 CM

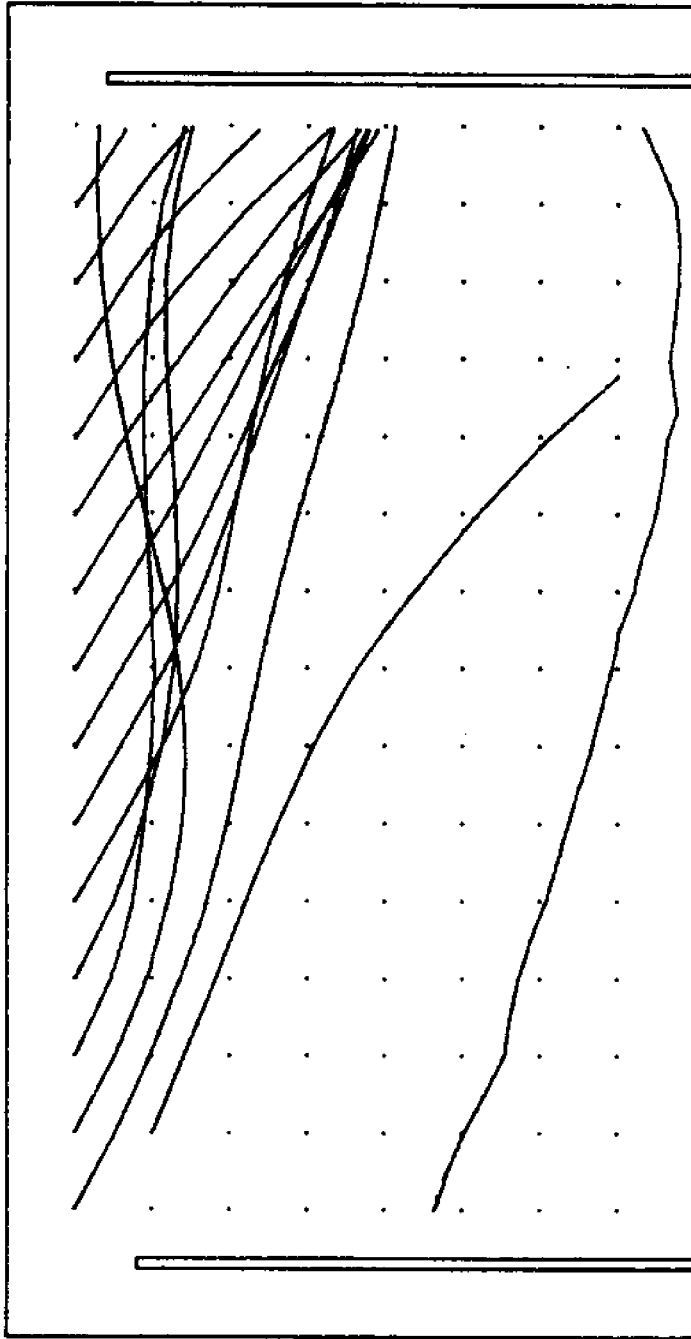
WAVE PERIOD: 3 SEC

APPROACH DIRECTION: 030 DEG CTN

Fig. 20. Wave refraction diagram for pre-fill bathymetry, MHW, 3-sec. wave period, and approach from 030 deg. CTN.

WILLOUGHBY SPIT AT 13-TH VIEW

GROINS 500 FT APART



BATHYMETRY: 8-22-84

STILL WATER LEVEL: MHW + 00 CM

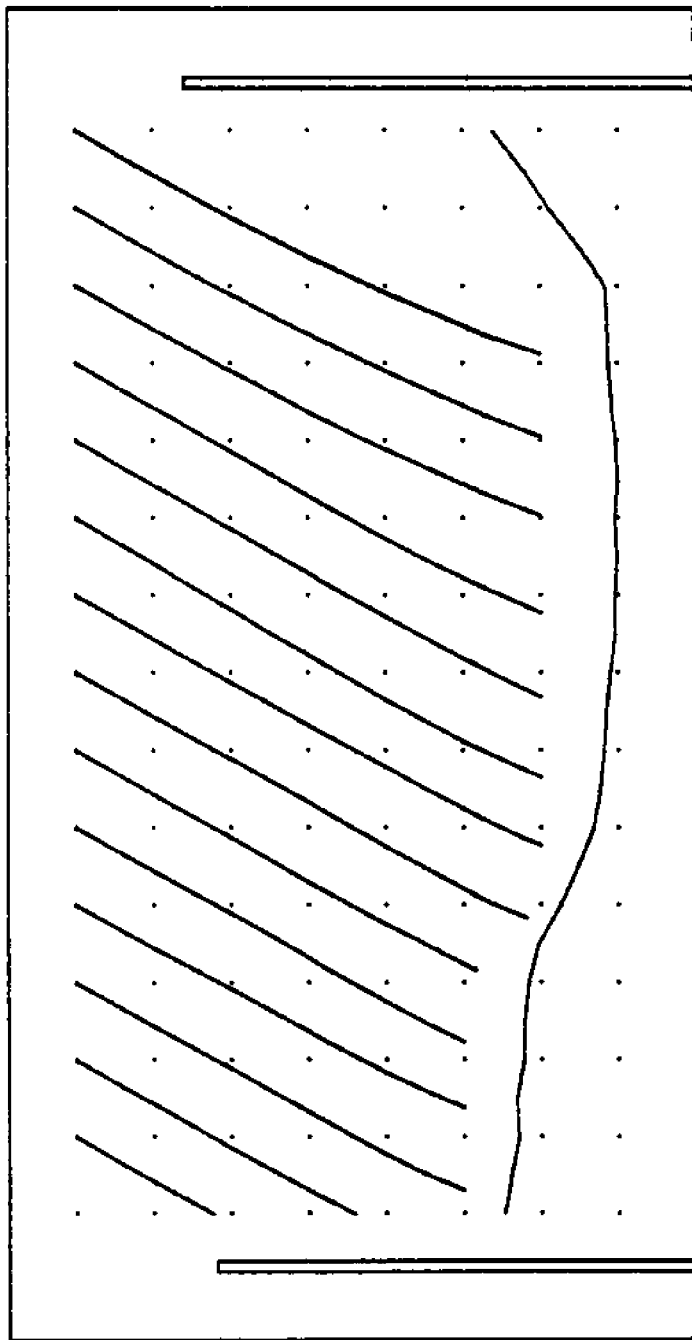
WAVE PERIOD: 3 SEC

APPROACH DIRECTION: 300 DEG CTN

Fig. 21. Wave refraction diagram for pre-fill bathymetry, MHW, 3-sec. wave period, and approach from 300 deg. CTN.

WILLOUGHBY SPIT AT 13-TH VIEW

GROINS 500 FT APART



BATHYMETRY: 4-23-85

STILL WATER LEVEL: MHW + 00 CM

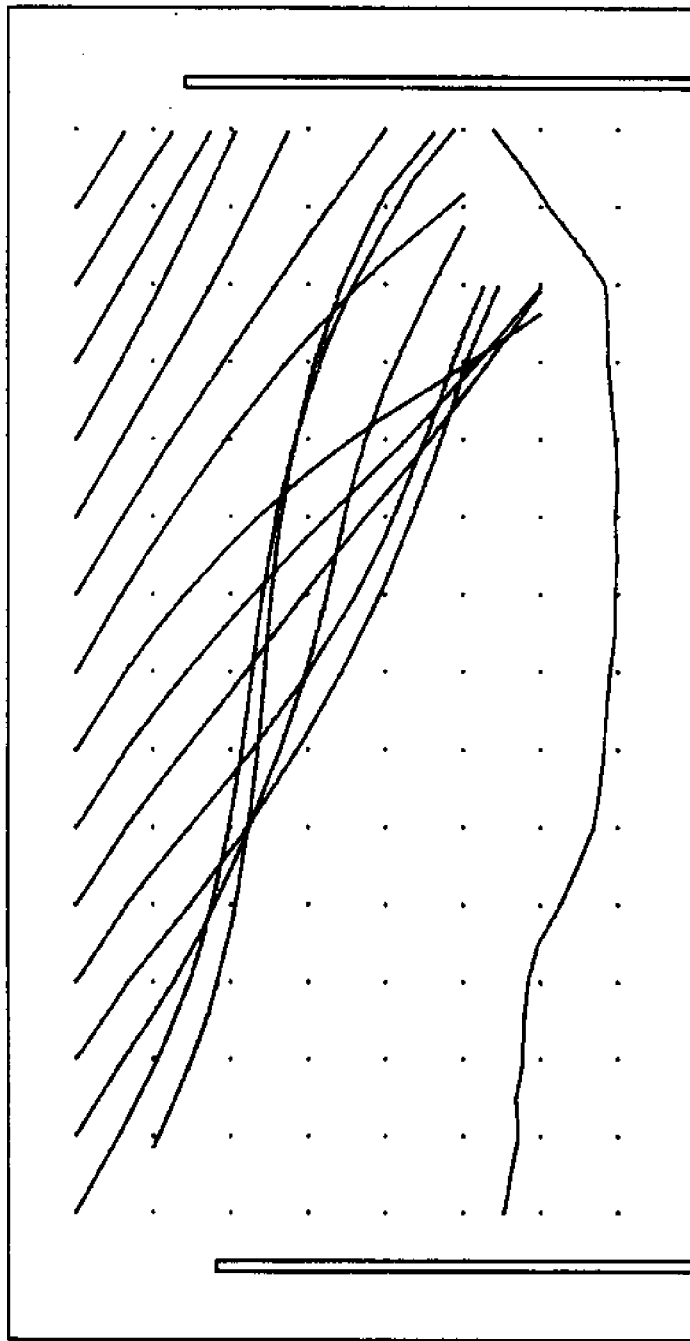
WAVE PERIOD: 3 SEC

APPROACH DIRECTION: 030 DEG CTN

Fig. 22. Wave refraction diagram for post-fill bathymetry, MHW, 3-sec. wave period, and approach from 030 deg. CTN.

WILLOUGHBY SPIT AT 13-TH VIEW

GROINS 500 FT APART



BATHYMETRY: 4-23-85

STILL WATER LEVEL: MHW + 00 CM

WAVE PERIOD: 3 SEC

APPROACH DIRECTION: 300 DEG CTN

Fig. 23. Wave refraction diagram for post-fill bathymetry, MHW, 3-sec. wave period, and approach from 300 deg. CTN.

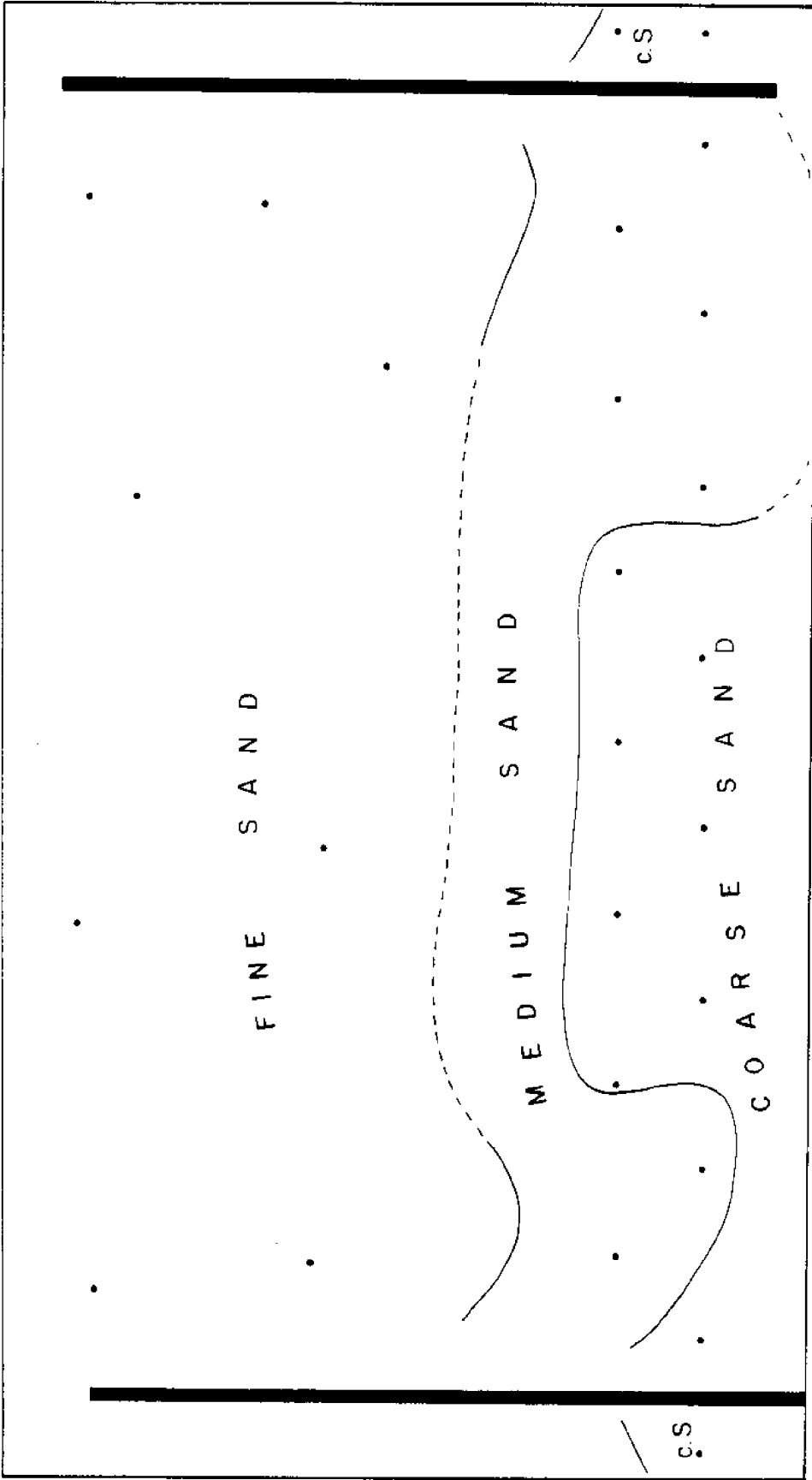
beach scarps preferentially developed there during the early retreat phase of the compartment shoreline following the placement of the fill.

BOTTOM SEDIMENT

Before the fill, coarse-grained sands (0.7 mm, mean diameter) were found along the shore, medium-grained sands (0.4 mm) were further offshore, and fine-grained sands (0.2 mm) occurred in the outer part of the compartment (Figs. 24, 25). Most modal diameters were in the range from 0.13 to 0.25 mm. Phi standard deviation averaged 0.68. Many samples were negatively skewed and contained particles up to diameters as large as 6 mm. The fill sediment, in contrast, is characterized by a mean particle size of 0.9 mm. Phi sorting is poor (1.32) and even though the distributions tend to be negatively skewed, they are more symmetrical than those of the pre-fill sediment. Broken shell comprises 50 percent of the larger size classes and 10 to 15 percent of the fine sand classes.

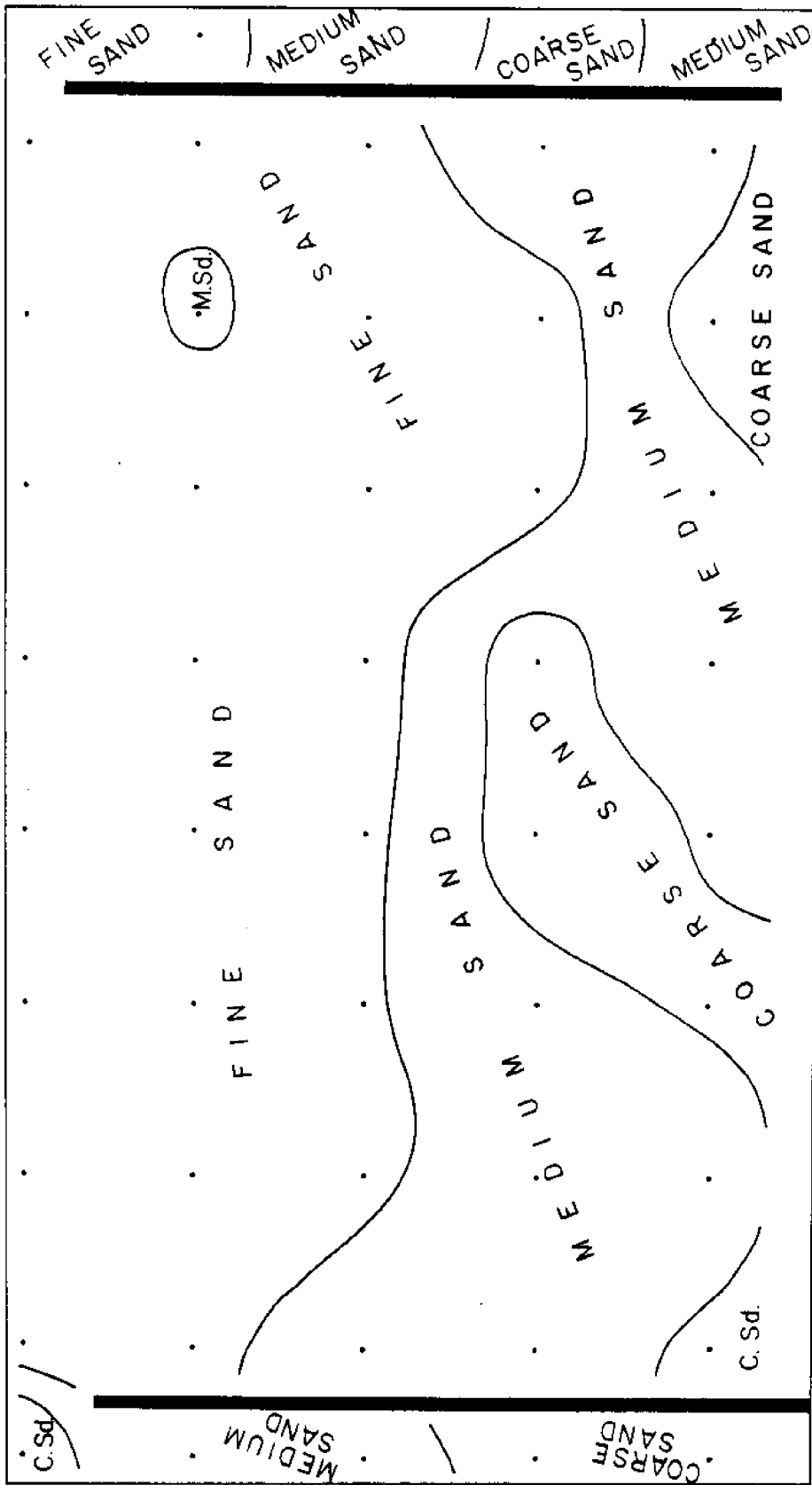
SHORELINE CONFIGURATION AND EVOLUTION

In describing the MLW shoreline in the test compartment at Willoughby Spit, the line connecting the seaward ends of the groins is a base from which distances are measured along the groins and three equispaced quarter lines. In Fig. 26A it is seen that the prefill shoreline of August to November 1983, was set back from the base line distances of 30, 44, 55, 63, and 45 m. The most recessed point was at the east quarter line. Between that point and the west groin, the shoreline was essentially a straight line the azimuth of which was 287 deg. CTN (clockwise from true north). The azimuth of the normal to this segment is 017 deg. CTN in good agreement with the azimuth of the principal fetch, 022 CTN.



M_g
 1/10 - 1/20 (1984)

Fig. 24. Sediment distribution in the test compartment at Willoughby Spit. The sampling period is prior to the placement of fill.



M₂ (5/14/84)

Fig. 25. A re-sampling of bottom sediment in the test compartment. Sampling period is pre-fill.

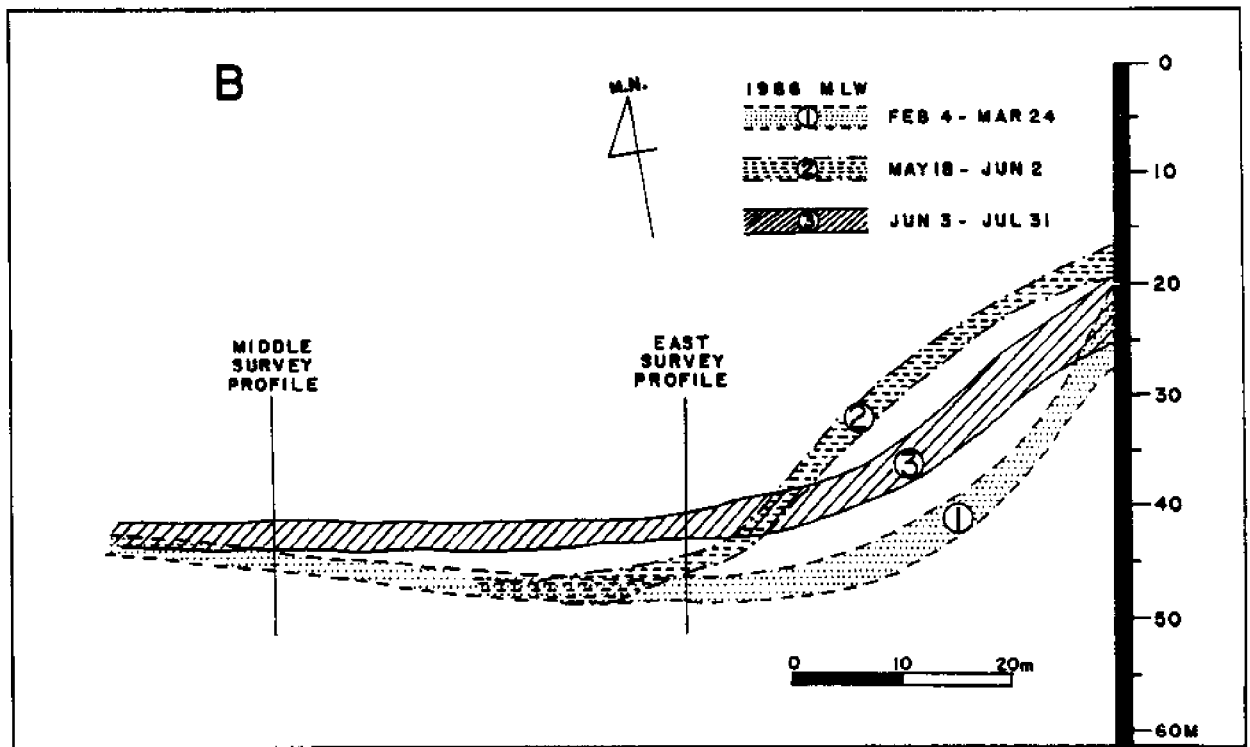
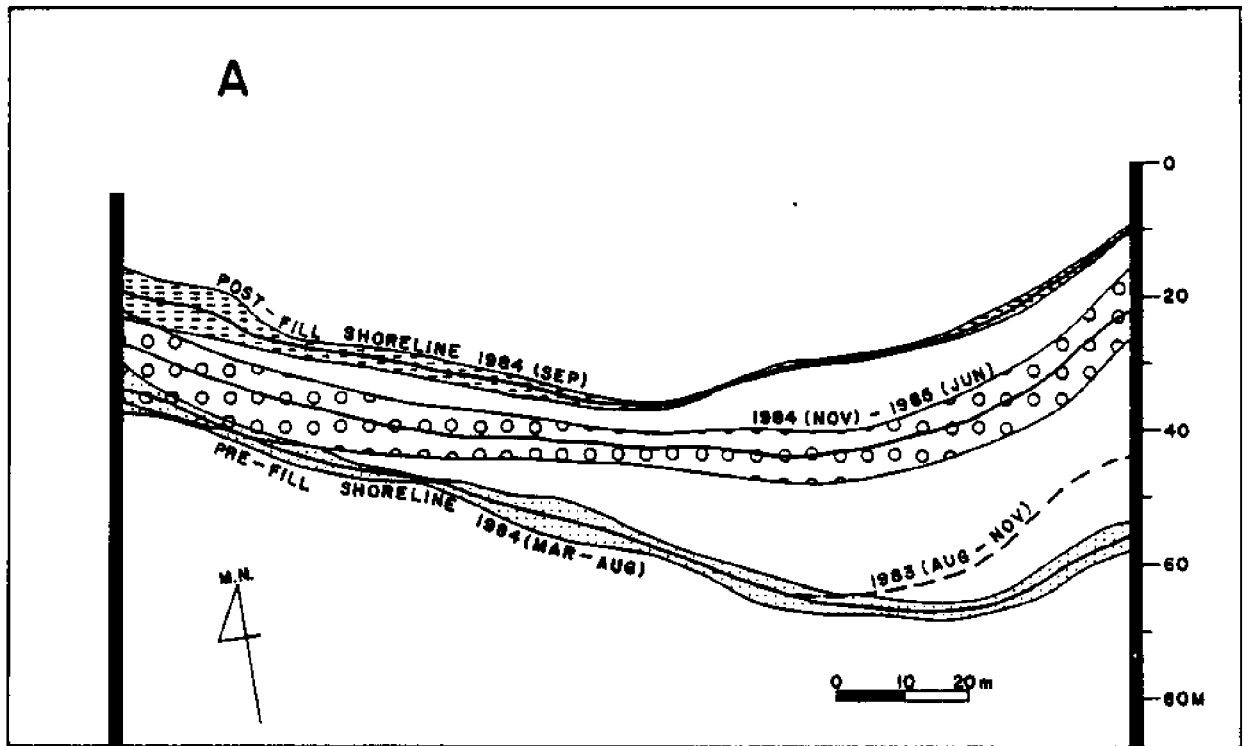


Fig. 26. Shoreline changes in the test compartment. A. Recession towards the pre-fill shoreline. Each band or envelope contains many shoreline surveys taken in the noted period; the average for the band is the central line. B. Details of a prolonged overwash episode at the east groin followed by redistribution of the overwashed sediment.

During the next four months, changes occurred only in the easternmost quarter. There was a shifting eastward and further retreat of the point of maximum recession. In this process the straight segment of the shoreline was lengthened. Retreat along the east groin was 12 m.

Approximately 5 weeks after the fill, the shoreline was 15, 26, 34, 27, and 9 m from the base line. On this new catenary-shaped curve, the point of maximum recession was nearly on the center line; the shoreline in the west half of the compartment was moderately curved and its mean azimuth was 280 deg. CTN. The average shoreline and its envelope are also shown for the period from November 1984 to June 1985. Recessions in the two elapsed months were 9, 9, 5, 16, and 11 m. The point of maximum recession shifted eastward and was between the center and the east quarter line. It is seen that after the fill, the shoreline evolved first rapidly and then slowly but always with a net tendency towards its pre-fill position and shape.

Periodically, when the water level is sufficiently high, sand can enter and leave the compartment along the shore. Movement is by level washing in the swash zone across a groin position under the action of broken waves and longshore current. The shoreline shape is altered, particularly near a groin, if an overwash episode persists or recurs frequently (Fig. 26B). For example, as illustrated in the figure, in May and early June, 1986, approximately 22 mo. after the placement of the fill, repeated overwashing occurred and the shoreline between the east quarter profile and the east groin advanced by 16 m owing to the deposition of overwashed sediment in the shadow of the groin. In the following 9-week period, changes in the envelope of the shorelines are suggestive of a partial redistribution westward within the compartment of the overwashed sediment.

From the date of fill to mid-October 1984, the mean shoreline in the compartment retreated at a rate of 72 m per year; for the next 16.5 mo., this rate was 0.75 m per year. Beginning in mid to late April 1986, the mean shoreline advanced to the position it occupied immediately following the initial rapid retreat. New sand on the foreshore was provided by the commencement of erosion of the toe of artificial dune ridge which had come within range of being vulnerable to attack and, which because of its steep forward slope, was capable of yielding a large volume of sand with a small retreat of the toe of the dune.

Redistribution of overwashed sediment depends, in part, on the occurrence of WNW to NW waves. As seen in Fig. 23 above, after refraction, the wave orthogonals of these waves converge at the shore in the eastern one-third of the compartment, while still manifesting some breaker angles open to the west. And as mentioned, scarps up to 55 cm in height when present are best developed and occur most frequently along the eastern quarter segment of the compartment shoreline.

At the same time that fill was placed in the groin system, growth of a new spit commenced at the west end of Willoughby Spit downdrift from the terminal groin (Fig. 27). The new feature was comprised of fill material and thus constitutes evidence for westward drifting of sediment. An initial MSL survey 2.5 mo. after the completion of the nourishment project, showed a spit 95.5 m long and 36 m wide. During the first seven months, the width of the spit remained relatively constant at 44.5 m while elongation occurred at a rate of 4.2 m per week. By early April, 1986, an overall length of 272 m was attained.

Spit volume was determined from profiles that extended from underwater toe depths across the feature. By April, 1986, volume of the spit was

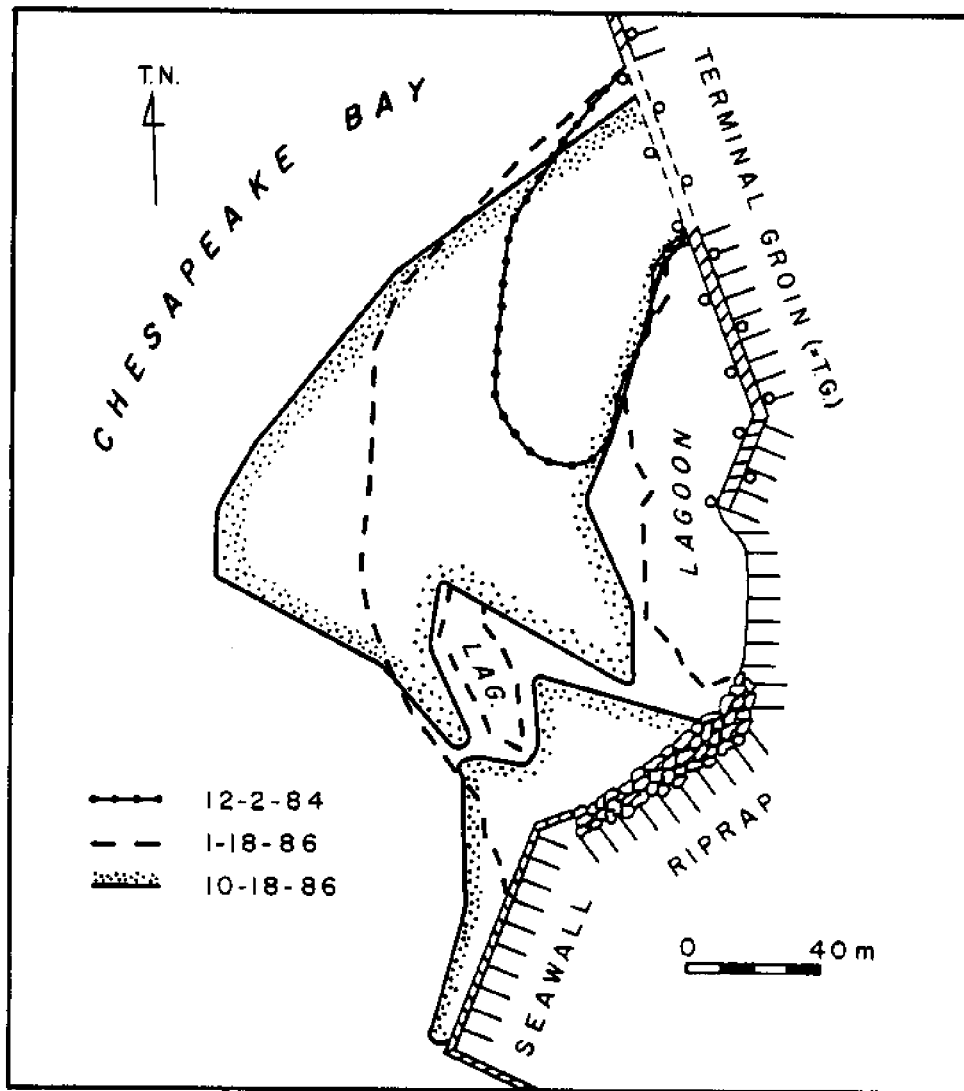


Fig. 27. Growth of a new split at the western end of Willoughby Spit following the placement of fill in the updrift groin system. Where the terminal groin is represented by broken lines, it has been covered by sand in transit to the west along the shore in the shore zone. (Provided to the author by R. Neville Reynolds).

32,518 cu m or 8 percent of the total volume of fill placed in the groin system. Average volume rate of growth of the spit was 19,975 cu m per year. If this rate were maintained, and if all fill sediment ultimately found a sink in the spit, the corresponding life of the fill would be 20 years. It is shown later that this estimate is actually erroneous and that the source of error is the omission of two factors from consideration: 1) much of the filled sediment is lost to the offshore directly from the system of groins; and, 2) the volume rate of sediment transport along the shoreline to the west is by no means constant with time, but instead decreases dramatically.

BATHYMETRIC ELEMENTS AND EVOLUTION

Surveys of beach topography and shore face bathymetry were made within the compartment 26 times during a three-year period by plane table surveying. A square element of the survey grid is 10 m on a side. Zero elevation of the surveys is 30 cm below MLW of 1983.

Before the fill (Fig. 28A), significant features of the beach and shoreface included: 1) the beach foreshore, the slope of which was 4 to 7 deg.; 2) an abrupt termination of the foreshore slope along the MLW line in the eastern part of the compartment; 3) a narrow berm in the west part of the compartment at an elevation of 1.5 m MLW; 4) a submerged bar the crest elevation of which was approximately -0.6 m MLW and was located at the mid-point of the line connecting the groin ends; 5) a channel whose axis enters the compartment from the west and is situated on the landward side of the bar; and 6) a broad shallow flattish area in the eastern one-third of the compartment. Along the wall of the east groin, the maximum difference that was found between the elevation of the updrift side and the elevation of the

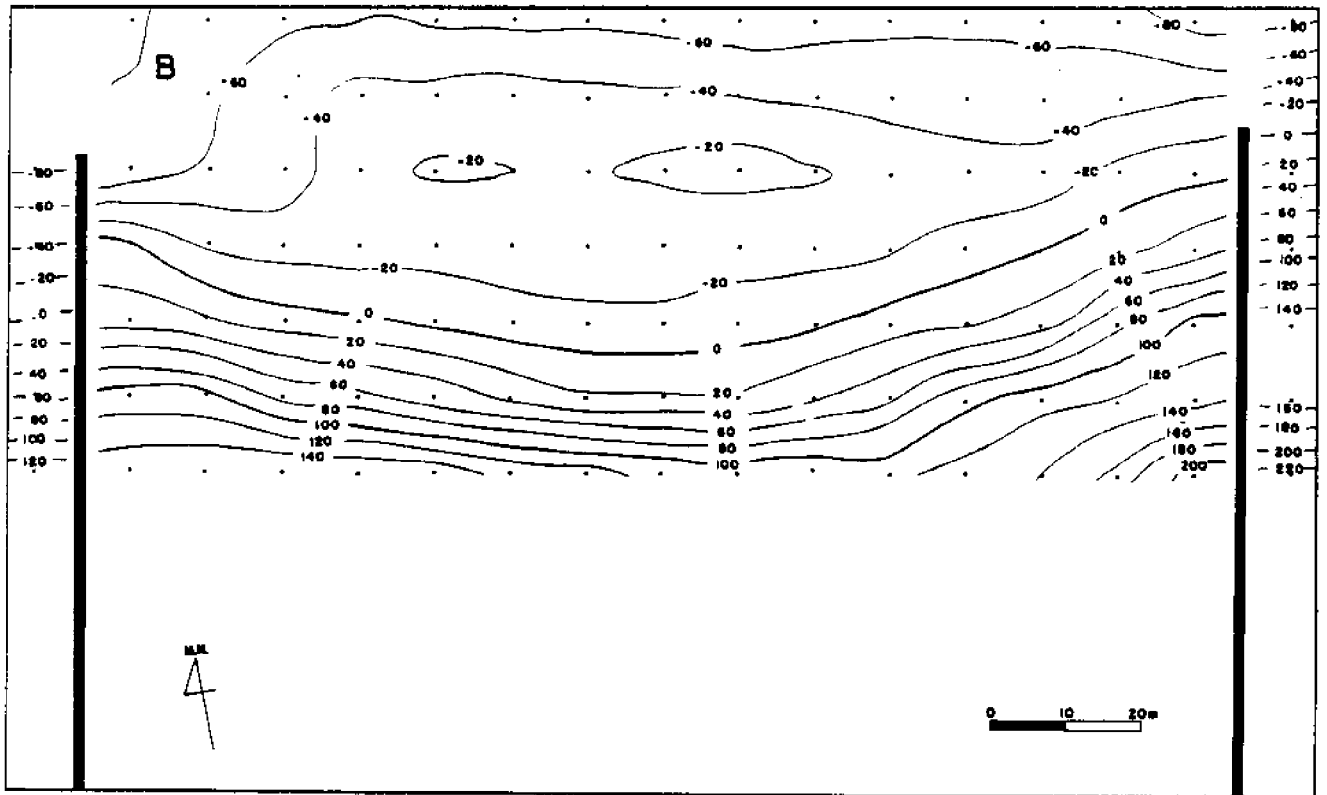
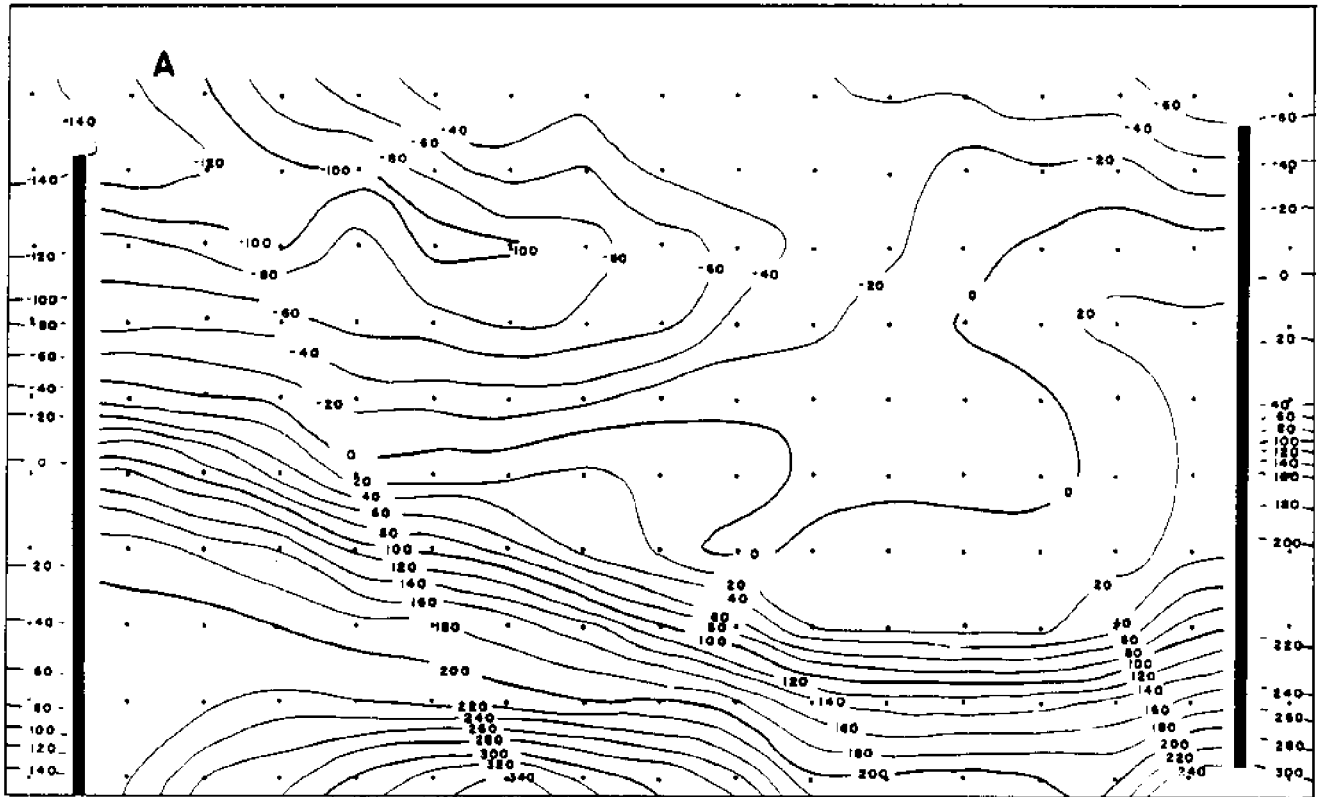


Fig. 28. Beach topography and shoreface bathymetry in the test compartment. Contour labels are in centimeters. MLW (1983) corresponds to the +30 cm contour. A. May 13, 1984; pre-fill. B. October 4, 1984; post-fill.

downdrift side was 1.7 m. An identical magnitude also occurred along the wall of the west groin. Among the 10 surveys taken before the fill, comparisons show little evidence of change.

The bathymetry approximately one month after the placement of the fill in the test compartment is shown in Fig. 28B. The entire beach, submerged and subaerial, has obviously been advanced seawards to the north by the placement of the fill. There is incipient development of a channel at the outer end of the west groin. A low ridge-like bar is evident along the line connecting the ends of the groins. In an east-west sense, the foreshore is dish shaped and nearly symmetrical.

The bathymetry sixteen months after the fill is shown in Fig. 29A where it is shown that the -80 cm depth contour had shifted 30 m landwards from its position following the fill. The bar was developed only in the west part of the compartment and the channel near the end of the west groin was clearly defined but had not reached its pre-fill size. Nearer shore the bottom over most of the compartment was gently sloping at 1 deg. Landwards was the ramp of the foreshore, the slope of which ranged from 4 to 5 deg. Farther landward was a berm at 150 cm MLW followed by the forward slope of the artificial dune.

Twenty-four months after the fill (Fig. 29B), the -80 cm depth contour had moved 11 m closer to shore and the earlier beach berm had been cut out by the further recession of the upper foreshore.

Maps of elevation difference were prepared from each consecutive pair of bathymetric surveys. For the one-year period before the fill, individual difference maps reveal only small changes. An examination of the sequence of difference maps for the pre-fill period shows a steady lessening of change with the passage of time.

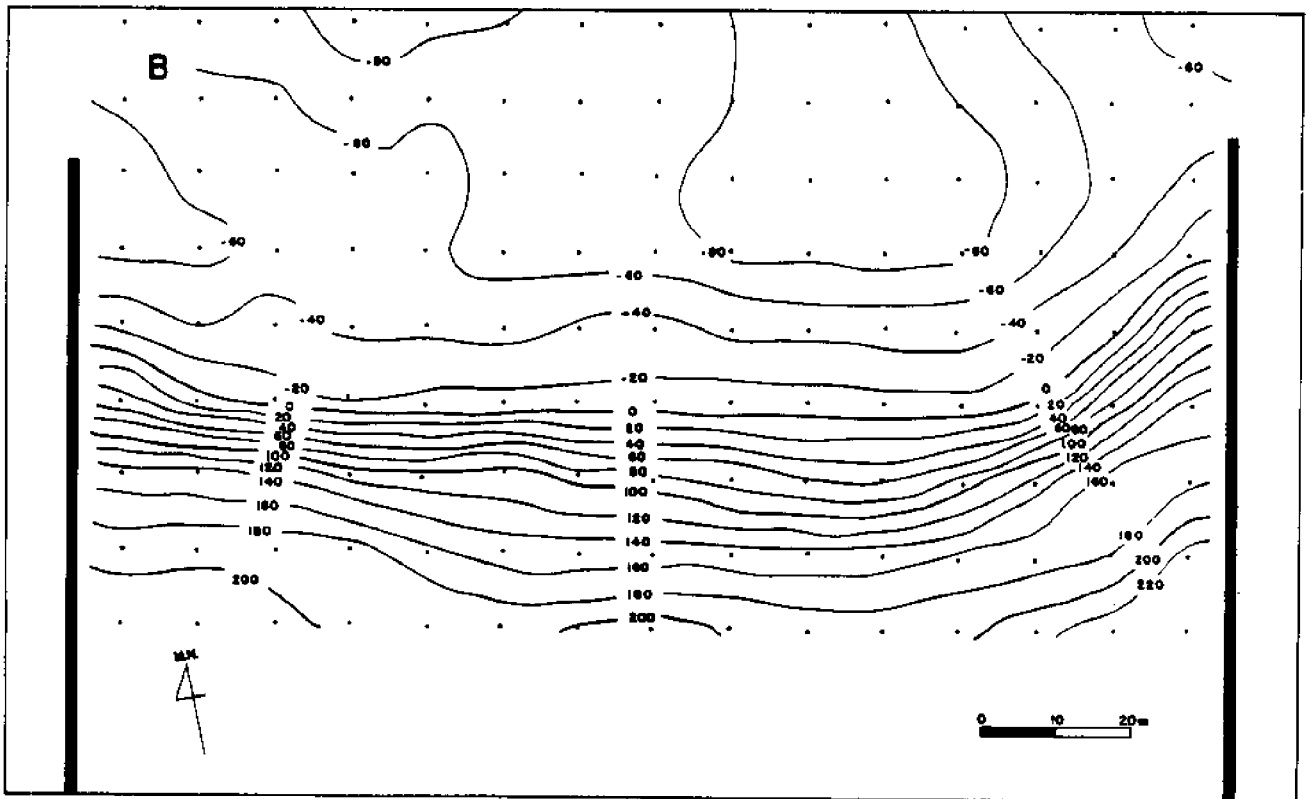
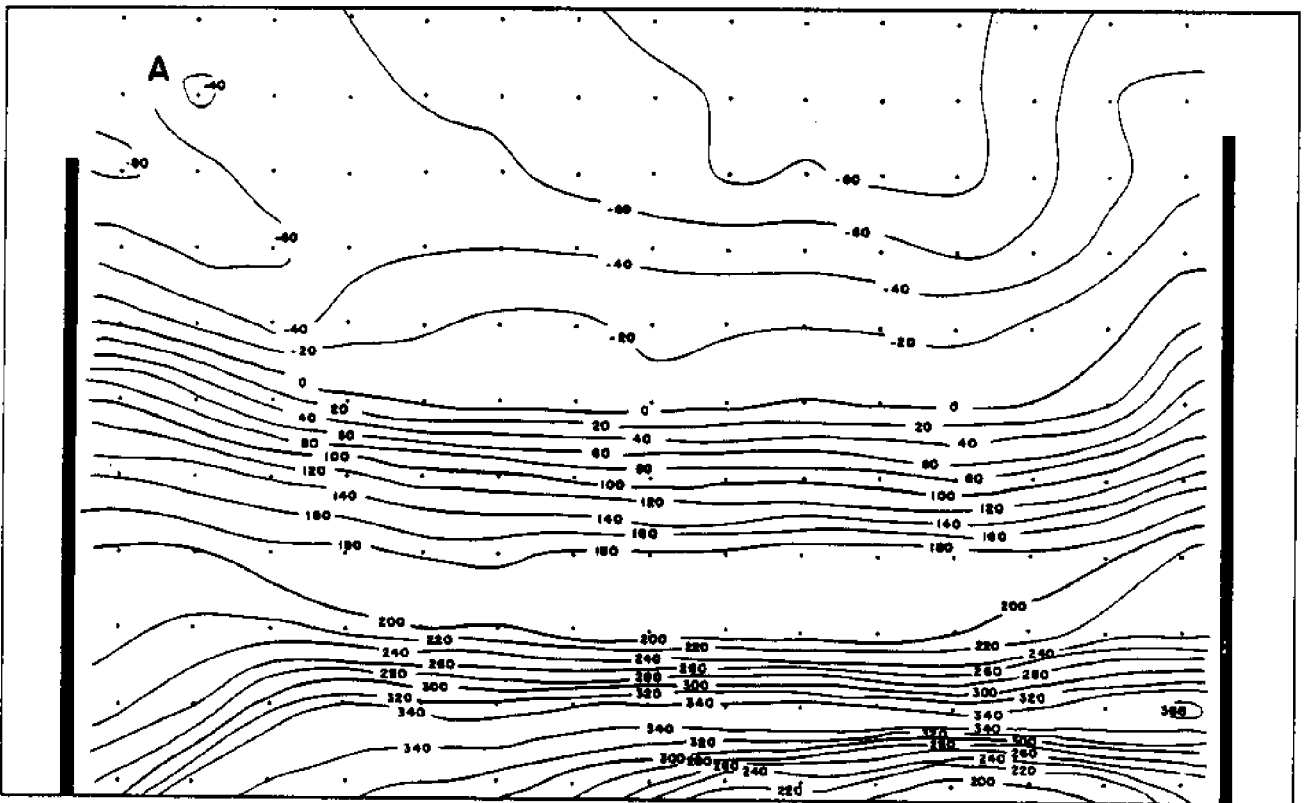
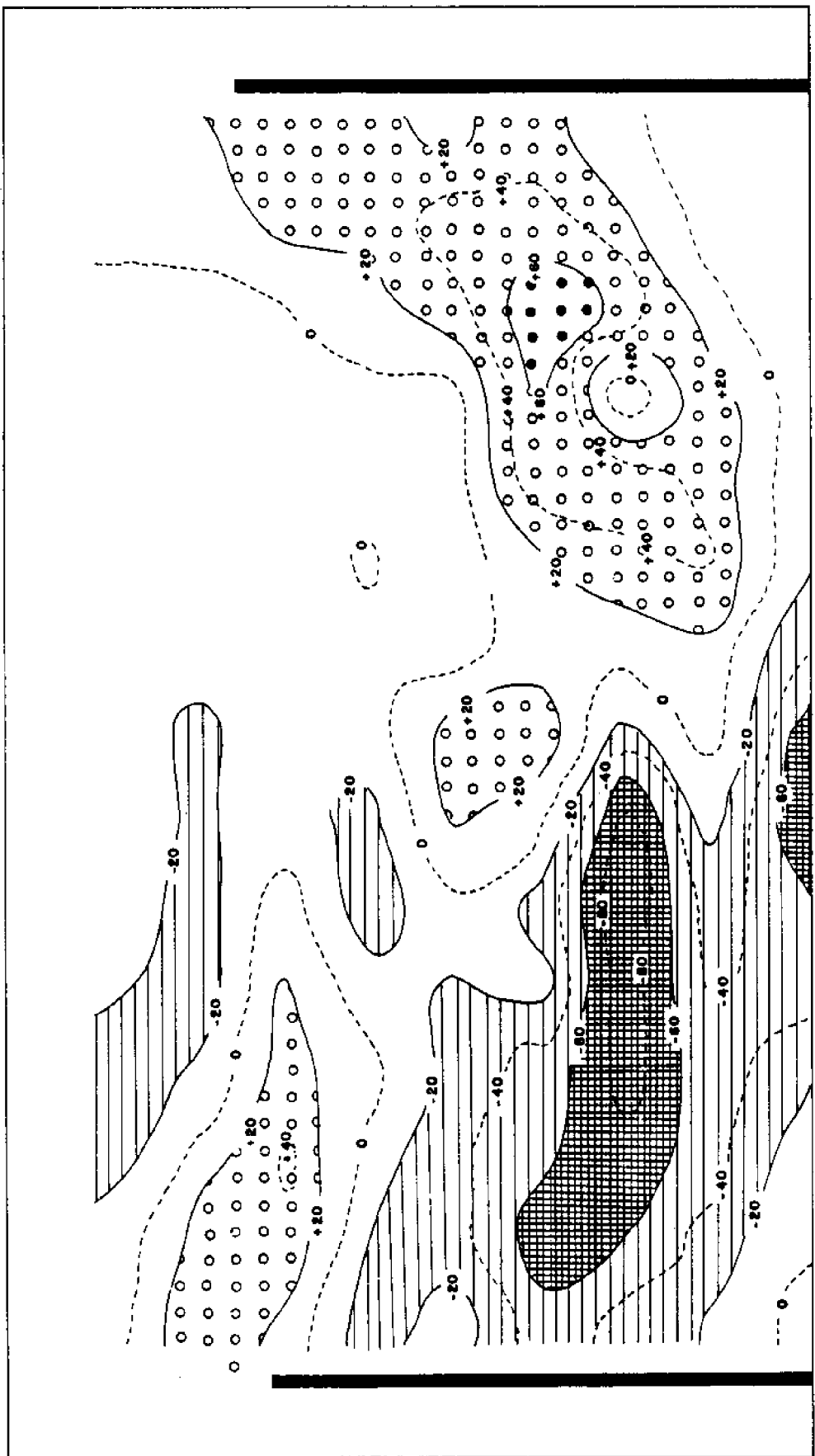


Fig. 29. Beach topography and shoreface bathymetry in the test compartment. Contour labels are in centimeters. MLW (1983) corresponds to the +30 cm contour. A. January 9, 1986; pre-fill; B. August 5, 1986; post-fill.

For the post-fill period, the most frequently encountered patterns of change are illustrated by four consecutive difference maps (Figs. 30-33) covering a period of some seven months. During an interval of frequent sediment overwashing, from mid-September to mid-November 1985 (Fig. 30), sand moved repeatedly from east to west across both east and west groins. The result is a bipolar pattern of net deposition in the eastern half and net erosion in the western half of the compartment along the shoreline. The site of the deposition corresponds with the wave shadow zone in the lee of the east groin. In the area of net erosion, the azimuth of the disequilibrium shoreline (i.e., the post-fill shoreline) relative to the crests of the dominant NNE-NE waves after refraction, results in westward opening breaker angles and hence, west-directed longshore currents at the shoreline. The heights of waves and breakers in the western two-thirds of the compartment often increases with distance to the west up to the groin wall, thereby increasing the potential for mobilization of bed sediment in that area.

In essence, there seems to be no reason for not viewing the accumulation of washed-over sediment at the east end of the test compartment as one-half the counterpart of the erosion of sediment at the west end of the compartment. In this view, it would be expected that in the adjacent downdrift compartment to the west, the sediment eroded in the west end of the test compartment would be found as an accumulation following overwashing. For the period covered by Fig. 30, the budget for the test compartment is comprised to two entries: 1) net gain of sediment in the east at the shoreline; and, 2) net loss of sediment in the west at the shoreline. This pattern is subsequently referred to as the overwashing pattern.



9/27 - 11/8 (1985)

ELEVATION DIFFERENCES IN CENTIMETERS

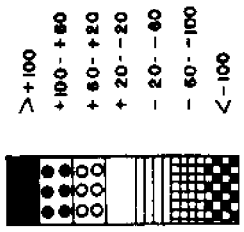


Fig. 30. Difference map; post-fill. September 27 to November 8, 1985.

The succeeding difference map (Fig. 31) again shows a bipolar pattern; however, the sense of the polarity is the reverse of that shown in Fig. 30. Net scour in excess of 1 m over the period of two months occurs in the eastern part of the compartment centered along and slightly above the MLW shoreline. Net deposition of sediment characterizes the western shoreline sector. Whereas, the disposition of net fill and net scour in Fig. 30 indicates a dominance of one-way overwashing from compartment to compartment, the pattern of Fig. 31 indicates a redistribution of the previously overwashed and deposited sediment within the test compartment. This pattern is subsequently referred to as the redistribution pattern. The algebraic sum of the patterns of Figs. 30 and 31 tends to zero but the net result of overwashing followed by redistribution has been an episodic transport of sediment to the west through the compartment along the shore.

In Figure 32, which adjoins Fig. 31 in time, a bipolar pattern of net accumulation and net erosion of sediment is again displayed; however, the sense of polarity is the same as that of the preceding difference map, i.e., it is also a redistribution pattern, although less intense in the degree of change.

In Figure 33, the bipolar pattern is again evident but this time it is reversed compared to the previous diagram with net accumulation of sediment of 1 m at the east groin and net removal of sediment along the shoreline at the west groin within the compartment. The four consecutive difference maps indicate a dominance of overwashing during an initial 6-week period, followed by a dominance of redistribution of the overwashed sediment during a 17-week period, followed by a dominance of overwashing of sediment for a period of 8 weeks.

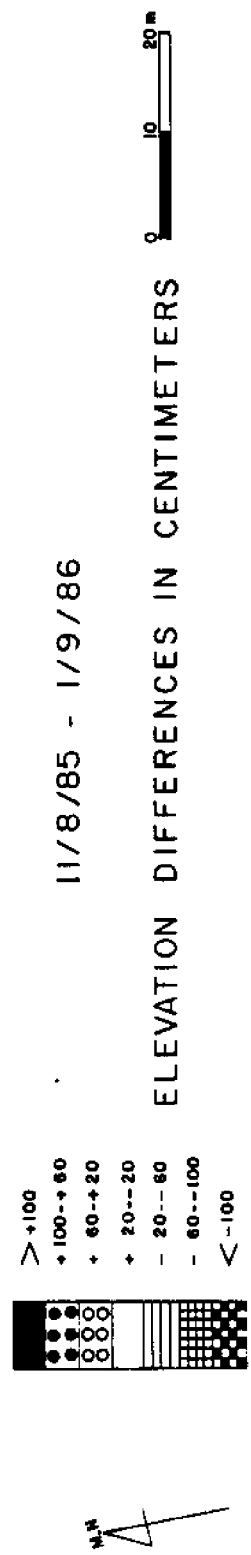
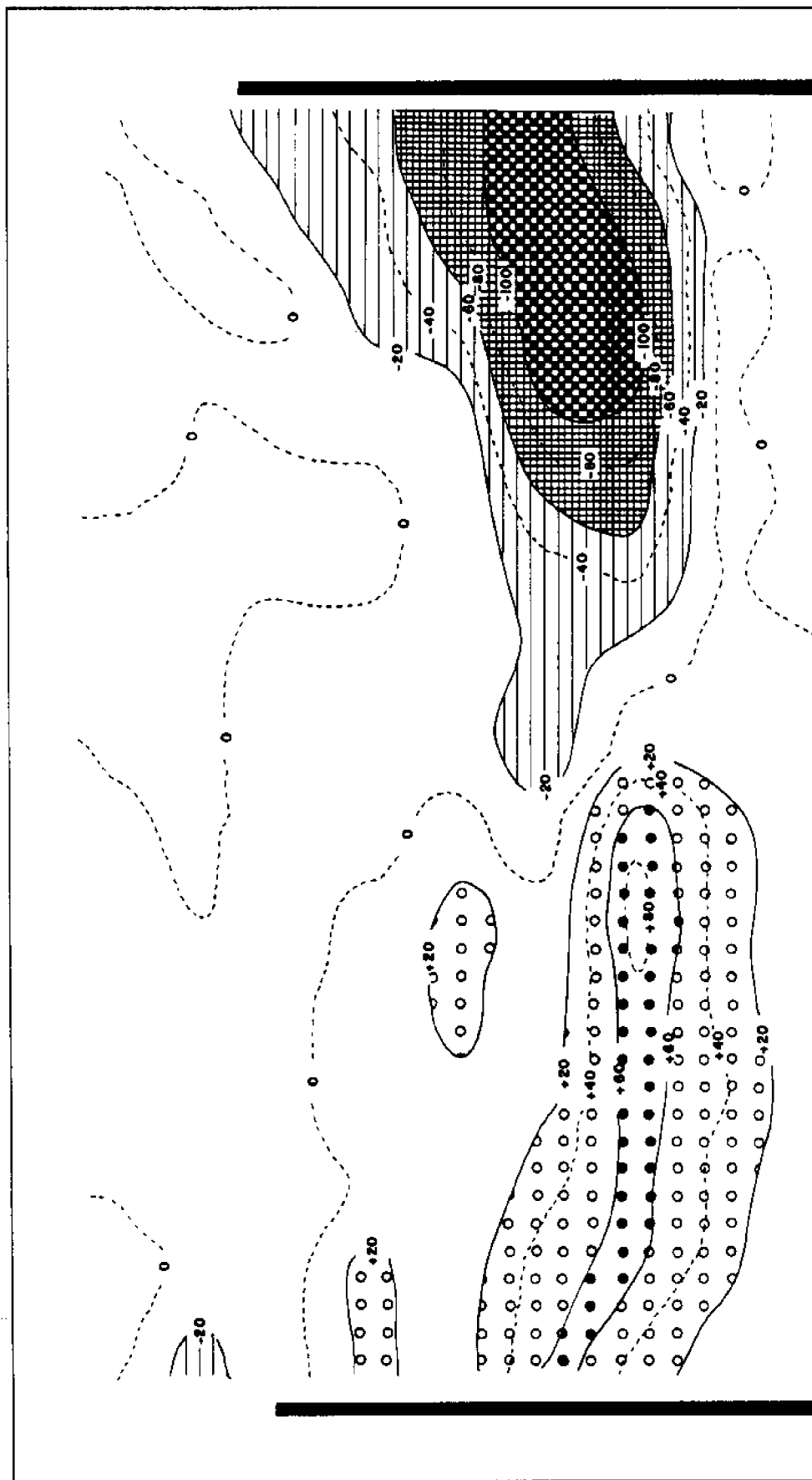
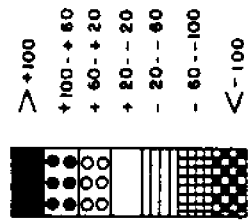
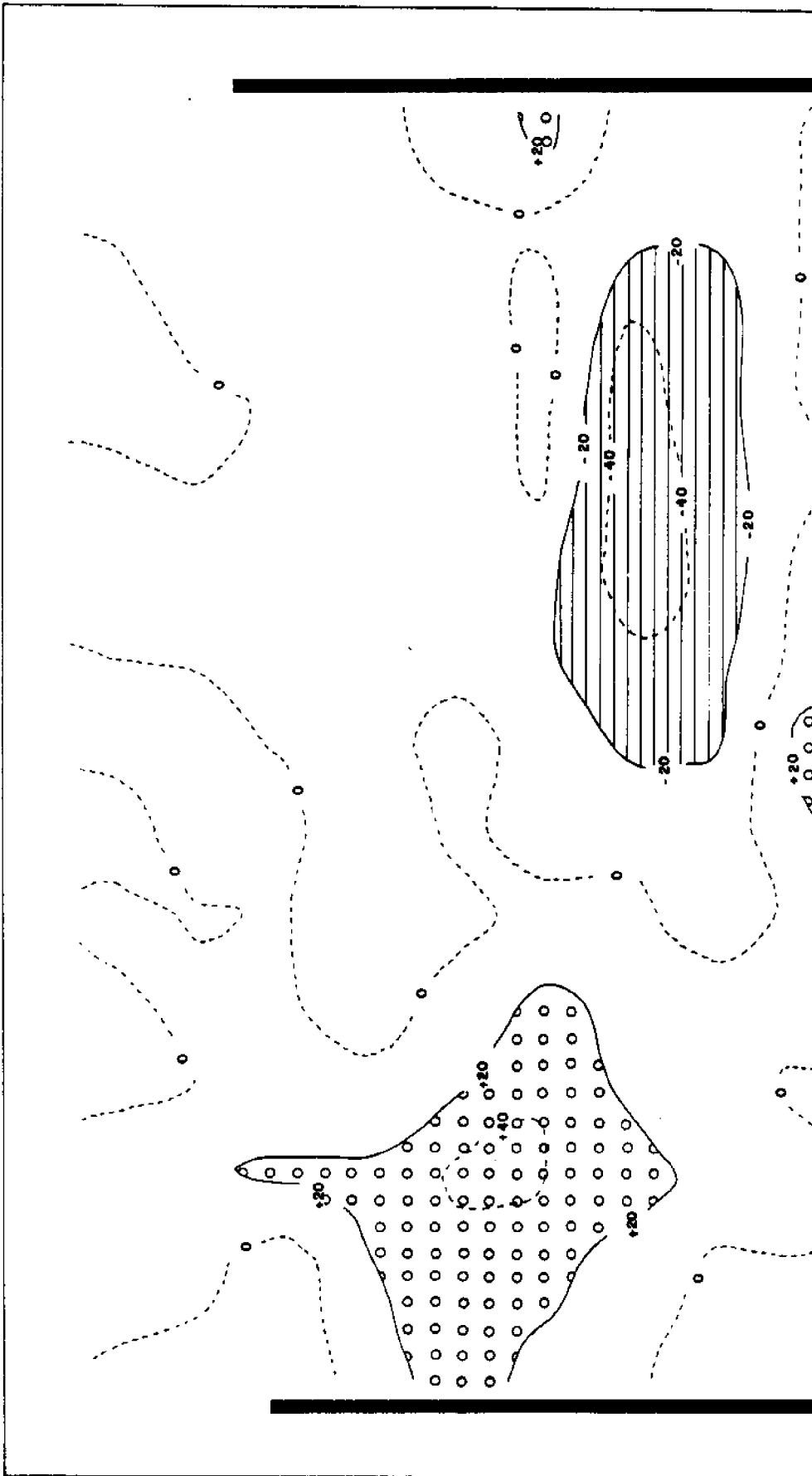


Fig. 31. Difference map; post-fill. November 8, 1985 to January 9, 1986.

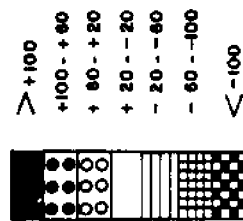
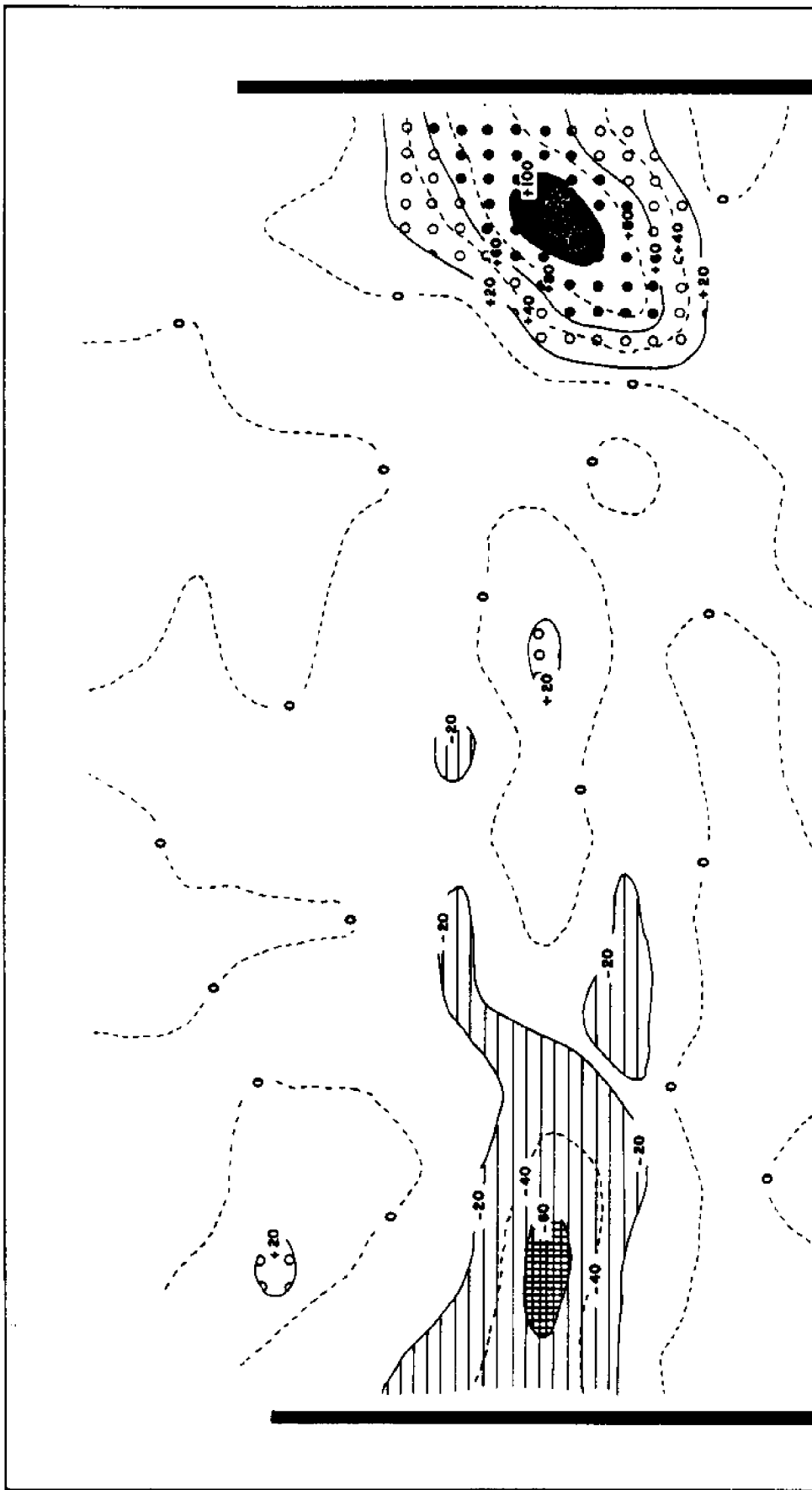


1/9 - 3/26 (1986)

ELEVATION DIFFERENCES IN CENTIMETERS



Fig. 32. Difference map; post-fill. January 9 to March 26, 1986.



3/26 - 5/23 (1986)



ELEVATION DIFFERENCES IN CENTIMETERS



Fig. 33. Difference map; post-fill. March 26 to May 5, 1986.

Change in the volume of sediment for the entire compartment is calculable from a given difference map by algebraically summing the change over all observation points and multiplying by a constant which reflects map area per observation point. From a sequence of such sums, each for a successive difference map, the volume of sediment in the compartment over time is determined by progressively cumulating the sequence of values (Fig. 34). An arbitrary starting volume of 5000 cu m was assumed for August 3, 1983.

In the pre-fill period, volume remained relatively constant. The upwards offset in August 1984 corresponds to the placing of 10,000 cu m of fill in the compartment. From that date onwards, the volume declines irregularly, but steadily on average, at a rate of 3114 cu m per year. If that rate were maintained, all the fill in the compartment would be lost in 3.2 years. This estimate is procedurally in error because of the assumption of the constancy of volume loss rate, and for another reason explained below.

An alternative computation of the rate of volume loss has been made, attention being given to whether new scour at a point is wholly, partly, or not at all in filled sediment. When this operation is done for each difference map and the sequence of values cumulated, a new curve is obtained (Fig. 34, dashed line). Averaged over time, the adjusted time-volume curve shows that the rate of loss of filled sediment is 1326 cu m per year or approximately 40 percent of the unadjusted rate. If the new rate were to be maintained, the fill in the compartment would be exhausted in 7.75 years. As before, the estimate suffers from an assumed constancy of loss rate. In the sections, below, this shortcoming is remedied.

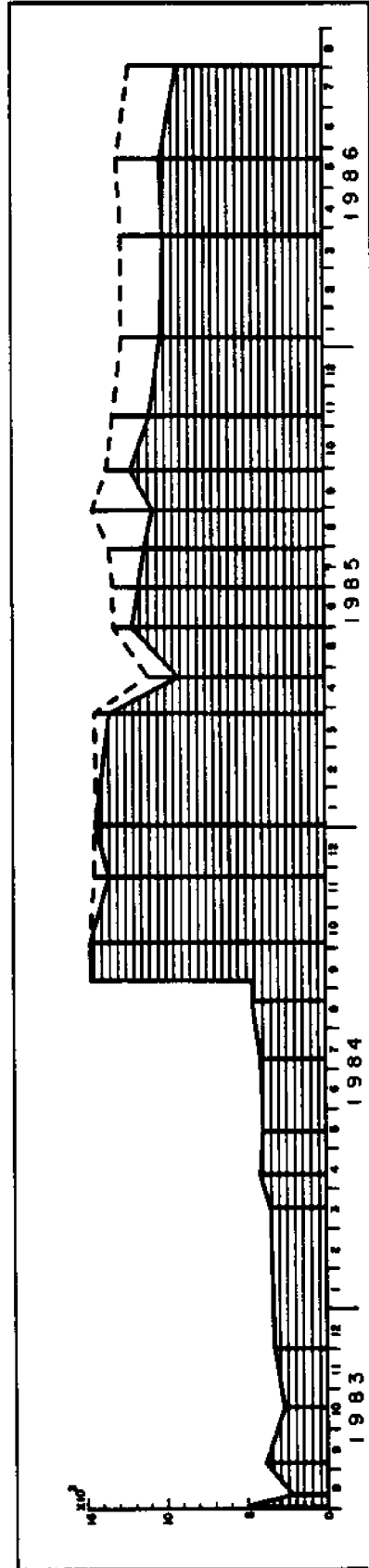


Fig. 34. Time-history of sediment volume in the test compartment. The shaded area gives the cumulation of values derived from the sequence of elevation difference maps. The dashed line is a corrected time-history curve allowing for whether erosion at a point is in fill or pre-fill sediment.

THE PROCESS SCHEMA

The findings of the study including measurements and observations as reported and discussed in the foregoing sections have led to the identification of two primary zones of shorewise sediment transfer at Willoughby Spit. Belt 1 is a nearshore zone, including the swash zone, where wave-associated processes dominate. Compartment-to-compartment transfers of sediment in this belt occur by groin overwashing at times of sufficiently elevated water levels (Figs. 26B, 30, 33, and 35). At these times, with longshore current motion to the west along the foreshore, moving sediment encounters no obstacle at a groin, but instead flows over a negative step (Figs. 35B, 35D). For the strongly recessed condition of the beach that existed just before the fill was placed (Figs. 35A, 35C), overwashing in Belt 1 required water levels 1.7 and 1.5 m above MLW at east and west groins, respectively. Recurrence times for superelevations of these magnitudes are 2.0 and 1.0 years. In contrast, immediately after the fill was placed (Figs. 35B, 35D), overwashing occurred twice per day, at each high water for several hours. With the slow retreat of the beach relative to the fixed profiles of the groins themselves it is evident that there would be a falling-off with time in the frequency of overwashing (Fig. 35). Other movements of sediment in Belt 1, namely, redistribution, occur along the shoreline but wholly within a compartment during times of lower water (Figs. 31, 32). The sediment-moving intensity of these within-compartment processes decreases with the aging of the fill as breaker angles along the compartment shoreline are slowly adjusted asymptotically towards zero. Finally, processes in Belt 1 are considered to be the chief contributors to the growth of the new spit at the west end of Willoughby Spit (Fig. 27)

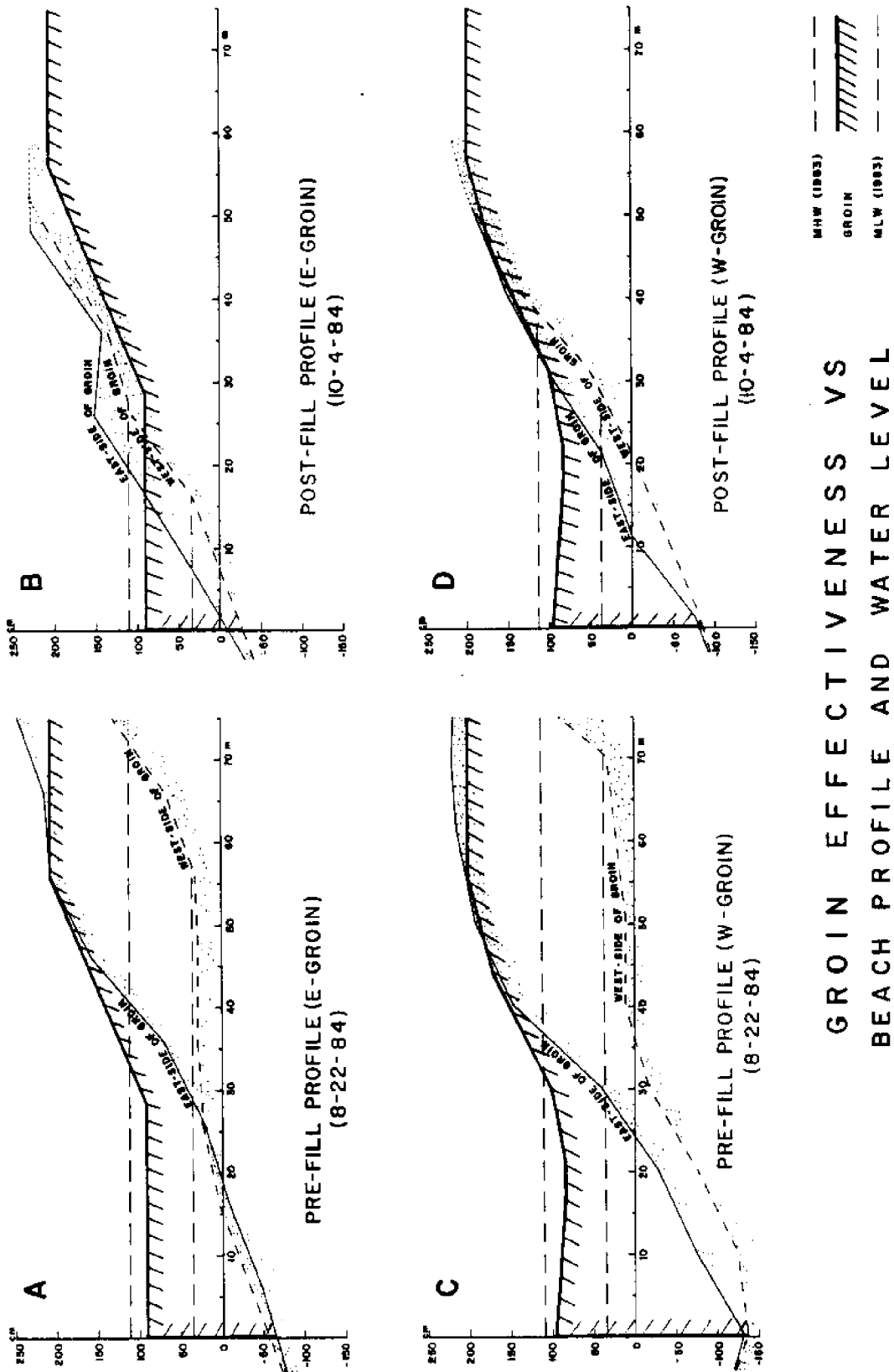


Fig. 35. Groin effectiveness related to sand level and water level. A. East groin, pre-fill profiles taken along the east and west sides of the groin. B. East groin, post-fill profiles taken along the east and west sides of the groin. C. West groin, pre-fill profiles taken along the east and west sides of the groin. D. West groin, post-fill profiles taken along the east and west sides of the groin.

judging from the position of the new spit and its shoreline relative to the sand-buried part of the terminal groin (see Fig. 27 and caption).

Belt 2 transfers of sediment occur also in the shorewise direction but in a zone that begins slightly beyond the ends of the groins. Here, tidal current action is visibly strong enough to move sand-sized sediment alternately to the east and west but with longer and stronger transport to the west (Fig. 11). Belt 2 receives sediment from Belt 1 through the action of shore-normal water motions concentrated at groin walls (Lundberg, in preparation). Other offshore-directed movements, that can occur anywhere in the compartment, are associated with asymmetry in particle motion due to wave-current interaction (Fig. 17C) and gyre spin-up. Shore-normal sediment movements of the foregoing kinds are chiefly responsible for the loss of sand from the compartment beach and nearshore zone to Belt 2 where the sediment is entrained by the transporting mechanisms characteristic of that zone.

THE ESTIMATION OF FILL LIFE

The processes of longshore sediment movement in Belt 1 at Willoughby Spit have been described in the earlier sections of this report. It will be recalled that intercompartmental transfer of sediment in the narrow breaker zone occurs when the longshore current encounters either a negative elevation step at a groin or no step; intercompartmental transfer in Belt 1 does not occur when the sediment carrying current is blocked by the groin wall. Two factors are determining: 1) elevation of the water surface relative to the top of the groin; 2) the elevation profile of the updrift beach relative to the elevation profile of the groin. The first factor is characterized by a probability density function such that increasingly higher elevations of

the water surface occur with decreasingly lower frequency. It also needs to be noted that the elevation of the groin top is greater with distance inland, increasing along the middle inclined section of the groin to the higher horizontal section at +6 ft. MLW.

The action of the second factor above depends on the length of time that has elapsed since a fill was placed. Immediately after a fill, sand levels in a compartment are high, and the position of the beach is advanced in the compartment. With the passage of time, the profile of the beach retreats landwards as sediment is lost and slopes are readjusted.

The result of the two factors taken together is that, immediately after the fill, intercompartmental transfers of sediment in Belt 1 operate for several hours at each high water, twice a day; however, after months of beach recession, only the larger tidal elevations at spring tides are great enough to enable Belt 1 action. With even further profile recession, a very large meteorologically-caused superelevation of the water surface is needed to permit Belt 1 sediment transfers from compartment to compartment to operate. At Willoughby Spit before the fill with the beach greatly recessed, a storm-related superelevation of the water surface of at least 3.7-4.4 ft. above MSL was required for activation of intercompartmental transfers of sediment along Belt 1. In the chapter on tides it was shown that elevations of this magnitude are to be expected once per year approximately. The frequency and efficacy of Belt 1 processes that move sediment from compartment to compartment are high immediately after a fill, but are progressively lessened in effectiveness with the aging (recession) of a fill.

As shown in the chapter dealing with shoreline adjustment within the compartment, as recession of the beach gradually takes place after a fill, the shoreline retreats differentially, aligning itself by rotation to the

action of the dominant waves so that the breaker angle everywhere along the shore gradually approaches zero with time. Because of the dependence of longshore transport of sediment on a finite, non-zero breaker angle, longshore transport of sediment within the compartment also approaches zero with time and offshore losses of sediment by rip-current action at groin walls are also progressively lessened.

This progressive decrease with time in the intensity of the acting processes of sediment removal from the compartment is the basis of the following mathematical description of post-fill shoreline change and sediment loss at Willoughby Spit.

The volume of filled sediment remaining in each of N compartments of a rectilinear groin system following a uniform fill can be described by a first order linear differential equation as follows:

$$\frac{dV_n}{dt} = - (j+k) V_n + k V_{n-1} \quad (1)$$

in which V_n is the volume of filled sediment remaining in the n th compartment; j is a rate constant pertaining to offshore-directed losses of sediment, i.e., the transfer of sediment from Belt 1 to Belt 2; k is a rate constant pertaining to longshore transfer of sediment in Belt 1 from compartment to compartment; and t is time. A definition sketch is given in Fig. 36. While transfer-out of sediment alongshore in the downdrift direction and losses offshore are occurring, there is a flux of sediment into a compartment in Belt 1 from the updrift compartment. Fill in equal amounts is initially placed in a finite number of discrete compartments, N ; compartments are empty for $n < 1$; there is a shoreline, but no

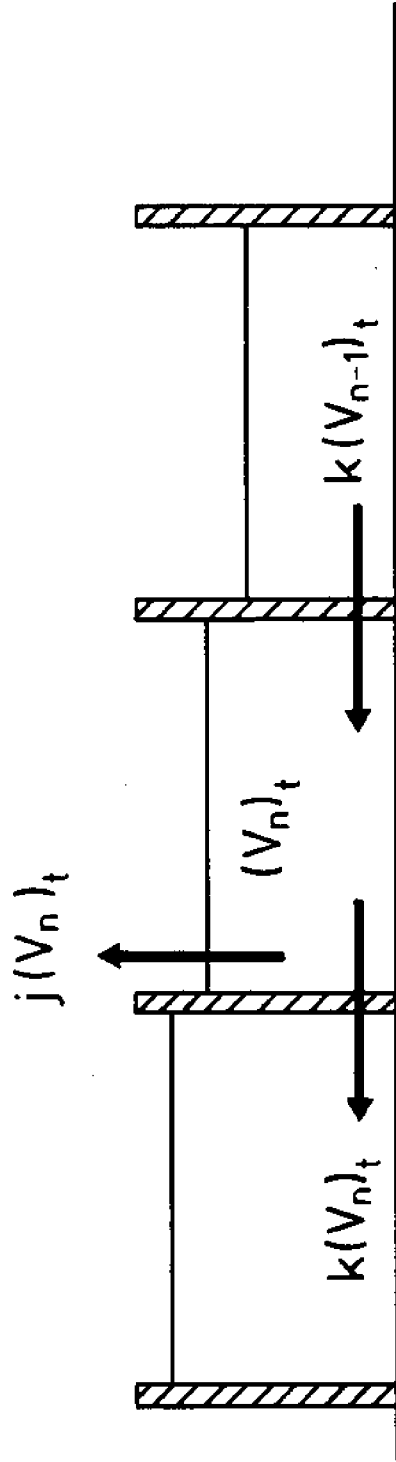


Fig. 36. Definition sketch. Three compartments of a rectilinear system of groins. Symbols are defined in the text.

compartments for $n > N$. No flux of sediment is directed into Compartment 1. Although the transports of sediment are actually episodic, relevant terms in Eq. 1 are interpreted as time averaged rates. Sediment that moves from Belt 1 to Belt 2 does not return to the compartments and is not deposited in the terminal spit. If some fraction of the sediment that is moved from Belt 1 to Belt 2 actually returns to the shore, then rate constant j can be construed as referring to the net rate of movement from Belt 1 to Belt 2. Constants j and k are uniform and invariant. Transport of sediment alongshore in Belt 1 is taken to be unidirectional in the direction of increasing n .

In Eq. 1, the rate of sediment loss from a compartment is greatest initially when a new sand fill has just been placed, V_n is largest, and shoreline displacement away from the equilibrium configuration is a maximum. Moreover, the transfer of sediment into the compartment from the updrift compartment is also large initially when there is a considerable quantity of sediment in the updrift compartment, and falls off later on when the volume in the updrift compartment is lessened, i.e., when recession of the subaqueous and subaerial beach in the updrift compartment has occurred.

The solution to Eq. 1 is

$$(V_n)_t = (V_1)_0 e^{-(j+k)t} \sum_{r=1}^n \frac{(kt)^{r-1}}{(r-1)!} \quad (2)$$

in which the subscript t indicates time dependency; the subscript 0 denotes $t = 0$. In Compartment 1, for example, the volume of sediment fill remaining experiences an exponential decrease with time, the rate of which is dependent on the actual magnitudes of j and k .

The cumulative volume of sediment transferred from compartment n to compartment $n+1$ in Belt 1 as of time t is given by

$$\begin{aligned} (L_n)_t &= k \int_0^t (V_n)_t dt, \\ &= (V_1)_0 \left\{ \sum_{s=1}^n R^s - e^{-(j+k)t} \sum_{s=1}^n R^s \sum_{r=1}^{n+1-s} \frac{(kt)^{r-1}}{(r-1)!} \right\} \end{aligned} \quad (3)$$

where $R = k/(j+k)$.

At Willoughby Spit, with reference to the fill placement of the present report, $N = 27$ and downdrift of the last compartment (i.e., $n = 27$) a terminal spit began to grow immediately following the placement of the fill in the groin system updrift. Eq. 3, with $n = 27$, expresses the cumulative volume of sediment that has issued from the last compartment at any time. In the absence of losses from the spit, this is equivalent to the terminal spit volume at any time.

Rate constants j and k are evaluated from Eq. 2 and 3 iteratively from the known conditions that: 1) in the test compartment ($n = 23$) the volume of fill remaining after 19 months was 80 percent of that placed initially in the compartment; and 2) the volume of the terminal spit after 19 months was 8 percent of the total fill placed initially in the system of groins. It is found that for these conditions $j = 0.0115$ and $k = 0.1250$ per month.

The loss of sediment from a compartment is due to two causes: 1) the excess of output over input in Belt 1; 2) offshore-directed losses of sediment as embodied in the j rate constant representing transfers of sediment from Belt 1 to Belt 2. In Fig. 37, it is seen that the affects of the

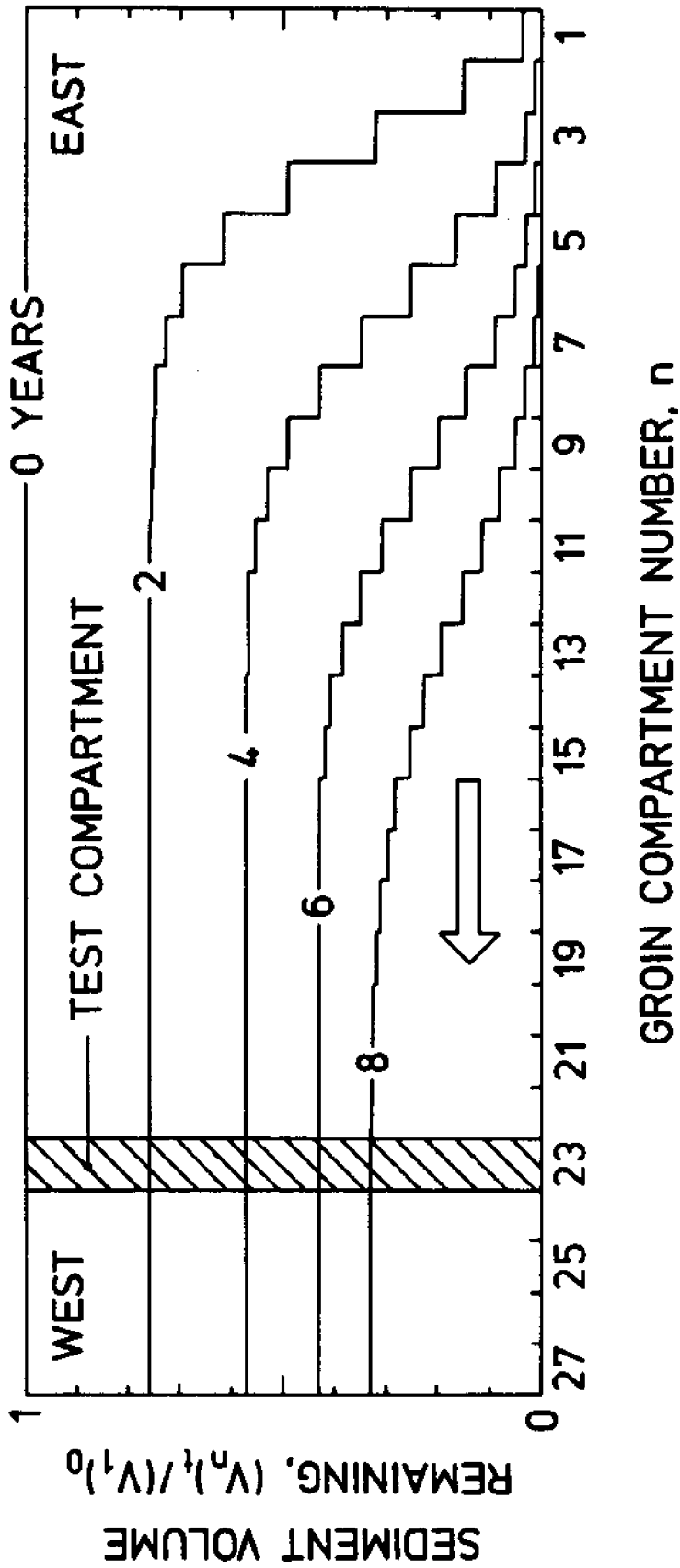


Fig. 37. Sediment remaining in the various compartments as a function of time post-fill. The results were obtained from Eq. 2 of the present report.

boundary condition imposed at the updrift end of the system propagate down-drift along the system with the passage of time and are stretched out. Losses arising from item 1 above are here termed longshore gradient losses, whether as a consequence of a boundary condition, as in the present equations, or to spatial changes in the rate constant k (changes of this kind in k are not a feature of the present analysis). The other losses, those associated with item 2 above, are here termed offshore losses and as set up in the present equations affect all compartments. They are, however, a priori (Eq. 1) volume-dependent as are all losses in the present formulation; that is to say, they fall off in intensity with time as is consistent with observations at the field site.

From an examination of Fig. 37 it is seen that in the test compartment ($n = 23$), as well as in other downdrift compartments, with reference to Belt 1 movements of sediment from compartment to compartment, the volume of sediment introduced into a compartment in unit time is very nearly equal to the volume of sediment exiting from the compartment in the same time period, i.e., early on, longshore gradient losses of sediment are essentially nil. The decrease in the volume of sediment remaining in the compartment is primarily attributable to offshore losses, even though sediment is seen pouring through the compartment along the shore during frequent episodic overwashing. With the passage of time, the depletion front eventually reaches a downdrift site, and longshore gradient losses become important, while offshore losses continue but, of course, weakened in intensity because of the passage of time. Finally, with approach to a terminal ideal static equilibrium all transports become negligible, a condition that was approximated by the state of the test compartment immediately before the placement of the fill. Long term recession (or aggradation) of the Willoughby Spit

shoreline could occur as a result of processes not considered in the fill longevity problem treated here.

It is to be noted that the ratio of j to k is approximately 1:10, an indication that offshore losses occur at a rate one order of magnitude smaller than longshore transport rates in Belt 1. It should be noted that offshore losses can occur, at least in part, distributed along a long front; whereas, longshore transport of sediment in Belt 1 takes place across a shore normal of small width. If transport intensity is expressed in terms of sediment volume moved per unit path width per unit time, then offshore losses per unit path width may occur on average at rates that are 1/100 or 1/1000 that of the longshore transport rates in Belt 1.

An estimate of the instantaneous rate of sediment transport alongshore in Belt 1 from compartment to compartment is calculable from one of the equations obtained. If the quantity $(Vn)t$, from Eq. 2, is multiplied by the rate constant k , the result is the rate sought for a location in the groin system depending on the choice of n , at a time t . Derived estimates of the instantaneous rates of sediment transport alongshore in Belt 1 for the study compartment ($n = 23$) are given below.

Time (years)	Sediment Transport Rate, Belt 1 (cubic meters per year)
0	15,000
2	11,382
4	8,637
6	6,553
8	4,958

Similarly, the offshore sediment transport rate can be calculated as the product of the quantity $(Vn)t$ and the offshore rate constant j .

Initially when $t = 0$ years, the offshore rate is 1,380 cubic meters per year from compartment 23; when $t = 8$ years, the offshore rate is 456 cubic meters per year from compartment 23. These offshore rates can be alternatively expressed by converting them to conventional units which are a "per unit path width" where the total path width is the distance between groins, 500 ft. (152.4 m). The following magnitudes are obtained: 0.29 cubic cm per sec. per meter of path width for $t = 0$ years; 0.096 cubic cm per sec. per meter of path width for $t = 8$ years. If the offshore transport is concentrated along the wall of the groin and occurs only there in a flow path 6 m in width, these magnitudes should be multiplied by a factor of approximately 25.

The longshore transport rates in the table above can also be converted to conventional units and placed on a "per unit path width" basis if the width of the longshore zone is assumed to be, say, 3 m. In this case, the longshore rates for compartment $n = 23$ for $t = 0$ and $t = 8$ years are 160 and 53 cubic cm per sec. per m of path width, respectively. The ratio between longshore sediment transport rate and offshore sediment transport rate on a "per unit path width" basis is approximately 550.

The volume of the terminal spit, according to the equations obtained, tends to increase nearly linearly during the first 5 months of growth. Thereafter the rate of volume growth continues to slow down, increasing only from 28.6 to 30.1 percent of the volume of the placed fill from year 8 to year 10.

The partitioning of the placed fill among the compartments, the terminal spit, and offshore losses is shown in Fig. 38. At the end of 10 years, retained fill in the system of groins decreases to 11.2 percent, the spit volume increases to 30.1 percent, and offshore losses accrue to 58.7 percent

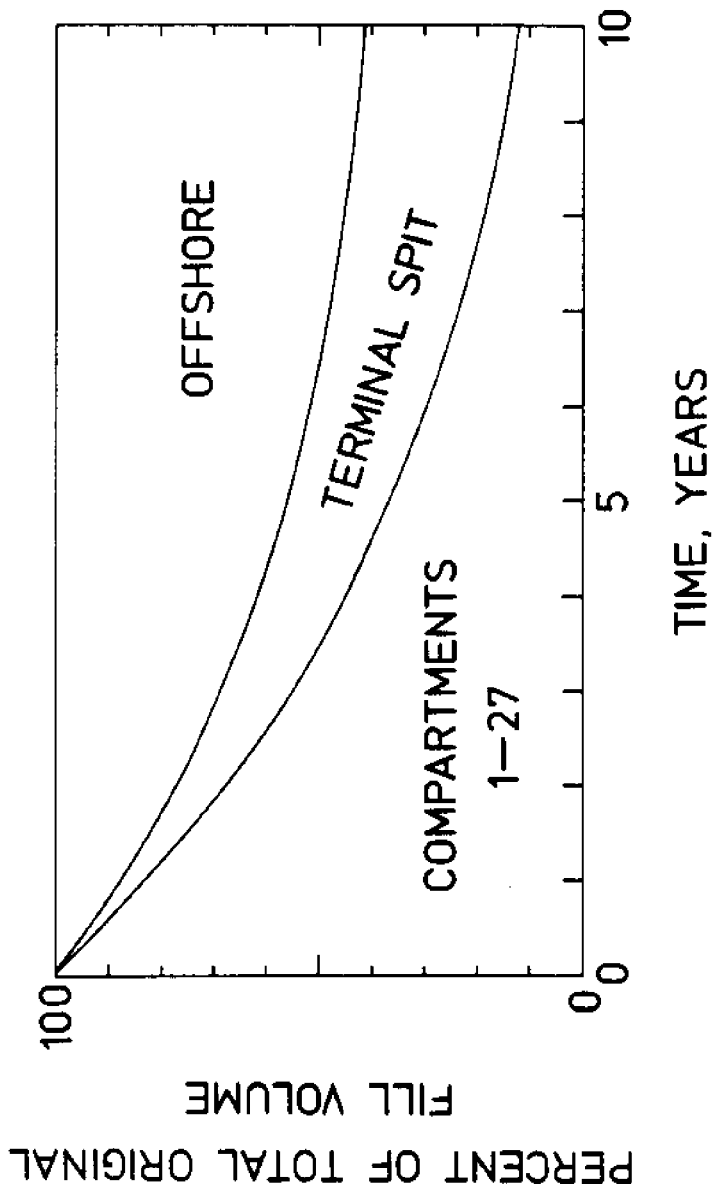


Fig. 38. Time history of the partitioning of the placed fill at Willoughby Spit among the groin compartments, terminal spit, and offshore losses.

of the placed fill volume. Half-life of the fill is 3.5 years. Effective life of the fill is 8.8 years, the latter being defined here as the time elapsed when 15 percent of the placed fill remains in the system of groins.

SUMMARY AND CONCLUSIONS

1. Placement of sand fill uniformly on a limited reach along a shore creates a transient condition of disequilibrium. In the case of the groin system at Willoughby Spit, pre-fill conditions were nearly those of static equilibrium: a) breaker angles within the compartments were statistically zero in adjustment to the dominant elements of the wave climate; b) sediment transport along the shore from compartment to compartment required a storm-related superelevation of water level of a magnitude that occurred approximately once in a period of one to four years. The analysis, given in the report, of the disequilibrium is made in terms of probable decay rate of the transient and the sediment-shifting processes that affect the decay--in this instance, the processes of fill loss from a groin compartment. The site studied is estuarine; shore-parallel tidal currents, of the area, acting close to shore just beyond the groin ends are as significant as waves in moving sediment.

2. Two processes of sand loss were identified: a) longshore gradient losses which arise when the rate of sediment transport increases in the direction of transport along the shore (in the present instance, the increase arises because of lowered values updrift caused by the progressive depletion of fill sediment from updrift compartments); b) offshore losses caused by the action of rip currents along groin walls, and the offshore-directed asymmetry in wave orbital velocity distribution near the bed (the latter arising from interaction of incident waves with quasi-steady currents generated by tidal action).

3. A differential equation is developed to describe the time-dependent decay of a fill transient over a rectilinear system of discrete groin compartments. Embodied in the equation and its solution are rate constants for both longshore and offshore transports of sediment. The constants are evaluated from the measured volumetric rate of growth of a new spit downdrift from the filled reach, and from the measured volume of filled sediment remaining in a test compartment versus time.

4. From the solution obtained, it is found that the half life of the fill at Willoughby Spit is 3.5 years; the effective life (85 percent lost) is 8.8 years; longshore transport rates decrease from 15,000 to 4,958 cubic m per year at a downdrift compartment from year 0 to year 8; offshore transport rates decrease from 1,380 to 456 cubic m per year from the same downdrift compartment from year 0 to year 8; re-calculated as transport per unit path width, longshore rates are approximately 550 times greater than offshore rates; after 10 years, 11.2 percent of the total original fill resides in the system of groin compartments, largely at the downdrift end, and 30.1 percent of the total original fill is lodged in the new terminal spit, and 58.7 percent of the total original fill has been lost to the offshore area.

5. T-head structures installed at the seaward end of each groin would increase the effective life of a hypothetical new fill by inhibiting offshore losses along groin walls. An increase of 45 cm in the elevation of the top of each groin, if and when they are rebuilt, would lessen the transfer of sediment from compartment to compartment thereby also postponing longshore gradient losses and delaying the arrival of the depletion front at a given compartment.

ACKNOWLEDGMENTS

The work described herein was supported by the Virginia Sea Grant College program, Project Number R/CP-1, the sponsoring federal agency being the National Oceanic and Atmospheric Administration, Department of Commerce. Graduate students Hyo Jin Kang, R. Neville Reynolds, and Dennis L. Lundberg worked long and diligently on the project and were engaged over a period of years in nearly constant discussion and interpretation of the results obtained. James R. Melchor of the U.S. Army Corps of Engineers, Norfolk District Office, provided through his office the long term loan of an electro-magnetic current meter to the study. Donald W. Mathias, Manager Environmental Services, City of Norfolk, provided the assistance of his office, and oversaw the filling operation. I alone take responsibility for the findings and conclusions of the present report.

REFERENCES CITED

- Balisillie, J.H. and Bruno, R.O., "Groins: An Annotated Bibliography," CERC Misc. Paper 1-72, U.S. Army Corps of Eng., 1972, 249 pp.
- Bloomfield, P., "Fourier Analysis of Time Series: An Introduction." John Wiley & Sons, New York, N.Y., 1976, 258 pp.
- Brown, E.I., Daley, E.L., Young, G.R., Bowman, F.O., Hale, R.K., Gelineau, V. and Saville, T., "Beach Erosion at Willoughby Spit, Va.," House of Representatives, 75th Congress, 3rd Session, Document No. 482, 1938, 28 pp.
- Byrne, R.J. and Anderson, G.L., "Shoreline Erosion in Tidewater Virginia," Special Rept. Applied Marine Sci. and Ocean Engineering, No. 111, Virginia Inst. of Marine Sci., Gloucester Point, Va., 1977, 102 pp.
- Cartwright, D.E., "Analysis and Statistics," in The Sea, Vol. 1, (M.N. Hill, ed.), Section V, Waves, pp. 567-589. Interscience Publishers, John Wiley & Sons, New York, N.Y., 1962, 864 pp. (See pp. 573-575: Properties of a Wave System in Terms of its Directional Energy System).
- Fleischer, P., McRee, G.J., and Brady, J.J., "Beach Dynamics and Erosion Control, Ocean View Section, Norfolk, Virginia," Tech. Rept. No. 50, Institute of Oceanography, Old Dominion University, Norfolk, VA, 1977, 185 pp.
- Grant, W.D. and Madsen, O.S., "Moveable Bed Roughness in Unsteady Oscillatory Flow," Jour. Geophys. Research, Vol. 87, No. C1, 1982, pp. 469-481.
- Harris, D.L., "Tides and Tidal Datums in the United States," CERC Special Report No. 7, U.S. Army Corps of Engineers, 1981, 382 pp.
- Longuet-Higgins, M.S., "Statistical Analysis of a Random Moving Surface," Phil. Trans. Royal Soc. London, Vol. A249, 1957, pp. 321-387. (See pp. 331-333: The Spectrum of the Surface in An Arbitrary Direction).
- Ludwick, J.C., "Tidal Currents and Zig-Zag Sand Shoals in a Wide Estuary Entrance," Geol. Soc. America Bull., Vol. 85, No. 5, 1974, pp. 717-726.
- Lundberg, D.L., "Groin-Associated Rip Currents Measured Using a New Digital Current Meter," Ph.D. Dissertation, Dept. Oceanography, Old Dominion University, Norfolk, VA, 1987, in preparation.
- Madsen, O.S. and Grant, W.D., "The Threshold of Sediment Movement Under Oscillatory Waves: A Discussion," Jour. Sedimentary Petrology, Vol. 45, No. 1, 1975, pp. 360-376.
- Melchor, J.R., "The Legend of Willoughby Spit, Fact or Fiction," Dept. Geology, College of William and Mary, Unpublished Report, 1970, 18 pp., 26 plates.

- Nagata, Y., "Observations of the Directional Wave Properties," Coastal Engineering in Japan, Vol. 7, 1964, pp. 11-30.
- Nagata, Y., "The Statistical Properties of Orbital Wave Motions and their Application for the Measurement of Directional Wave Spectra," Jour. Oceanog. Soc. of Japan, Vol. 19, No. 4, 1964, pp. 169-181.
- Thompson, E.F., "Wave Climate at Selected Locations Along U.S. Coasts," CERC Tech. Report 77-1, U.S. Army Corps of Eng., 1977, 364 pp.
- Tomlinson, J.H., "Groynes in Coastal Engineering," Rept. No. IT 199, Hydraulics Research Station, Wallingford, Oxon, OX10 8BA, England, 1980, 21 pp.
- Ursell, F., "Edge Waves on a Sloping Beach," Proc. Roy. Soc. (London), Series A, 214, 1952, pp. 79-97.
- USACE (United States Army Corps of Engineers), "Willoughby Spit and Vicinity, Norfolk, Virginia, Hurricane Protection and Beach Erosion Control Study," Feasibility Rept. and Final Impact Statement, Parts 1 and 2, Supporting Documentation, 1983.
- USACE (United States Army Corps of Engineers), "Preliminary Design for Disposal of Dredged Material from Thimble Shoal Channel on West Ocean View Beaches, Norfolk, Virginia," Final Report, Waterway Surveys & Engineering Ltd., Virginia Beach, Virginia, 1984, 76 pp.
- Vitale, P., "Sand Bed Friction Factors for Oscillatory Flows," Jour. Waterway, Port, Coastal and Ocean Division, ASCE, Vol. 105, No. WW3, 1979, pp. 229-245.
- Willis, D.H. and Price, W.A., "Trends in the Application of Research to Solve Coastal Engineering Problems," IN Nearshore Sediment Dynamics and Sedimentation (J. Hails and A. Carr, Eds.), Chap. 5, pp. 111-121. John Wiley & Sons, New York, N.Y., 1975, 316 pp.
- Wood, W.L. Jr., "Horizontal Particle Velocity Profiles Beneath the Crests of Waves Breaking on a Submarine Bar," Tech. Rept. No. 3, Dept. Geology, Michigan State Univ., ONR NR 388-089, 1970, 68 pp.